CRANFIELD UNIVERSITY

Ejay Nsugbe

Particle Size Distribution Estimation Of A Powder Agglomeration Process Using Acoustic Emissions

School Of Aerospace Transport And Manufacturing

PhD Acoustic Sensing

PhD

Academic Year: 2014 - 2017

Supervisor: Professor Andrew Starr

September 2017

CRANFIELD UNIVERSITY

School Of Aerospace Transport And Manufacturing
PhD Acoustic Sensing

PhD

Academic Year 2014 - 2017

Ejay Nsugbe

Particle Size Distribution Estimation Of A Powder Agglomeration Process Using Acoustic Emissions

Supervisor: Professor Andrew Starr
September 2017

This thesis is submitted in partial fulfilment of the requirements for the degree of Doctor Of Philosophy

(NB. This section can be removed if the award of the degree is based solely on examination of the thesis)

ABSTRACT

Washing powder needs to undergo quality checks before it is sold, and according to a report by the partner company, these quality checks include an offline procedure where a reference sieve analysis is used to determine the size distributions of the powder. This method is reportedly slow, and cannot be used to measure large agglomerates of powders. A solution to this problem was proposed with the implementation of real time Acoustic Emissions (AE) which would provide the sufficient information to make an assessment of the nature of the particle sizes.

From the literature reviewed for this thesis, it was observed that particle sizes can be monitored online with AE but there does not appear to be a system capable of monitoring particle sizes for processes where the final powder mixture ratio varies significantly. This has been identified as a knowledge gap in existing literature and the research carried out for this thesis contributes to closing that gap.

To investigate this problem, a benchtop experimental rig was designed. The rig represented limited operating conditions of the mixer but retained the critical factors. The acquired data was analysed with a designed hybrid signal processing method based on a time domain analysis of impact peaks using an amplitude threshold approach.

Glass beads, polyethylene and washing powder particles were considered for the experiments, and the results showed that within the tested conditions, the designed signal processing approach was capable of estimating the PSD of various powder mixture combinations comprising particles in the range of 53-1500 microns, it was also noted that the architecture of the designed signal processing method allowed for a quicker online computation time when compared with other notable hybrid signal processing methods for particle sizing in the literature.

Keywords:

Signal processing, process monitoring, time domain, online monitoring, non-invasive monitoring, amplitude threshold.

Publications Made From Thesis

All manuscripts were drafted by E.Nsugbe and listed co-authors either assisted with the data collection/analysis or provided feedback and corrections on the manuscripts.

Journal Publications:

-E.Nsugbe, A.Starr, C.Ruiz-Carcel **Monitoring The Particle Size Distribution Of A Powder Mixing Process With Acoustic Emissions: A Review.** Engineering Technology Reference, pp. 1–12 ,doi: 10.1049/etr.2016.0139

-E.Nsugbe, A Starr, I Jennions and C Ruiz-Carcel **Online Particle Size Distribution Estimation Of A Particle Mixture In Free Fall With Acoustic Emission** submitted to Journal Of Particulate Science And Technology (Revisions Suggested)

-E.Nsugbe, C Ruiz-Carcel, A Starr, and I Jennions **Estimation Of Fine And Oversize Particle Ratio In A Heterogeneous Compound With Acoustic Emissions** submitted to Multidisciplinary Digital Publishing Institute: Sensors (Revisions Suggested)

-E Nsugbe, C Ruiz-Carcel, A Starr and I Jennions **Particle Size Distribution Measurement Of A Heterogeneous Powder Mixture Using Acoustic Emissions** to be submitted to Powder Technology

Conference Publications:

-E. Nsugbe, A Starr, P Foote, C Ruiz-Carcel and I Jennions **Size Differentiation Of A Continuous Stream Of Particles Using Acoustic Emissions** IOP Conf. Series: Materials Science and Engineering 161 (2016) 012090 doi:10.1088/1757-899X/161/1/012090 (**Best Paper Award**)

- E. Nsugbe, A Starr, I Jennions and C Ruiz-Carcel **Online Particle Size Distribution Estimation Of A Mixture Comprising Of Similar Sized Particles With Acoustic Emissions** The 6th International Conference on Manufacturing Engineering and Process (**Best Technical Presentation**)

- E. Nsugbe, A Starr, I Jennions and C Ruiz-Carcel **Particle Size Distribution Estimation Of A Mixture Of Regular And Irregular Sized Particles Using Acoustic Emissions** 27th International *Conference* on Flexible Automation and Intelligent Manufacturing

Co-Authored Journal Publication:

-C Ruiz-Carcel, A Starr, and E. Nsugbe **Estimation Of Powder Mass Flow Rate In A Screw Feeder Using Acoustic Emissions** Published In Powder Technology

In loving memory of my Godfather “Uncle Odion” and also former Reader in Electronics Engineering At Sussex University “Dr Lionel Ripley”.

….R.I.P to both of you.

“ …the only people who tell you that you can’t do something are the ones who failed. And I’m not going to tell you that you can’t do something, because I did it and you can too. So don’t listen to negative people. The only person who decides what you can do is you. ”

-Paul Stanley/Christopher Irvine

ACKNOWLEDGEMENTS

All praise and gratitude be to my creator for all the mercies, strength, wisdom and guidance he has shown to me over the duration of the PhD.

I would like to thank the man who hired me and gave me the opportunity to come down to Cranfield and work as part of a consortium full of bright academics, he served as my supervisor, line manager and voice of reasoning over the course of my PhD and his name is Professor Andrew Starr. Thank you for being supportive, understanding and flexible with me as I matured over the years.

I would like to thank Professor Ian Jennions for agreeing to step in when help was needed and going on to guide and capably assisting me with my research as my co-supervisor. I would like to thank my colleague, friend and PhD mentor, Dr Cristobal Ruiz-Carcel for the abundant help, support and guidance which he selflessly provided me. I would also like to extend thanks to Professor Peter Foote who provided me with assistance in getting started with my research prior to his departure. And also many thanks to my internal review team which comprised of the perfectionist Professor Stewart Williams and the man with an eye for detail Professor Stephen James.

Many thanks to you all for seeing my potential and guiding me into becoming a much stronger version of myself.

I would like to thank the likes of Claire Duckitt, Claire Martin, Paul Gould and Dave Smyth for providing me with access to the production site as well as relevant process information when it was needed. I would also like to acknowledge the support of partners Procter & Gamble, IIT, Ajax, Centre for Process Innovation, the University of Birmingham, the University of Leeds, and the University of Durham. This research is part of Chariot and The Advance Manufacturing Supply Chain Initiative (AMSCII) which is a government supply chain fund which is helping to rebuild British manufacturing prowess.

Big thanks to the guys at the particle characterisation lab, Christine Kimpston at the Scanning Electron Microscope lab, David Ayre and the rest of the crew that supported me here at the Cranfield University community.

And last but not the least, I would like to acknowledge and extend my gratitude to my family and friends, for the unconditional love and support which all of you have shown me during this journey. As always, special thanks to my parents for allowing me to go out there and carve my own pathway in life while constantly supporting me every step of the way, sister Hanna(and soon to be lawyer) for her love and support, and also Grandparents and aunts for their continuous well wishes.

TABLE OF CONTENTS

LIST OF FIGURES

LIST OF TABLES

LIST OF EQUATIONS

$$C = f\lambda \quad (2.1) \text{ –Page46}$$

$$C1 = \sqrt{E(1-V)/\rho(1+V)(1-2V)} \quad (2.2) \text{ –Page46}$$

$$C2 = \sqrt{E/2\rho(1+V)} \quad (2.3) \text{ –Page47}$$

$$\mathrm{V}(t) = S(t) * \mathrm{G}(t) * \mathrm{R}(t) \quad (3.1) \text{ –Page63}$$

$$\mathrm{S(t)} = (fmax\left(\sin\left(\frac{\pi t}{tc}\right)\right)^{3/2}, \ 0 \text{ for } 0 < t < tc \quad (3.2) \text{ –Page63}$$

$$t_c = 4.53\left(4\rho_1\pi\left(\left(\frac{\delta_1+\delta_2}{3}\right)\right)^{\frac{2}{5}}\right) r_1 v_0^{-1/5} \quad (3.2.1)\text{-Page63}$$

$$f_{max} = 1.917\rho_1^{\frac{3}{5}}(\delta_1+\delta_2)^{\frac{2}{5}} r_1 v_0^{6/5} \quad (3.2.2)\text{-Page64}$$

$$\delta_1 = (1-\mu_i^2)/(\pi E_i)$$

$$V(t) = U(t) * I(t) \quad (3.3) \text{ –Page64}$$

$$M = \frac{1}{n}\sum_{i=1}^{n}|x| \quad (3.4) \text{ –Page66}$$

$$M_1 = \frac{1}{n}\sum_{i=1}^{n}|x_1| \quad (3.5) \text{ –Page66}$$

$B_1+B_2+B_3+B_4+B_5+B_6=100\%$ (7.1) –Page111

B_1= can be estimated using PSD model 1 (7.2) –Page111

$B_2 = B_{3456} - B_1$ (7.3) –Page111

$B_3 = B_{456} - B_{12}$ (7.4) –Page111

$B_4 = B_{56} - B_{123}$ (7.5) –Page111

$B_5 = B_6 - B_{1234}$ (7.6) –Page111

$$B_6=100\%-B_{12345} \quad (7.7)\text{ –Page111}$$

$$F(t) = \sum_{t=1}^{n} 2mv_i\delta(t-t_1) \quad (8.1)\text{ –Page126}$$

$$F(t) = 2mvfp \quad (8.2)\text{ –Page127}$$

$$P_{AE}= \eta\frac{F(t)}{\Delta A} \quad (8.3)\text{ –Page127}$$

$$C= \zeta/D^2 \quad (8.4)\text{ –Page127}$$

$$f_p=C\frac{\Delta Av}{\Delta A}=CV \quad (8.5)\text{ –Page127}$$

$$J= P_{AE}\Delta Av=2\eta mv^2f_p=2\zeta\eta f_p= 2\zeta\eta mv^3/D^2 \quad (8.6)\text{ –Page127}$$

$$E=\int_0^T Jdt = \int_0^T \frac{\pi}{3}\zeta\eta\rho_s V3Ddt, \quad (8.7)\text{ –Page127}$$

$$P_D=\sum_{t=1}^{T} x^2_k =E^a_k(D_j) \quad (8.8)\text{ –Page128}$$

$$\sum_{j=1}^{N} \lambda_j P_k^a(D_j)x_j = P_{mix,k}^a, k = K \quad (8.9)\text{ –Page133}$$

$$V(t)=S(t)*G(t)*R(t) \quad (9.1)\text{-Page140}$$

LIST OF ABBREVIATIONS

AE-Acoustic Emissions

PSD-Particle Size Distribution

DOE-Design Of Experiment

P&G-Proctor and Gamble

CPI-Centre For Process Innovation

FBRM-Focus Beam Reflectance Measurement

NIR-Near Infrared Spectroscopy

PAT-Process Analytical Technology

FPGA-Field Programmable Gate Array

Chapter 1

1.1 Introduction

The Particle Size Distribution(PSD) is an important quality attribute of various kinds of particle processing settings that range from granulators, batch agglomeration mixers, coal milling plants, fluidised beds and pneumatically conveyed systems.[1] With the reason for this being that the PSD is a quality attribute that influence the bulk and flow properties of the powders, gives as indication of the level of mixing, can serve as an indication of process efficiency, and can also have an influence on pipe erosion in the case of pneumatically conveyed systems.[2-4]

Procter and Gamble (P&G) require an online PSD monitoring platform in their powder agglomeration process, as it is believed that this will provide a way of monitoring the quality of the powder in-process and provide the future opportunity for process optimisation to take place within the production loop. [5,6] This thesis details the steps taken to design a PSD estimation model which can be used for different types of powders and can be implemented online. The problem will be investigated with using the design space approach supported by the Design Of Experiments (DOE), and it will involve the design of a series of goal driven experiment whose results will be used to comprehend the behaviour of the material in-process and help investigate how the proposed Process Analytical Technology (PAT) can be used to monitor the desired process quality attribute.[7]

1.2 Project Background

1.2.1 Chariot Project

This work was conducted as part of the Chariot project, a partnership focused on creating high value compact products to extend the UK's supply chain reach. The three year project commenced in 2014. It aimed to develop innovations in the manufacturing chain for specialist powders that can be used for a wide range of consumer goods.[1,2] The project was made up of eight partners:

P&G, Centre For Process Innovation (CPI), International Innovative Technologies, Ajax Equipment Limited and the Universities of Leeds, Birmingham, Durham and Cranfield University. The partnership brought together world class research capability to focus on particulate formation, online measurement and analysis. The main motivation for the project stemmed from the fact that the traditional means of washing powder production was not efficient in terms of resources or cost. The Chariot project not only aimed at the formulation of new innovative ways of producing powder but also the subsequent reduction in environmental impact and cost of manufacturing associated with the production. [1, 2] The overall project analysed the milling of powder and particles, and also researched into the effects of new and different finding equipment designs on material properties and performance. The flowchart in Figure 1.1 shows the research themes in the Work Packages and how they feed into each other. The work reported in this thesis results from WP6s, which was focused on the monitoring of the particle changes using acoustic emission.

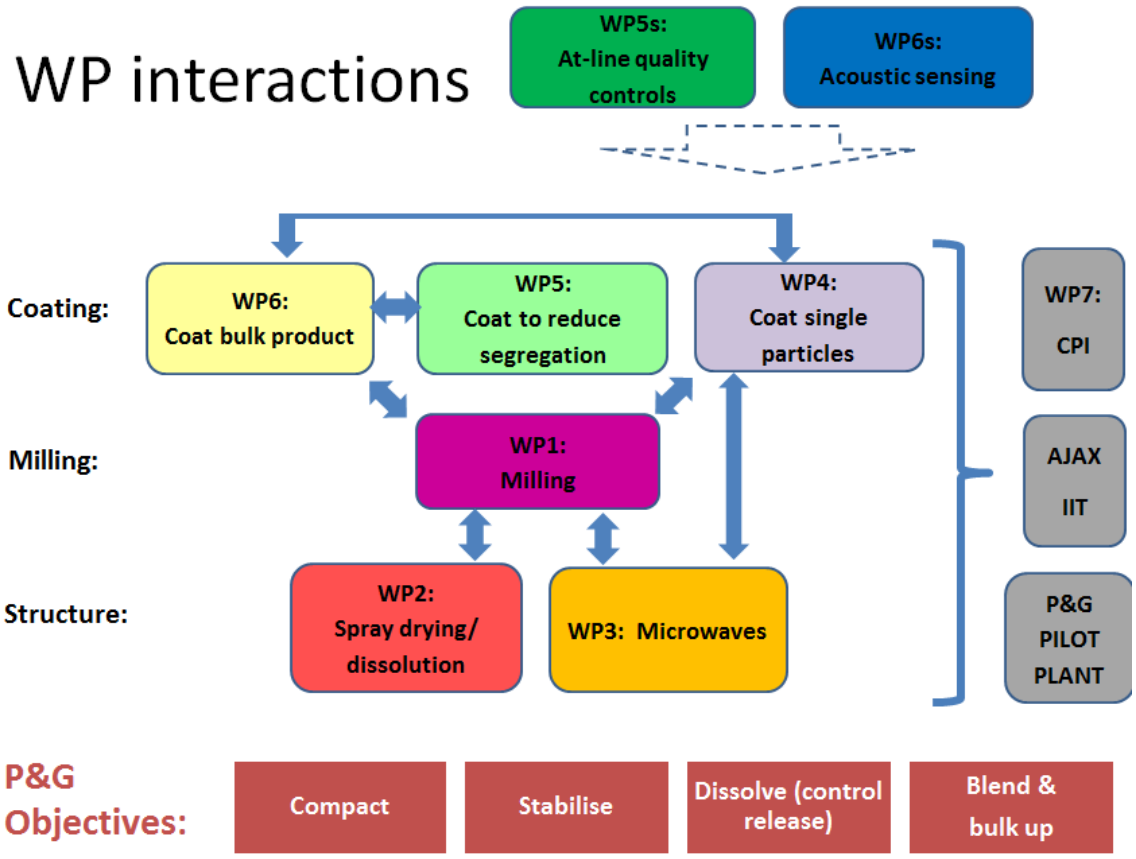

Figure 1.1: Schematic Views Of Work Packages Interactions

1.2.2 Washing Powder Manufacturing Process

The washing powder compound comprises of solids and liquids, the solid materials in the compound include; builders, enzymes, fillers and bleaches. While the liquid materials include; surfactants, perfumes and binding liquid.

During the production process, all the solids are dispensed into a “crutcher”, which is a large reaction vessel and mixer, with an internal temperature of 80º Celsius. Using a spiral screw inside the crutcher, the raw materials are mixed into slurry, which is then discharged from the Crutcher into the drop tank in batches. Aided by a series of pumps, this slurry is supplied continuously to the spray drying tower. Hot air flows into the spray drying tower at a temperature of 400º Celsius, and this in combination with some nozzles converts the slurry into dried “blown powder”. With the means of a conveyor and air lift, the blown powder is transported into the mixing drum - which is the final production phase

before packing. Figure 1.2 shows a schematic representation of the various stages involved in the production of the washing powder.

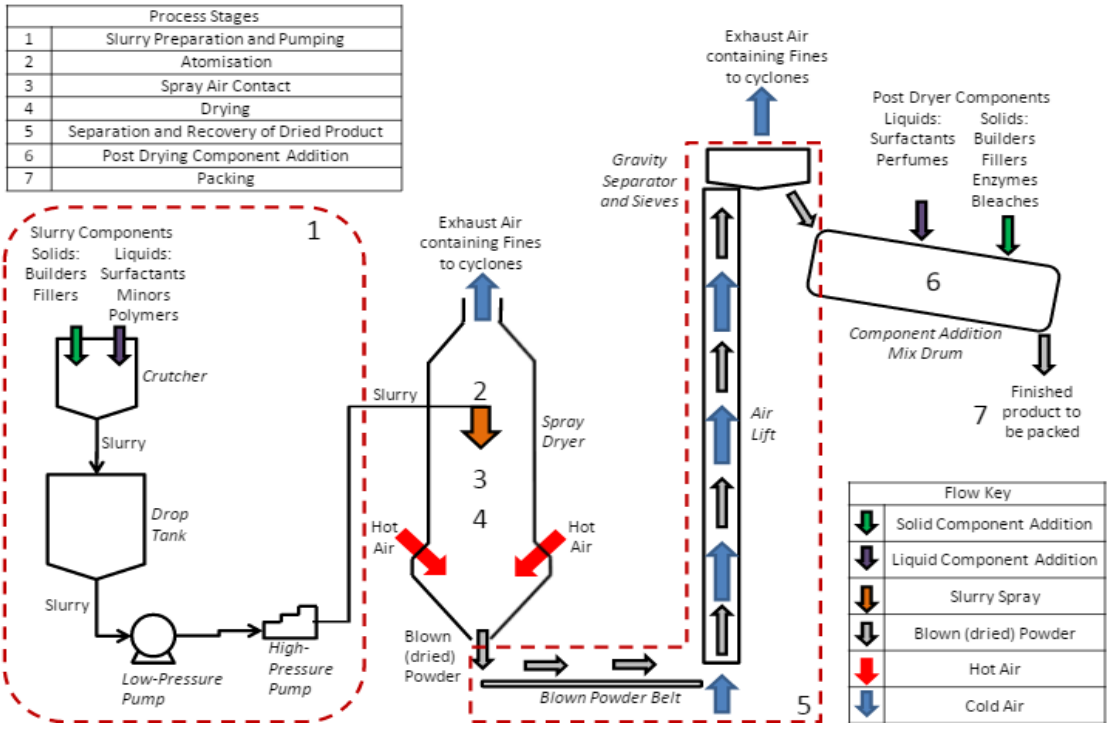

Figure 1.2: Schematic Representation of the Washing Powder Production Process

The mixing stage is where all component materials from all the prior processes illustrated in Figure 1.2 are finally integrated before packaging commences, this stage determines the final physical characteristics of the finished product prior to packing and also presents the final opportunity to perform a product quality check and thus is regarded as the critical phase of production. This area has been of particular focus of this research for this reason. Figure 1.3 shows a picture of a batch mix drum at a P&G plant.

Figure 1.3: Picture of a batch mix drum at a P&G plant

The blown powder, solids (builders, fillers, enzymes and bleach) and liquids (surfactants and perfumes) are simultaneously dispensed into the mixing drum where mixing takes place for 12 minutes. In the 10th minute a non-ionic binder and perfume are added to the mix, after which it is mixed for the final 2 minutes before packaging commences.

1.2.3 Post Production And Proposed Method

The washing powder compound needs to fulfil certain quality standards before they can be sold, in the P&G production setting the necessary quality checks are carried out offline. These offline quality checks consist of a wet chemistry test which involves the analysis of the compound in the liquid phase in order to identify and quantify the presence of various chemicals in the composition which would be typically unmeasurable by physical means, while the physical inspection is done by way of sieving to measure the ratio of “fines”(<500microns) to “oversize”(>500microns) particles from a sample taken out of a finished batch. Both of these offline checks have been described as slow and in the case of the wet chemistry test has been described as expensive. This research is focused on the implementation of real time process

monitoring sensors to measure a physical attribute of the powders that can be used to interpret overall product quality and help provide future opportunity for a closed loop approach to real time process control.

1.3 Aims and Objectives

1.3.1 Aim

For the theme which this research is based around, the PSD was chosen as the quality attribute to be monitored as it is hypothesised that this will give an indication of the flow properties of the powders, extent of agglomeration and also provide a way of assessing the overall efficiency of the powder production chain.[8] Acoustic Emissions (AE) was selected as the sensing tool to use in this research, details of the selection process and justification are explained in chapter 2.

Thus the aim of the research is the design of a method capable of estimating the PSD of various powder mixtures using AE.

1.3.2 Objectives

The associated objectives in achieving the aim of the thesis include;

1. Establish the relationship between AE and particle size
2. Understand the variables which influence the AE
3. Detect variations in the PSD of various mixtures using AE

1.3.3 Key Steps Involved

1. Selection of appropriate sensors and signal processing approach
2. Design and build an experimental bench-top approach to monitor powder samples
3. Process the acquired signal using appropriate algorithms to extract information about the process

1.4 Thesis Outline

The objectives of this thesis are addressed in subsequent chapters as follows;

Chapter 2: this chapter discusses the chosen research methodology and the application of the Design Of Experiment methodology in identifying the key process variables present in the mix drum which were used to design the benchtop experimental rig. A review of the state of the art in particle size measurement was done in this chapter in addition to an explanation of the down selection process and justification of selecting AE, in addition to a review of the work done by previous authors in the field and identifies a knowledge gap and potential contribution to literature which this thesis will be providing.

Chapter 3: this chapter discusses the benchtop experimental design, AE signal source, sensor of choice, theoretical model established by previous authors which links particle size and AE, and how this was used to design a signal processing method which will be used to extract particle size information from an acquired AE signal.

Chapter 4: this chapter is based around the size differentiation of sieved glass beads and polyethylene particles, in order to be able to validate the relationship stated in the theoretical model in the previous chapter.

Chapter 5: covers the estimation of the PSD of different combination of mixtures comprising of the chosen experimental particles using the designed signal processing method and an interpretation of the results of the various mixtures using the theoretical model which describes particle-AE relationship.

Chapter 6: involves experiments which aim to replicate the offline physical quality check procedure at P&G using washing powder and the designed signal processing method.

Chapter 7: details the steps taken to estimate a particle size distribution of the washing powder compound comprising of 6 size categories

Chapter 8: an algorithm comparison case study was carried out in this chapter with a time-frequency based approach used by Ren et al, in order to be able to benchmark the perform of the designed PSD estimation method.

Chapter 9: discusses and concludes the advances made in the area of AE as an online tool for monitoring PSD in powder processes, as well as future work and recommendations in this area

2 Literature Review

This section details the research methodology which will be used to investigate the research problem. A review of various measurement techniques that can be used to monitor particle sizes has been presented, along with a justification of the selection of Acoustic Emissions (AE). This is followed by a review and critical analysis of previous studies in this area, along with the identification of a knowledge gap and potential contribution to literature.

2.1 Research Methodology

Predominantly used in the pharmaceutics, Process Analytical Technology (PAT) involves the identification of Critical Process Parameters (CPP) used to make a certain product, and the understanding of how these affect the Critical Quality Attributes within the specific process limits.[9] The implementation of this framework would allow for consistent product quality in addition to helping to reduce production costs and waste.[9]

There are a number of PAT tools which aid in process understanding and when applied in a process provides a structured pathway for the acquisition of the relevant process information, in addition to continuous improvement and risk mitigation approaches. [9] These tools include; Multivariate tools for design, data acquisition and analysis, Process Analysers, Process control tools and knowledge management tools. [9]This research will be focused on the selection of an appropriate process analyser and effective data analysis tools for the case study being investigated as part of this research.

Implementing a robust PAT system requires an understanding the various physical and chemical properties influencing product quality, as well as knowledge of how these factors vary with alterations in process parameters (e.g. mixer rotating speed and binder addition).

A design space approach is a useful tool for comprehending the interaction between input variables and process parameters, and how they influence final

product quality. [11] This approach aids in understanding how a certain product acts under a range of operating conditions, and is useful in developing a versatile process to deal with variability in input materials and process parameters. [11]

From Figure 2.1, it can be seen that the design space is a subset of the knowledge space. The knowledge space embodies the available process information including regions of possible failure; the design space makes reference to the acceptable operating conditions where the output product is of adequate standard. [10] Further process optimisation could occur in order to narrow a set range of normal operations which is named as the ‘control space’, although operation within the design space region can be treated as acceptable.[10]

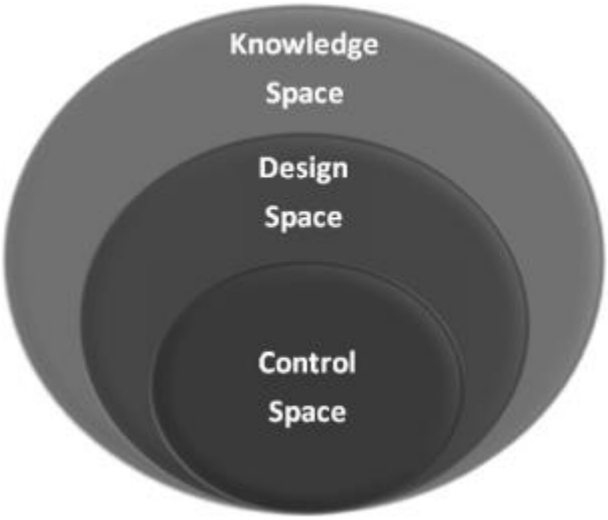

Figure 2.1 Design Space Approach Schematic [10]

Commonly used in conjunction with the design space approach to understand interaction between variables, is a statistical method referred to as Design of Experiments (DOE).[10,12] The DOE works with statistical standards to create goal-driven investigations, which are based on concurrently varying a number of factors in a controlled environment.[10,12]

The investigations are usually a simulation of the real process, involving a number of desired variables. Supporting these investigations with statistics aids in clearly distinguishing between causal and correlative relationships, thereby making it possible to identify the root causes of variability and how they influence the operating process. [10]

This research problem will be addressed with the design space approach and supported by the Design of Experiments (DOE) technique.

2.1.1 Design Of Experiments

2.1.1.1 Introduction

In order to gain better understanding of a process, experiments are designed to assess what inputs have a pivotal influence on the process output and what the expected output of the process should be in various cases.[11]

DOE is a useful tool that can be used to achieve objectives such as machinery inspection notification, output process variation reduction and waste reduction in manufacturing. [11]

2.1.2 Components Of Experimental Design

Using a simple washing powder example as illustrated in Figure 2.2 and following the DOE approach, the three components of an experimental design and their effects are considered.

- **Factors**: otherwise referred to as input parameters, they can either be controllable or uncontrollable. The controllable factors in the experiment are the ingredients (e.g particles) used, the speed of the drum, to name a few. [12] The uncontrollable factors may include external interferences (e.g. temperature).
- **Levels:** this includes the amount of each material used, e.g. the amount of particles dispensed into the mix drum.[12]
- **Response:** this is the final experimental outcome. At the end of the experiment, pivotal outcomes are assessed to determine the factors that

would produce the best overall quality characteristics. In the case of the final washing powder box, a key measurable feature would be particle size.[12]

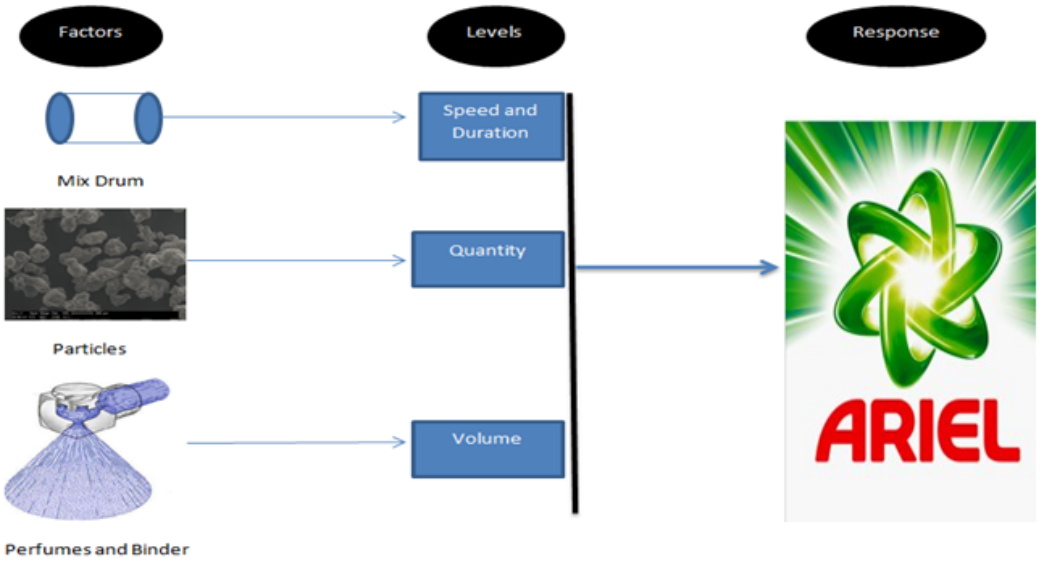

Figure 2.2 Levels of Components of Experimental Design Involved In Making A Box Of Washing Powder

2.1.3 Application Of Design Of Experiments (DOE)

The DOE method has been applied in this research as a factor reduction tool in order to eliminate some non-critical variables present in the factory mix drum, which would make it possible to design a controlled benchtop experimental rig that focuses on the specific factors of interest.

Below is a list of the various process factors present in the mix drum and a supporting justification behind the elimination or reduction of each factor. Table 2.1 shows a list of each factor alongside their associated reduction/elimination equivalent.

Machine Rotating Speed: the machine rotating speed provides the force which sets the particles in motion and allows for mixing to occur, Figure 2.3 illustrates the results of a Discrete Element Modelling (DEM) study

carried out by Yang et al which describes how the increase in the rotating speed of a drum mixer gives rise to a number of flow regimes.[13] During the slumping phase the particles are lifted and dumped in an occasional avalanche like motion, in the slumping-rolling phase the flow begins to show signs of change as the time between each avalanche begins to reduce, in the rolling stage the rotating speed at this point causes an excitation of the particles at the top of the pile as the particles begin to move quickly while the particles at the bottom show signs of slow movement, a further increase in the speed gives rise to the cascading regime while an additional increase induced the cataracting flow pattern where the particles move at a high enough velocity to be hurled off the bed of particles and interact freely with the wall of the mixer, in the final phase which is regarded as the centrifuging stage, the particles adhere to the walls of the mixer to the strong centrifugal forces caused by the high mixing speed. [13]

The experimental rig which will be designed for use in this research will be based around the cataracting stage of the mixing, as this has been viewed as the stage of mixing where the particles obtain maximum attainable velocity and produce particle wall interaction in free flow before the mixer speed increases and the particles adhere to the walls of the mixer due to the strong centrifugal forces present in the centrifuging regime. [13] It is also worth noting that at the cataracting flow phase, the fluid number which can be described as the ratio of the inertia to gravity force in a flow, is less than 1 at this point.

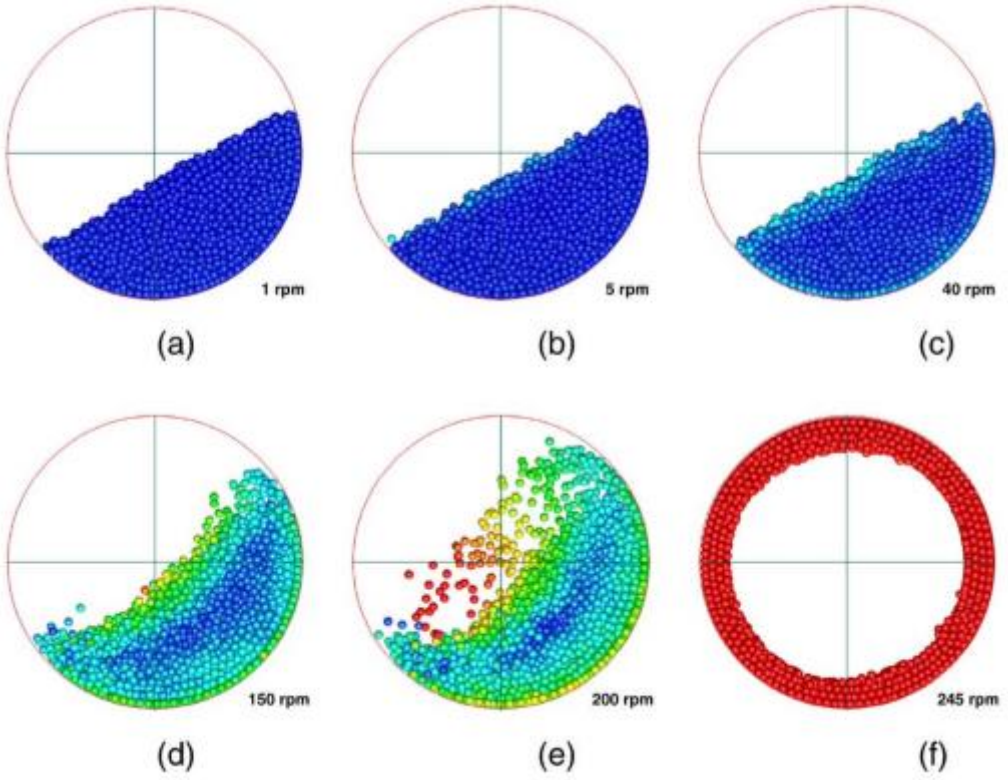

Figure 2.3: Picture illustrating the Discrete Element Modelling (DEM) results illustrating various flow patterns in a mix drum (a=slumping, b=slumping-rolling, c=rolling. d=cascading, e=cataracting, f=centrifuging) [13]

- Flow rate: in the mix drum, in addition to the PSD of the particles, the flow rate is primarily influenced by the mixer rotating speed and the amount of the agglomeration binder present. This suggests that flow rate variations would be present during the mix process as the powders combine for a fixed duration before the binder is added to the mix later on during the mix cycle. To simplify the experiment, one flow rate will be used for all experiments. A funnel will also be used to ensure that the powder flow rate is constant for all experiments. During the funnel selection procedure, various funnels were tested. The majority of funnels gave a constant flow rate, but it was seen that certain funnels produced a bimodal flow rate in a random sequence. The funnel which produced a unitary flow rate and allowed for powder free flow without blockage was

selected as the candidate funnel for the experimental rig. The candidate funnel produced a dispensation rate of 19.3g/s.

- Binder: a liquid is used during the mixing process as a binding agent to enable the particles agglomerate. As this work is based around the PSD estimations of powders in free fall and not agglomeration, this experimental factor has been eliminated and will not be included in the experimental setup.

- Particle impingement body: the inside of the mix drum which the particles impinge on during mixing is made of aluminium, therefore an aluminium plate of uniform thickness was selected as the particle impingement body.
- Mix duration: as the benchtop experimental rig will be setup to monitor powder flow dispensed through a funnel and not a mixing process, the experimental factor becomes inapplicable in this case and can thus be eliminated.

- Particle Number: there are 15 different types of particles in the washing powder compound which was used in the laboratory-based experiments conducted, so for each experiment where washing powder was used, the 15 constituent particles were present in the mixture. In other experiments where we wished to have a more controlled investigation, this number was varied systematically depending on the aim of the experiment and involved the use of glass beads and polyethylene particles. A microscope image of the washing powder particles can be seen in Figure 2.4.

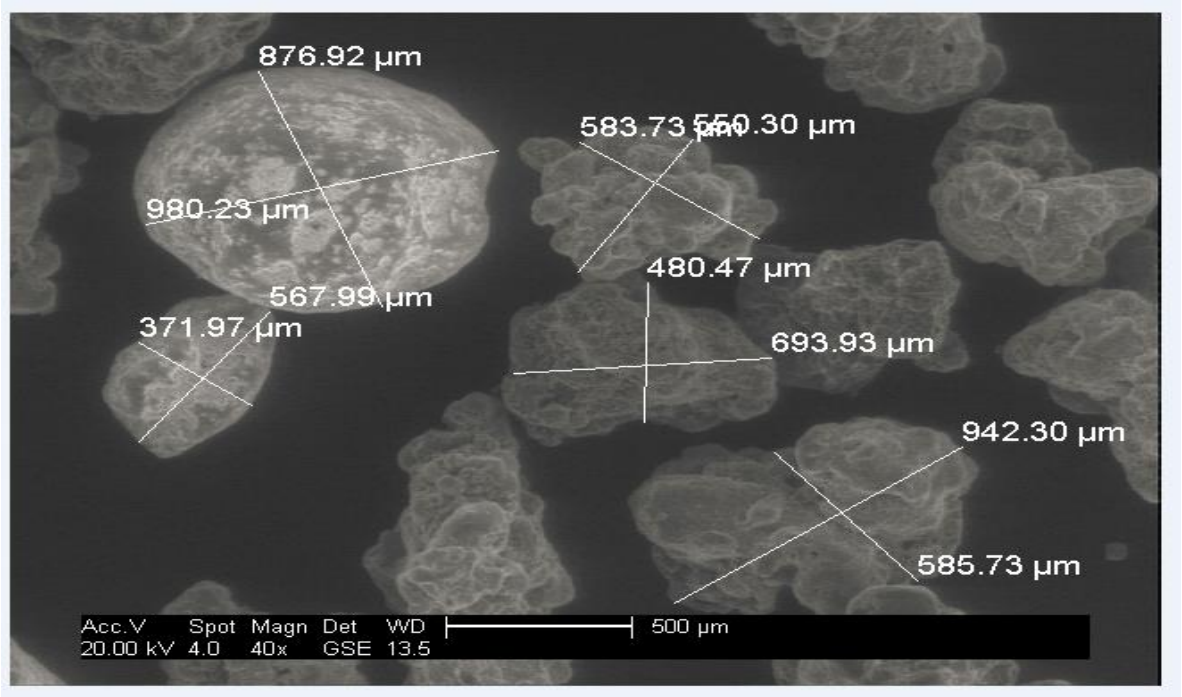

Figure 2.4: Microscope Image of Washing Powder Particles

- Machine noise: as these investigations to be carried out are based on the free flow of powders dispensed through a funnel, there will be no rotating components in the experimental rig and therefore machine noise would not be present.

Table 2.1: Table Showing the Various Process Variables in the Mix Drum and Their Respective Reduction Equivalent

Process Variable	**Reduction Equivalent**
Machine Rotating Speed	Free fall with gravity
Particle Number	Number varies depending on experiment
Binder addition	Factor eliminated
Particle impingement body	Aluminium plate of uniform thickness
Mix duration	Factor eliminated

Flow Rate	One constant flow rate
Machine noise	Factor eliminated

2.2 Particle Size and Particle Size Distribution

The term ‘particle size’ typically describes diameters of spherical approximations to particles that typically range from nanometres to millimetres.[1] The particles produced by most real life particle-processing plants tend to vary in size - which means they are polydisperse, therefore it is useful to not just measure the particle sizes but also to establish the Particle Size Distribution (PSD) in a process.[1] The PSD of a mixture of particles is an important quality check factor as this influences the bulk and flow properties of the particles.[8] This has thus led to the development of various particle monitoring technologies which are detailed in section 2.3.

2.3 Process Analytical Technology Used In Particle Size Monitoring

An array of sensing methods exists for monitoring the particle mixing process both intrusively and non-intrusively, with each type of sensor having its own unique signal processing method.[10] The following are a list of widely used sensor technologies for monitoring particle sizes in powder processes:

-Sieving and Weighing: this is the simplest and oldest form of particle size analysis and involves the sorting of particles on the basis of their size, irrespective of their other physical properties. [17] A typical sieving process consists of placing a known mass of powder on a sieve with a known aperture size and providing an impulse to the sieve in order to allow the particles pass through the sieve apertures. [17] In certain cases, sieves containing different aperture sizes are stacked on each other and regarded as layer sieves, which

are quivered until the particles begin to go through the respective apertures in the different sieve layers and stop when they reach an aperture which they cannot pass through.[17] The amount in each sieve layer is weighed at the end of the process and calculated as a percentage of the total mass of the particles put in the sieve and used to form a PSD.

-**Electrostatic Sensing**: this sensing method is based on the principle of particles emitting electrostatic charges as they interact with each other in-process; with a working electrode and appropriate signal processing method, information on particle size can be uncovered.[18] Working in a pneumatically conveying particle setup, Zhang et al applied a time domain analysis approach to obtain a particle size indicator of the electrostatic signal produced by the particles with a constant mass flow.[18]

-Imaging: this technique involves the use of image processing techniques to estimate particle sizes in-process using a camera. The images obtained are first converted into binary before a pattern extraction technique is used to separate any possible granule overlap prior to particle size and shape calculation.[10,19] Watano et al used an image processing system to detect the endpoint for both a fluidised bed and a shear granulator.[10,19] The images were acquired using a Charge Coupled Device (CCD) camera and supported with an optical fibre for lighting and an air purge to prevent powder adhesion.[10,19] The image sensing unit was positioned above the fluidised bed chamber and the acquired images were pre-processed using a circle pattern matching algorithm to reduce granule overlap.[8] Upon calculation of the size and shape of the particles, some correlation was observed with a sieve analysis. The disadvantage of imaging is that the probe is large and equipment modification is required to position the probe inside the vessel. In addition, considerable expertise is required to develop a robust control system. [10,19]

-Near Infrared Spectroscopy (NIR): this concept is based around the absorbance of light with the molecular vibration of hydrogen bonds.[11] Water is easily absorbed in the NIR region (1400-1450nm) which is where the first overtone (molecule moving from ground state to excited state) in the OH stretching band is located, as well as in the 1900 and 2000nm region which consists of OH stretching and OH bending bands.[15] Particle physical features such as size and density influence the amount of light reflected back[15]. The primary downfall of this technique is the heavy equipment calibration associated with the equipment prior to use as well as the complex analysis methods involved in isolating the features of interest.[15]

-**Focus Beam Reflectance Measurement (FBRM):** a compact FBRM device comprises a laser beam attached to the top of a probe with the aid of an optical fibre.[20] It is assumed that the beam would rarely pass through the centre of the particles; therefore measurements are referred to as chord lengths instead of diameters.[20,21] It works on the principle that once a beam touches a granule, by finding the product of the velocity of the beam and the duration of the light reflected back, the length of the particle chord length can be determined.[21] With the FBRM thousands of chord lengths can be acquired per second. These measurements are used to form a chord length distribution from which particle sizes can be estimated online, but the main downside of this technique is that the measurement probe must be placed into the material of interest and cannot measure anything more than 2mm away.[10]

-Vibration: with the aid of an invasive vibration probe comprising an accelerometer behind a concave target plate, Stantiforth et al used vibration to monitor particle size growth in a high shear granulator and planetary mixer. In the case of the high shear granulator, the root mean square of acceleration was related to the granule conditions and could be used to track granule size growth and detect an end point.[14,16] For the planetary mixer, the peak velocity and

peak to peak displacement readings corresponded to evolution in the particle size distribution of the granules and increments in their densities.[14,16] The challenge with this monitoring method lies in the establishment of a relationship between the size of the particles to the acquired vibration displacement.[15,16]

-Acoustic Emissions (AE): both the audible and ultrasonic domains have been applied to monitor particles in-process.[10] The sources of the emissions have been thought to emanate from either a particle-particle contact or particle-equipment contact.[22] AE has the ability to work online and does not require direct contact with the product of interest or any form of equipment modification, with the only form of contact required being the mounting of the sensor on the particle processing equipment.[10] Due to this setup arrangement, the AE signals are reflective of the whole process and not a specific localised area. Another advantage of AE sensing is the fact that ultrasound waves (high frequency sound) disperse well through solid bodies (process equipment) and poorly through air, which may suggest that the bulk of the AE signals acquired would emanate from the process being monitored and would be free from audible background noise.[10,22,23]

In addition to monitoring particle size, AE has been seen to be able to monitor process transition, particle density and flow rate.[8] The main challenge with the technique remains the establishment of a relationship with signal processing algorithms capable of extracting information about particle size and process behaviour from the acquired AE signal.[10]

A summary of the different monitoring methods taken from various case studies can be seen in Table 2.2.

Table 2.2: Various Particle Size Measurement Sensing Methods

Monitoring Method	**PSD range**	**Sensor Placement**	**Reference**
Electrostatic Sensing	100-1000 microns	Non-invasive	[18]
Imaging	250-1000 microns	Invasive	[17][24]
Near Infrared Spectroscopy(NIR)	37-1000 microns	Invasive	[25-27]
Focus Beam Reflectance Measurement(FBRM)	1-1000 microns	Invasive	[28-31]
Vibration	38-150 microns	Non-invasive	[32]
AE	63-1200 microns	Non-invasive	[3,4]
Sieving and Weighing	5-1000 microns	n/a	[33]

2.4 Acoustic Emissions

This research is based on the use of acoustic emissions in the extended ultrasonic region to monitor the PSD of the washing powder during mixing. Apart from being a non-invasive monitoring method, due to the small size (53-1500 microns) of the particulates being monitored and noisy production area,

acoustic sensing in the ultrasonic region will be investigated because of its insensitivity to audible background noise and has also been seen to possess primary sensitivity to frequencies at which particulate events occur.[22]

'Acoustics' is a compound term used to define how vibrational waves are generated, transmitted and received. In particles, vibration waves can either be parallel or perpendicular to the wave direction.[36] Both can be characterised with the wave equation as can be seen in equation 2.1.;

$$C = f\lambda \quad (2.1)$$

Where *C* = speed, *f* = frequency, and *λ*=wavelength

The speed depends on the elastic properties and the density of the propagation medium, while the frequency is a direct reciprocal for the duration for one sinusoidal cycle tone.[36] For mixing processes, AE are understood to originate from particle-particle, particle-wall contact, in addition to the friction generated by contact and flow.[22]

2.5 Impact Dynamics and Elastic Waves

As structural borne AE signals are going to be acquired in this research, it is important to understand the phenomena of impact dynamics and the resulting elastic waves dissipated. During any impact, contact bodies generate elastic waves that radiate away from the contact region, and these elastic waves are either propagated in a longitudinal or transverse direction as shown in Figures 2.5 and 2.6.[34] Their velocities are independent and can be expressed as seen in equations 2.3 and 2.4.

$$C1 = \sqrt{E(1-V)/\rho(1+V)(1-2V)} \quad (2.2)$$

$$C2 = \sqrt{E/2\rho(1+V)} \quad (2.3)$$

Where *C1* = longitudinal waves, *C2* = shear waves, ρ= density, *V*=Poisson's Ratio, *E* = Young's Modulus

A third type of wave also exists, called a Rayleigh wave, in semi-infinite media. Figure 2.7 shows an image of a typical Rayleigh wave.

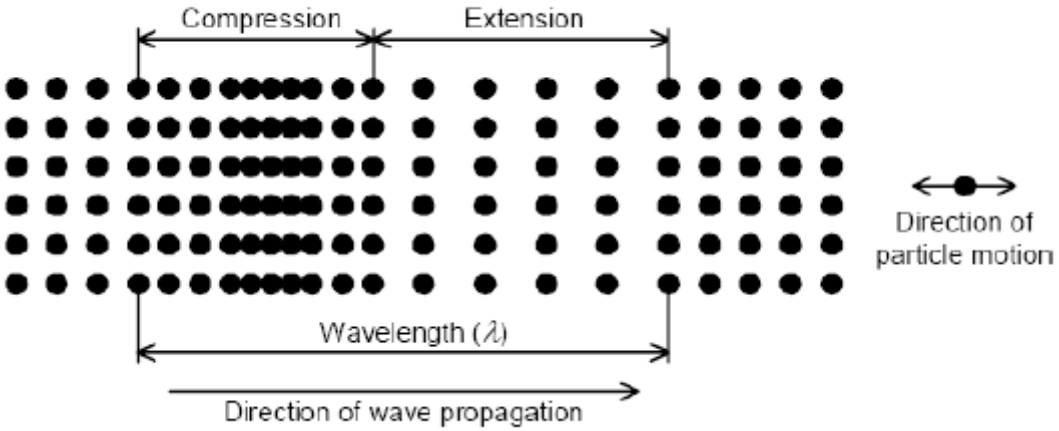

Figure 2.5: Longitudinal Wave [34]

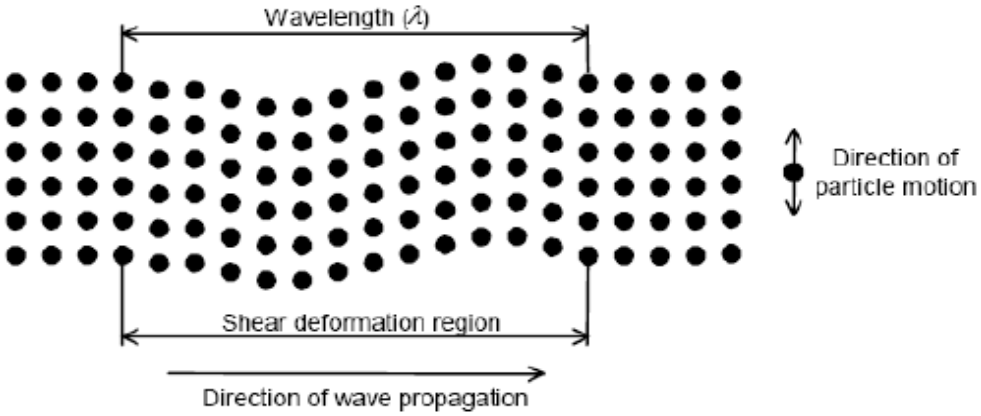

Figure 2.6: Transverse Wave [34]

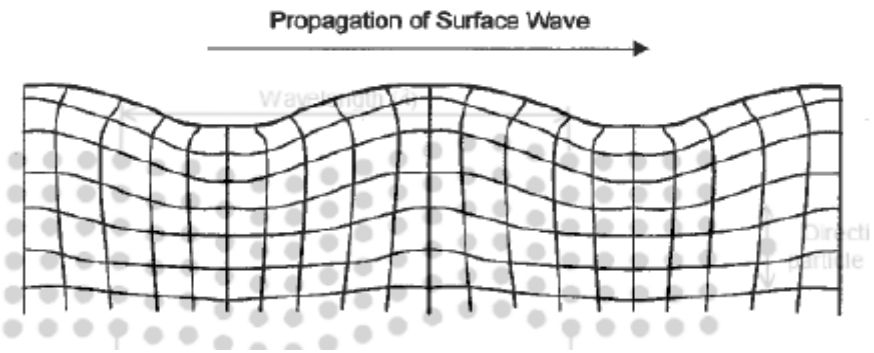

Figure 2.7: Rayleigh Wave [34]

For infinite mediums bounded by two surfaces (aluminium plates, for example), more sophisticated propagation modes are produced and are called Lamb waves. The two common Lamb wave mode types are called symmetric and asymmetric wave modes, both of which can be seen in figures 2.8 and 2.9.

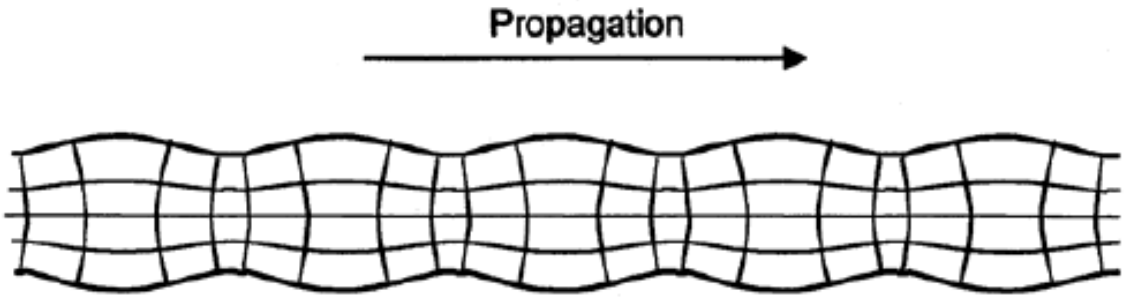

Figure 2.8: Symmetric Wave Mode [34]

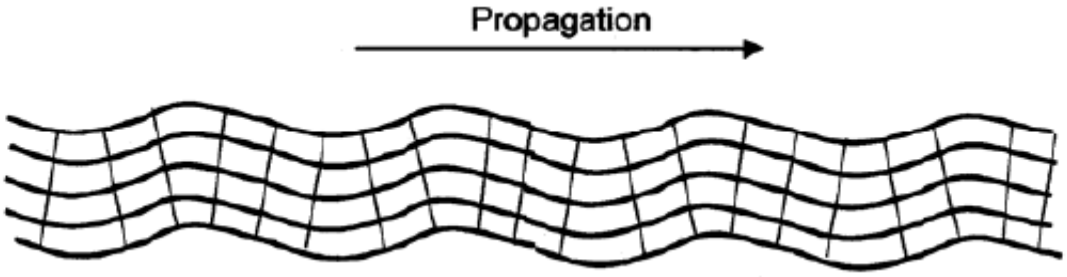

Figure 2.9: Asymmetric Wave Mode [34]

The impingement particles move in an elliptical manner in Lamb waves and the amplitudes of the motions both parallel and perpendicular to the impingement

medium (plate) depend on mode and frequency in a rather complicated manner.[34]

Hunter solved the force-time equation for the scenario of an elastic deformation around an indentation, in the investigation of the energy absorbed by elastic waves upon impact, under the assumption that the elastic impact occurred at right angles to the surface and by means of the Fourier components of a normal transient force.[34] It was seen that upon impact of a steel sphere on a steel target plate, the energy converted into elastic waves is less than 1% of the total incident kinetic energy.[34]

2.6 Analysis Of Previous Work

The literature shows that Leach and Ruben were the pioneers in using acoustic emissions in the sizing of particles. Using an ultrasonic condenser microphone and a rotating drum as can be seen in Figure 2.10, the relationship between the particle size and the resulting acoustic emissions for glass and metallic spheres ranging from 50 microns to 3cm was investigated.[37-39]

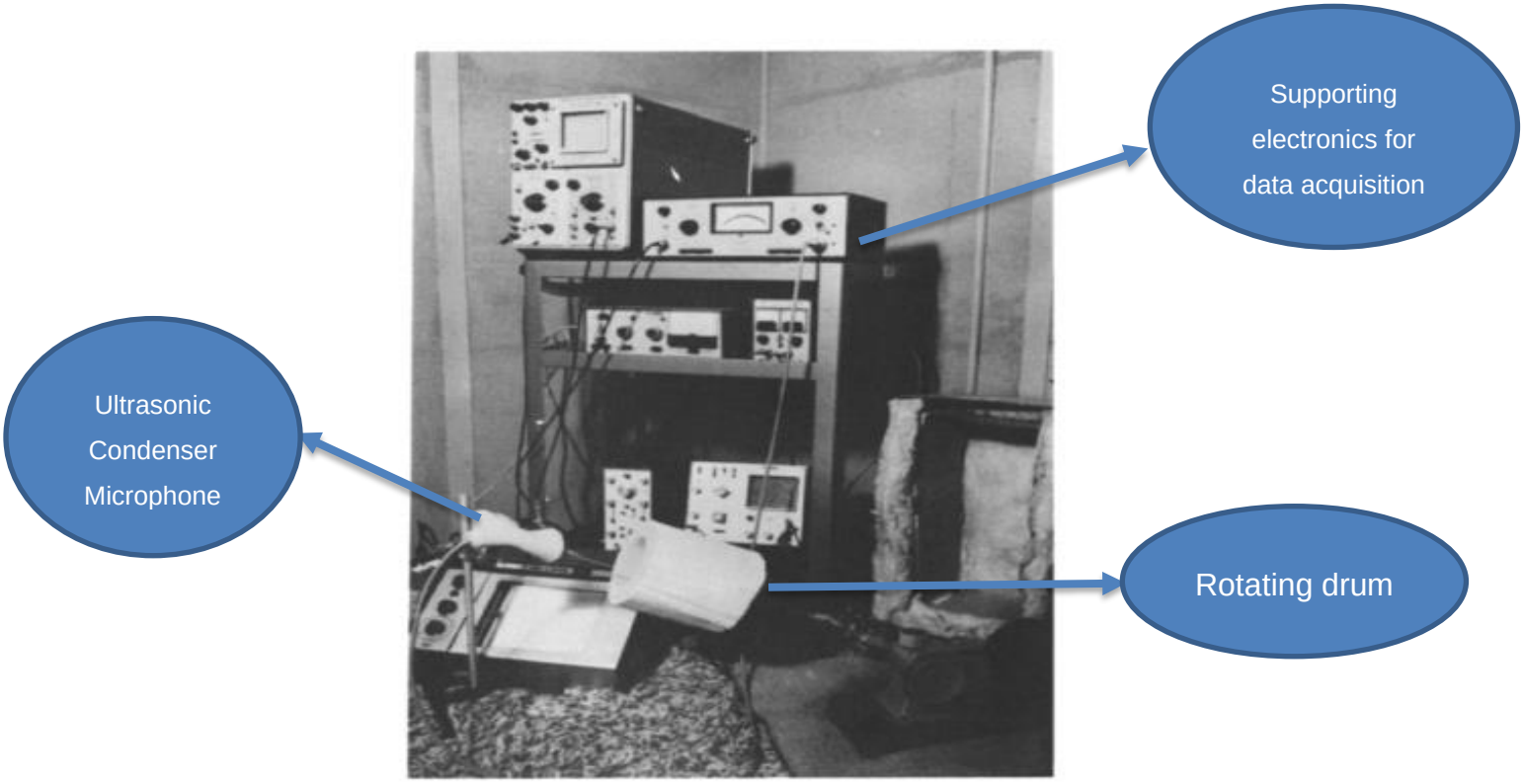

Figure 2.10: Experimental setup showing white drum and condenser microphone [37]

Buttle and Scrubye et al proposed a quantitative particle sizing approach with AE Sensors to monitor spherical bronze and glass particles dispensed on an aluminium target plate.[38] Using a de-convolution technique, particle size information was extracted from the resulting AE signal. With an understanding of the origin, propagation and acquisition of the signal, this method, known as quantitative acoustic emission analysis, can be used to uncover particle information, although this method is unlikely to work in a practical setting as aside from the de-convolution required, it would struggle to work where signals are susceptible to noise and the particle impacts overlap.[40,41]

Papp et al used multivariate data analysis to investigate the relationship between various physical properties (size, moisture content) of the particles and the steady evolution of the AE taking place during their formation for two different granulators offline.[8,42-45] Acoustic Emission sensors were mounted on the outer wall of each granulator, which comprised a bottom driven impeller and a side driven chopper.[8] For the duration of each granulation process, the impeller and chopper were operated at 250 and 1000rpm respectively. It was observed that any frequency peaks that are present at the beginning of the granulation process remain present till the end of the process.[8] Papp's results suggest that the AE frequency has an inverse relationship to the particle size being impacted.[8] Thus, the assumption then becomes that the decrease in the average frequency can be correlated with the granule growth during the process.[9] Bastari et al and Chen et al used a data driven approach based around trained neural networks to estimate particle sizes, but as the system is based on a neural network, the decision making process is not completely understood.[3,46]

Hybrid signal processing methods were adopted by Hu et al and Ren et al. Hu et al utilised a time domain based amplitude threshold approach to help classify particles of different sizes but the method was seen to be inaccurate in

classifying particles under 90 microns.[41,4] Ren et al used a wavelet based algorithm to estimate the sizes of different particles but due to the nature and calibration of the signal processing method, the designed model would not be adaptive enough to work in settings where powder mix ratio varies significantly.[4] In terms of audible acoustics, Hansuld et al was able to track the various phases and end point of a granulation process using a condenser microphone and conducting a frequency domain analysis of the audible acoustic signal.[10] Briongos et al used audible acoustics in a fluidised bed, and found that only a state space analysis technique was able to identify various phases during the mixing process.[43]

2.7 Summary Of Previous Work and Knowledge Gap Identification

From the literature uncovered, there is enough evidence to suggest that particle sizes can be monitored using AE. The quantitative particle sizing approach used by Buttle et al would be incapable of working in an industrial environment due to the deconvolution steps required to estimate particle sizes.[40] Bastari et al and Chen et al applied data driven signal processing approaches that included the use of a trained neural network to estimate particle sizes, but as the method used was a data driven approach, it would not be sufficient in this research as a measurement system whose decision making process can be understood is required.[3,46] A time domain threshold based particle sizing approach was developed by Hu et al to estimate particle sizes but his model was unable to detect particle sizes under 90 microns, and this was attributed to the overall noise in the experimental setup.[41] The wavelet based algorithm proposed by Ren to estimate particle sizes in a fluidised bed, relied heavily on the calibration stage which requires a tuning process.[4] This suggests that the model is unsuitable for processes in which the final particle mix ratio varies significantly.

It would appear from the uncovered literature that there does not exist a hybrid particle sizing approach sensitive enough to work in a process where the final

particle mix ratio varies. This is important for the case study being investigated in this research, because the sponsor company is interested in measuring PSD deviation in real time. Therefore in this research, a hybrid signal processing particle sizing method, that can be used in powder processes and is sensitive enough to detect significant PSD variations, would be a significant advantage. This appears to be the knowledge gap from the literature and would form the body of knowledge being contributed to the literature by this research.

2.8 Conclusion

In this chapter, the research methodology which will be used to investigate the research problem has been outlined. A range of sensors capable of monitoring particle sizes has been reviewed, and AE was chosen as the particle monitoring technique to be used due to being non-invasive, insensitive to background noise and possessing primary sensitivity to regions which particle events emanate. Related works in this area of applying AE for particle size monitoring have been reviewed and critically analysed and it was seen that there does not exist a hybrid particle sizing approach sensitive enough to work in a process where the final particle mix ratio varies. Therefore the design of a hybrid signal processing particle sizing method that can be used in powder processes and is sensitive enough to detect significant PSD variations, is the key aim in this research.

3 Experimental Rig Design

3.1 Introduction

This chapter discusses the design of the benchtop experimental rig capable of monitoring powder free and the data analysis procedure and signal processing method which is based on a theoretical model which show that Acoustic Emissions (AE) carry sufficient information required to estimate the sizes of particles.

3.2 Experimental Setup

With the application of the Design Of Experiment(DOE) as detailed in section 2.1.3, the experimental rig has been designed around the cataracting flow regime which is the final phase where the particles are in motion and impinge against the mixer wall and particle velocity is at maximum shortly before they become attached to the mixer wall due to the heavy influence of the centrifugal force in the centrifugal flow regime phase.[13] The concept which the experimental rig has been designed around suggest that the work done in this thesis will primarily be applicable in processes where the cataracting flow regime or equivalent exists and the fruid number of the flow is less than 1.

The experimental rig used in this research was based on the dispensation of a known mass of powder at a known rate, from the funnel placed at a known height, which fell freely under the force of gravity to a target plate to which an AE sensor was attached. A diagram of the final experimental rig and a picture showing the sensor placement can be seen in Figure 3.1 and 3.2.

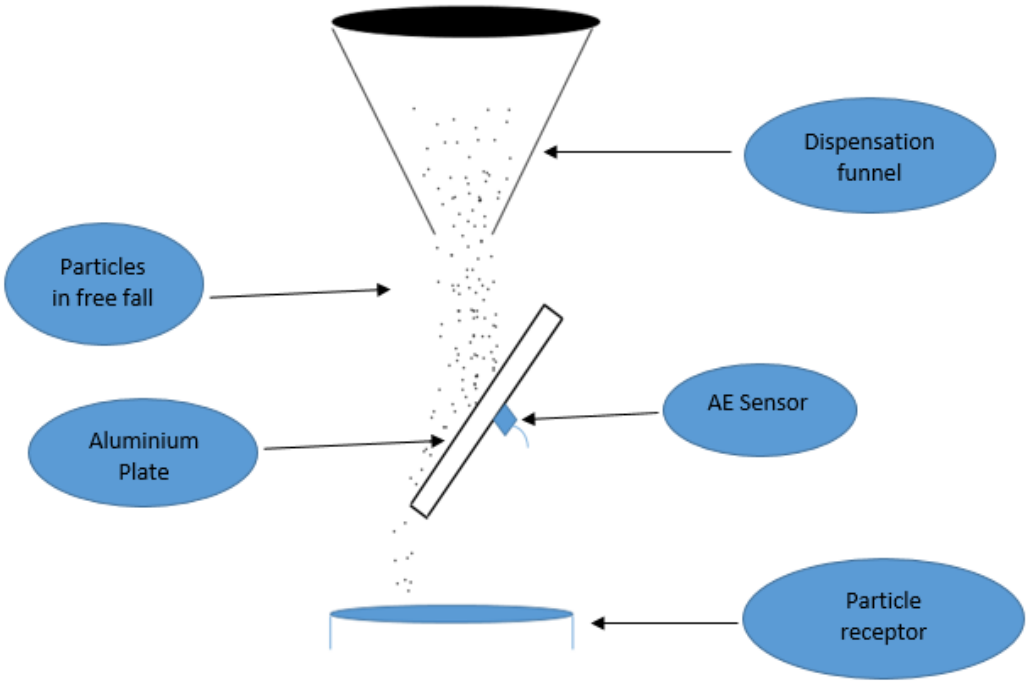

Figure 3.1: Experimental Setup

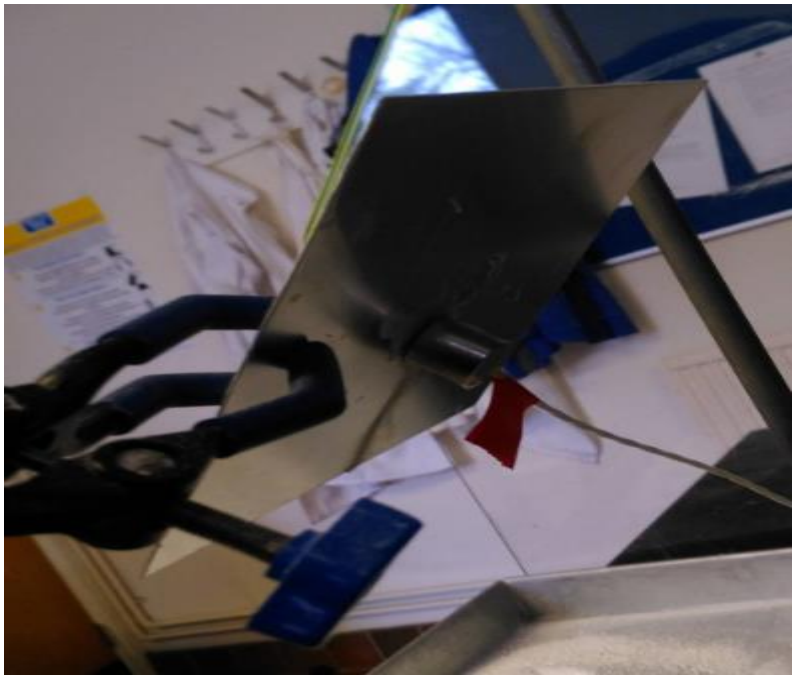

Figure 3.2: Placement of the sensor

The aluminium plate sheet chosen as the target plate comprises dimensions 11x18x8cm with a density of 2.7g/cm^3, Poisson's ratio of 0.35, young's modulus of 69GPa and a uniform thickness of 0.7mm, with the AE sensor attached to the back of the plate using beeswax adhesive as can be seen in Figure 3.2, was inclined at an angle to prevent build-up of powder in and around the impact area. The funnel was chosen as a source of powder dispensation as it was seen to be capable of producing a repeatable source of powder dispensation and would not produce any form of external interference to the AE signal which is being acquired. [47] Experiments were carried out which involved the variation of the height of the funnel in order to determine the final height from the target plate as the impact velocity of the particles is an important parameter which influences the resulting AE signal of the impinging particle.[47] Before the final height was set, the funnel height was varied until a height was reached where particles were distinguishable and the flow rate was repeatable. The final chosen height was 12cm and theoretical studies carried out by Pecorari et al with similar particles, a model that accounted for air viscosity and a drag co-efficient of 0.5 suggested that this height is sufficient for the particles to attain terminal velocity before impact.[48] The funnel dispensation aperture was 2cm in width and the surface on the plate which most of the impacts took place on can be estimated to be 36cm^2. An example AE signal obtained from a washing powder sample can be seen in Figure 3.3. From the AE signal in Figure 3.3 it can be noted that the impact peaks are of highly varied heights, this is because the washing powder compound is a heterogenous powder mixture and comprises of wide distribution.(53-1500microns)

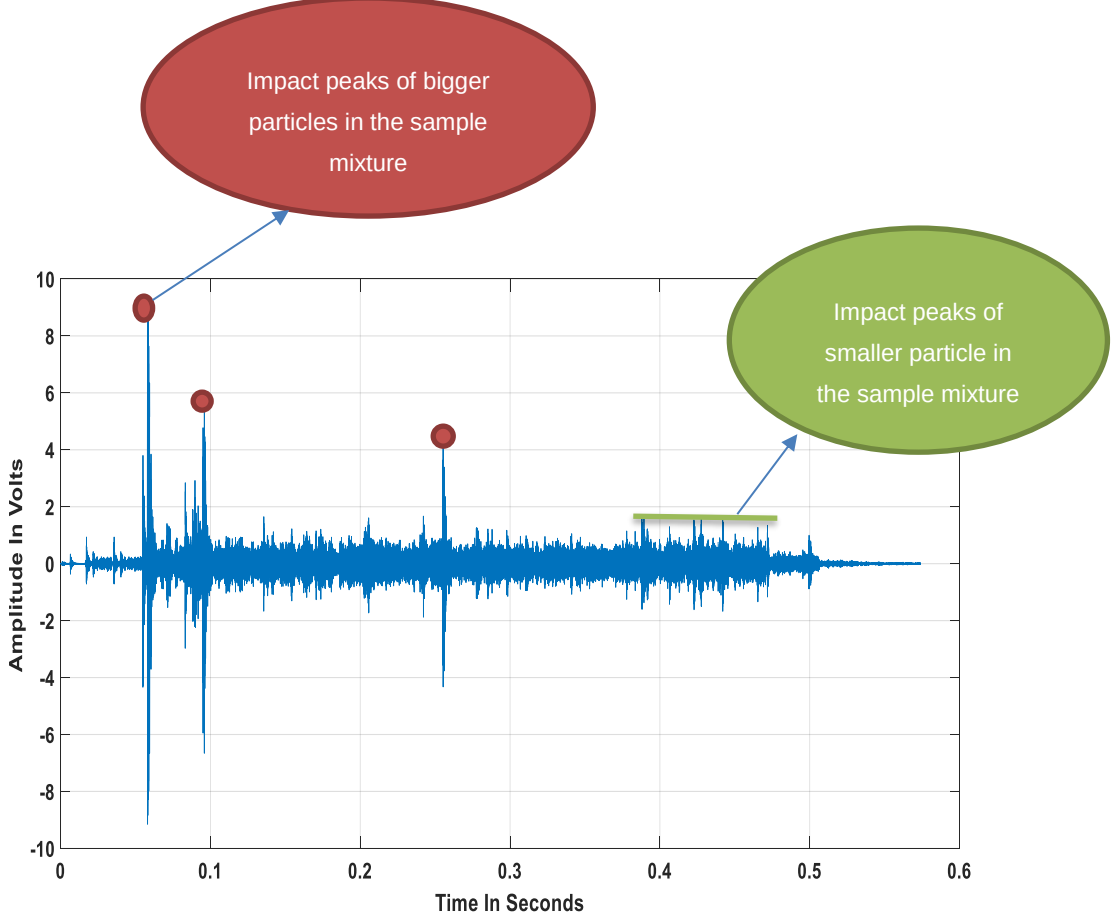

Figure 3.3: Sample AE Signal Of Washing Powder

3.3.1 AE Signal Source

In this study, the source of the AE waves are thought to emanate from the dispensed particles impacting the aluminium plate which serves as the wave propagation medium for the acoustic stress waves generated by the particle impacts.[40,48] These waves are then recorded by a structural borne AE transducer attached to the back of the plate and the resulting signal from waves of these kind are typically of a low amplitude and thus possess high frequency characteristics.[49] The simultaneous impacts caused by the particles hitting the target plate, produce an AE signal which consists of overlapping burst events which can be characterised by their amplitudes and correlated to particles of a certain size.[41]

3.3.2 AE Sensor

The sensor used was the PCI-2 Physical Acoustic sensors by Mistras.[50] The sensor bandwidth spans 100K-1MHz and a sampling rate of 1Ms was used during the acquisition. Figure 3.4 shows the block diagram of the signal processing

chain. The acquired signal goes through a preamplifier before being sent through a filter. This filtered signal is sent to the Analogue to Digital Converter where it is digitised and passed to a Field Programmable Gate Array (FPGA) where sampling and signal averaging takes place. The final digitised waveform is continuously streamed to the hard-disk of the computer.

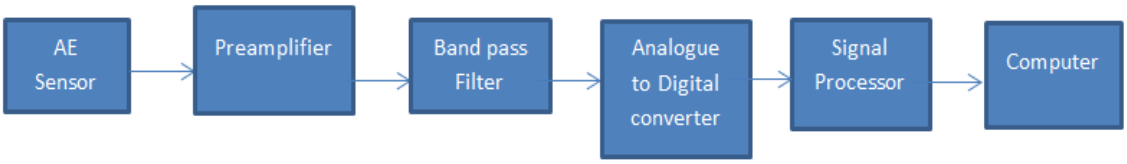

Figure 3.4: Block Diagram Of The Sensor Signal Processing Chain [50]

3.4 Experimental Particles

By applying the DOE sequence, two sets of particles were chosen for the experimental work in this research.[11] Glass beads were chosen to represent the washing powder particles with a regular geometry and high density, while polyethylene particles were chosen to represent the irregular sized particles in the washing powder compound with low density. Microscope images of the glass beads and polyethylene particles can be seen in Figures 3.5 and 3.6 respectively.

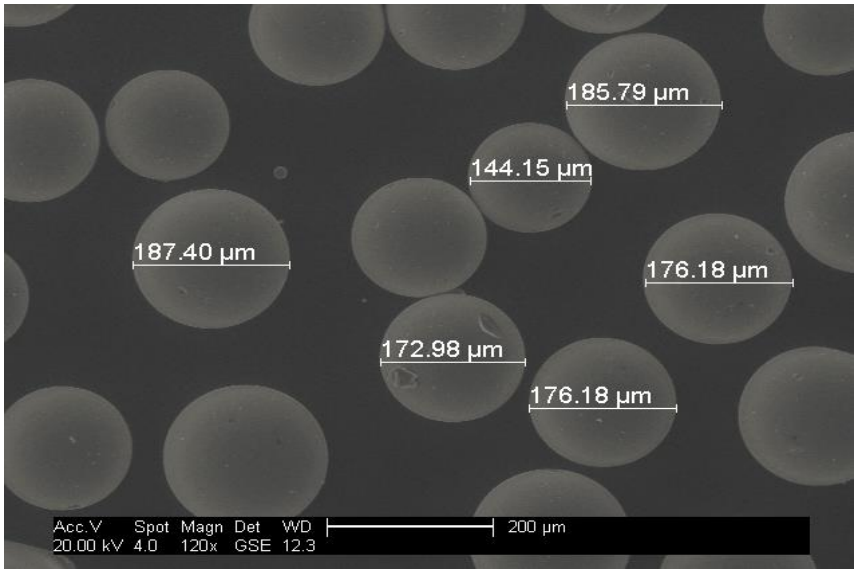

Figure 3.5: Microscope Image Of Glass Beads Particles

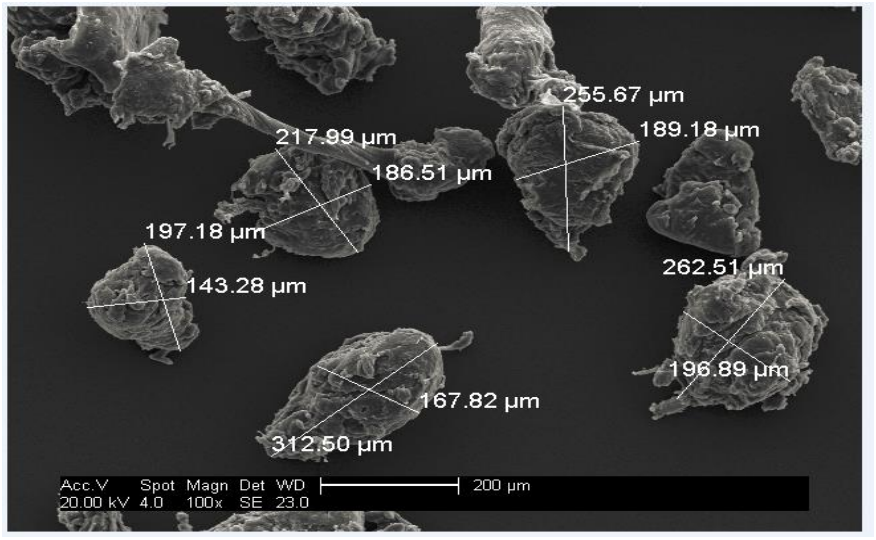

Figure 3.6: Microscope Image Of PE Particles

3.5 Rig Repeatability Tests

To ensure that the experimental funnel produced a repeatable flow rate for different powder mixtures, the dispensation rate was measured for different powder mixtures using two sets of glass beads. The experimental funnel was hung from a Honeywell model 31 Low Range Precision Miniature Load Cell capable of measuring between 50g-500g which was used to measure how the mass in the funnel varied over time.[51] Details of the glass beads and the mix ratios used for the experiments can be seen in Tables 3.1 and 3.2.

Table 3.1: Glass Beads Details

Class 1/Small	150-212 microns
Class 2/Big	425-600 microns

Table 3.2: Powder Mix Ratio Table

Class 1 Particle Percentage	**Class 2 Particle Percentage**	**Experiment Repetition**
100%	0%	4

80%	20%	4
60%	40%	4
50%	50%	4
40%	60%	4
20%	80%	4
0%	100%	4

For each experimental run, a known mass of powder was loaded into the funnel and allowed to flow out freely while the load cell monitored how the mass of powder in the funnel changed with time. The load cell was supported with an acquisition programme in Labview and a sampling rate of 10KHz. This sampling frequency was chosen in order to ensure enough data points were acquired during each experimental run in order to be able to fit a curve that can be relied on.

For each experimental repetition, data was acquired for 5 seconds - the graph in Figure 3.7 shows a sample Load-Time plot for a 60/40 mix ratio experiment.

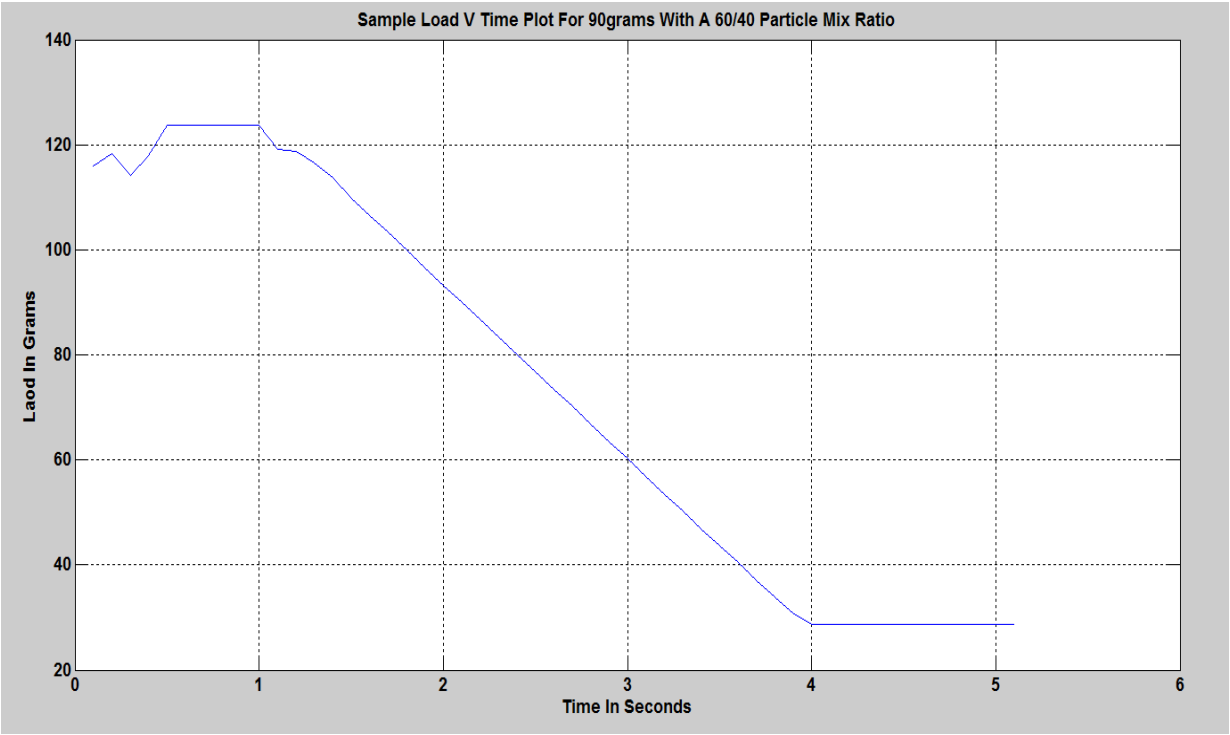

Figure 3.7: Load against Time Plot For 90 grams of Powder With A 60/40 Mix Ratio

From Figure 3.7, it can be seen that once the funnel is unblocked, it begins to dispense powder at a constant rate until all the powder has been dispensed. This is evident by the straight line observed between 1.2 and 4 seconds. It is worth noting that even though the full mass of the powder has been dispensed, the load measured by the load cell will not drop to zero due to the weight of the funnel suspended on the load cell.

To calculate the flow rate, a constant segment of the acquired load vs time graph was isolated and the slope of the line was estimated. This calculation was done for all experimental runs and the results can be seen in the graph in Figure 3.8.

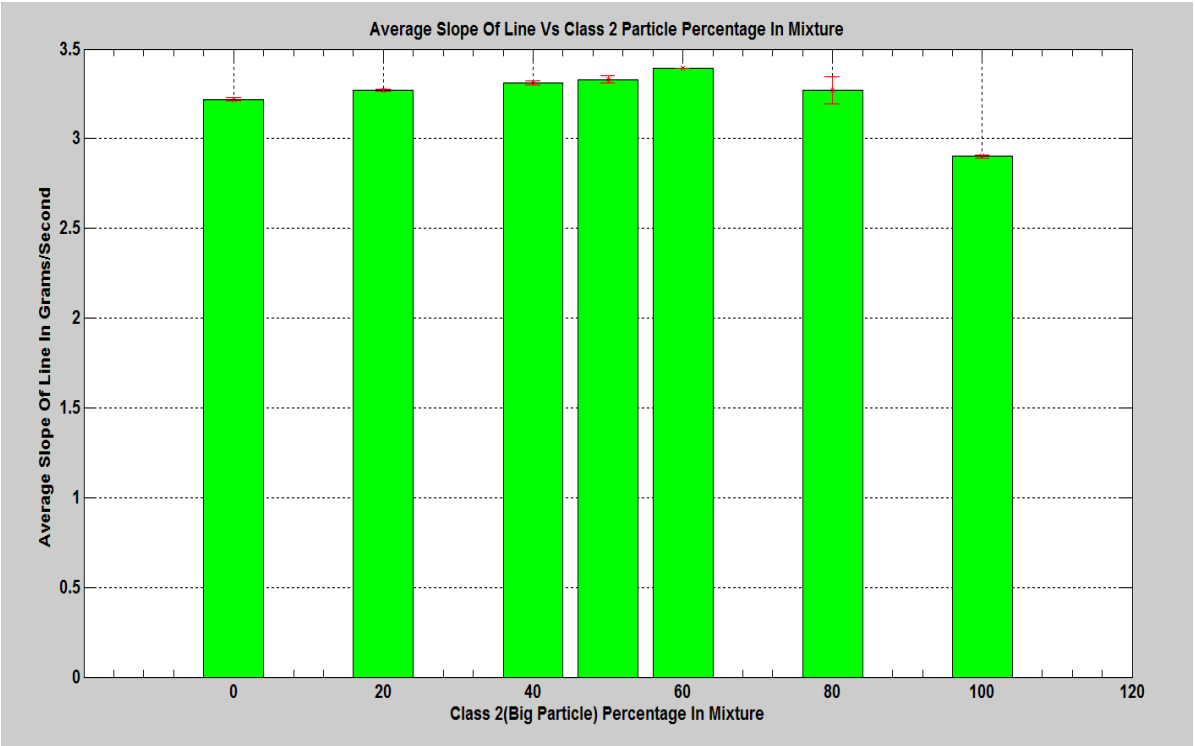

Figure 3.8: Graph Showing Average Slope of Line against Class 2 Particle Percentage In Mixture

From Figure 3.8, it can be seen that the average slope of the line, i.e.flow rate, only deviates by a small amount (maximum of 0.04) from the average value; this result suggests that the flow rate can be said to be repeatable for each powder mix ratio. It can also be noted from Figure 3.8 that the average slope value appears to increase until the class 2 particle percentage exceeds 60%, and this is thought to be because the glass beads are spherical in nature, the packaging is maximised between the spheres as the mix ratio increases which also increases the flow rate until the optimum packaging point is reached, once the optimum packaging is exceeded it can be noted that the flow rate begins to experience a reduction.

3.6 Signal Processing Method

3.6.1. Particle Sizing With AE - Theoretical Background

When a particle hits a plate, elastic stress waves are generated which are linked to the forces which the particle produces on the plate.[41] The particle size is a key factor which influences the magnitude of the resulting force of a particle impinging a plate.[40] The associated surface displacements caused by stress waves can be recorded with a transducer, and by applying physical modelling steps in addition to deconvolution methods, Buttle et al were successful in quantitatively obtaining the particle size from individual impact events.[40]

The acoustic emission signal which is recorded by the transducer is not solely dependent on the nature of the particle and the dynamics of impact, but also on the physics of the stress wave propagation through the plate and the instrument's response to surface displacements.[41] This process is shaped by a flow chain of the various processes and can be seen in Figure 3.9.

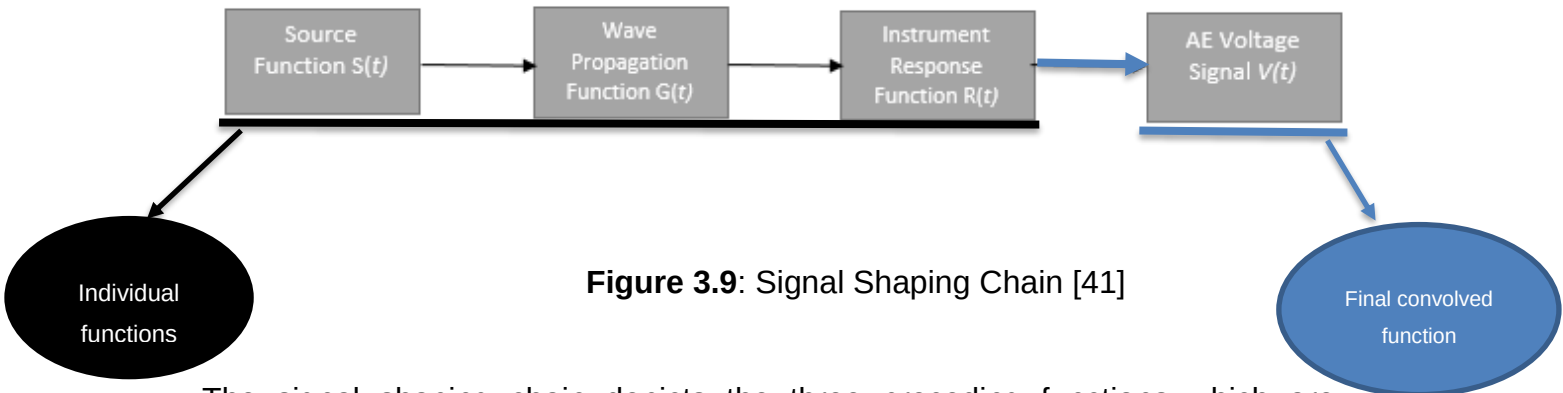

Figure 3.9: Signal Shaping Chain [41]

The signal shaping chain depicts the three preceding functions which are convolved through a convolution process to give the output AE voltage signal which is the source for the data analysis and signal processing which particle information will be extracted from, with the convolution representing a mathematical integral operation on two functions where a third function is

produced which is usually a product of the pointwise multiplication with respect to the two original functions.[52]

Under the assumption that both the wave propagation material and sensing instrument can be modelled as Linear Time Invariant (LTI) systems, the AE voltage signal consists of a convolution of the preceding three blocks and its mathematical representation can be seen in equation 3.1.[40]

$$\mathrm{S}(t) * \mathrm{G}(t) * \mathrm{R}(t) = V(t) \quad (3.1)$$

Where:

$\mathrm{S}(t)$=source function/ source of the acoustic signal

$\mathrm{G}(t)$=wave propagation function

$\mathrm{R}(t)$=Instrument response function

'*'represents a convolution

The source function S(t) represents the force-time history and can be estimated using Hertz's theory of contact for solid bodies and is based on the assumption that the impact is normal, fully elastic and the particle is spherical. The force which the particle imposes on the plate can estimated with equation 3.2.[41,53]

$$\mathrm{S(t)} = (fmax\left(\sin\left(\frac{\pi t}{t_c}\right)\right)^{3/2}, \ 0 \text{ for } 0 < t < tc \quad (3.2)$$

Where:

Particle contact time = t_c=$4.53\left(4\rho_1\pi\left(\left(\frac{\delta_1+\delta_2}{3}\right)\right)^{\frac{2}{5}}\right)r_1 v_0^{-1/5}$ (3.2.1)

Peak Compression Force =f_{max} = $1.917\rho_1^{\frac{3}{5}}(\delta_1+\delta_2)^{-\frac{2}{5}}r_1^2 v_0^{6/5}$ (3.2.2)

$\delta_1 = (1-\mu_i^2)/(\pi E_i)$

Symbols E and μ represent Young's modulus and Poisson's ratio, while the subscripts 1 and 2 stand for the particle and plate respectively. ρ_1 refers to the mass density, r_1 stands for the equivalent radius and v_0 refers to the approach velocity of the particle. With the knowledge of the particle's approach velocity, properties of the plate and particle, the particle size can be theoretically estimated from the source function.[41,53]

In a homogenous elastic medium, the propagation of stress waves can be modelled by the elastodynamic wave equations of motion.[53] A solution to the elastodynamic wave equation can be formed using Green's function which describes the response of the wave propagation medium to a single force applied in a fixed direction. Green's function $G_{in}(x,t,l_0,T)$ describes the displacement in direction 'i' at a point 'x' at time 't' due to a unit impulse force at a location 'l' in the direction 'n' at a time 'T'.[53]

The transducers used to record the AE events of particles hitting a plate are normally assumed to have a flat response between two frequencies. For structural borne sensors the actual response of the sensor is a function of the impedance matching between the sensor and the wave propagation medium.[8] The instrument response function mathematically establishes the relationship between the surface displacement and the sensor's waveform. The sensor output waveform can be expressed as a linear convolution between the surface displacement and the sensor's response function as can be seen in equation 3.3. [41,53]

$$V(t) = U(t) * I(t) \qquad (3.3)$$

Where I(t) is the sensor's instrument response function and U(t) is the displacement to the wave propagation medium which could still be present independent of the sensor. Calibration of the sensor can be performed through a transfer function approach and can be found from inversion of the Fourier transform.[54] Once the Green's function of the wave propagation medium and the instrument response function have been determined, their effects can then be de- convolved from the acquired AE signals.[40,41,53] With a knowledge of the AE source, wave propagation medium and sensor response function, a method known as quantitative particle sizing can be used to estimate particle sizes with the aid of deconvolution methods.[40]

Working with the principles of the signal shaping chain and assuming the particle impingement medium and sensor are both linear time invariant systems, Hu et al developed a model that was based on the relationship between the maximum AE voltage which corresponds to the maximum compression and is proportional to the peak compression force.[41] Hu et al supported this model with a signal processing algorithm which was based on a threshold method that links the maximum AE amplitude within a set threshold to particles of a certain size.[41] The experimental results showed that this signal processing method was unable to detect particles below 90 microns diameter. Looking closely at the method used by Hu et al, it would appear as though the maximum amplitude feature is not robust enough to be used when dealing with smaller particles and may also be difficult to work with in a practical environment which has a lot of process noise.[49]

Under the same assumptions proposed by Hu et al, if the maximum AE voltage corresponds to the maximum compression and is linked to the peak compression force, then it can be hypothesised that the mean of these resulting forces above a predefined threshold can be correlated to a particle of a certain size.

Mathematically this can be expressed as;

Where;

x/x_1=AE voltage amplitudes

n=number of values in the set being considered

M/M_1 =AE signal mean

i=indicates that the mathematical operation should start with the first number in the set being considered

Case of unmixed particles

$$M = \frac{1}{n}\sum_{i=1}^{n} |x| \qquad (3.4)$$

Where | x |>Threshold

Case of particle mixtures

$$M_1 = \frac{1}{n}\sum_{i=1}^{n} |x_1| \qquad (3.5)$$

Threshold1<| x_1|>Threshold2

3.7 Conclusion

In this chapter, details of the design of the experimental rig which was used in this study was discussed. Using a DOE sequence, the rig was designed to have reduced factors when compared to the industrial scale mixer while retaining the key factors and attributes, the experimental particles which was used in this thesis was also presented here.[11] Validation experiments carried out, helped to confirm that the rig possessed good repeatability for the different particle mixtures considered. Also, the experimental particles which was used for later chapters were identified and presented here.

The theoretical model established by Buttle et al for quantitative particle sizing was presented in this chapter and it helped show from a theoretical perspective that AE signals produced by a certain particle hitting a target plate contains information about the size of the impacting particle itself.[41,53] From the

principles proposed in this model, a general model for an output, given a certain input was proposed for cases of unmixed and unmixed particles in equations 3.4 and 3.5 and formed the core of the signal processing method which was used to analyse acquired AE signals in this thesis.

4 Particle Size Differentiation

This chapter details the results of the first experimental study carried out in the project, which was aimed at differentiating sieved particles of different sizes. While observing the capability of the signal processing method detailed in chapter 3, sieved unmixed particles of different sizes were used to reduce variability during the experiment. Polyethylene and glass beads were used to represent the irregular and regular sized particles present in the washing powder compound, and the successful differentiation of these particle sizes provides evidence to suggest that the designed signal processing approach can classify particles of different sizes and geometry, and can also be extended to estimate the PSD of powder mixtures.

4.1 Experiment Details

4.1.1 Experiment Procedure

All experiment repetitions were carried out using the rig shown in Figure 3.3. For each run, the exit of the funnel was blocked while a measured mass of powder was poured into it. After that, the funnel was unblocked, the full mass of powder was allowed to flow freely on the target plate, and the particle impacts were recorded using the attached AE sensor.

4.1.2 Experiment Particles

The powders were filtered into narrow bands with a dry sieving method as shown in Table 4.1, using an Endecotts layer sieve.[33]

Table 4.1: Particle Class Information

Particle Type	**Size Distribution**	**Bulk Density In g/cm^3**
Polyethylene	53-63 microns	0.21
	64-125 microns	0.22

	126-150 microns	0.25
	151-250 microns	0.34
Glass Beads	150-212 microns	1.49
	213-300 microns	1.53
	425-600 microns	1.59

4.1.3 Particle Sizing Approach

An amplitude threshold was used to support the signal processing method proposed for particle size differentiation. The threshold helped identify the optimal point in the signal at which the best particle size classification could be made.

4.1.3.1 Related Literature Threshold Rules

Hu et al's threshold is based on 3 principal rules, and the first is to detect all possible peak candidates in the signal.[41] Next, for every three peak candidates, the middle one (which is also higher than the other two peaks) is taken to be the primary peak. Finally, any other peaks below a further user defined threshold are regarded as pseudo peaks due to the presence of noise, and are eliminated. This threshold method would not be effective when there is a wide distribution of particles involved, due to the first rule that involves the selection of one primary peak from a group of three.[41] Another author, Ivantsiv et al used a simpler threshold rule to detect peaks at set intervals; however using this rule means that particles which fall between the defined detection interval will be missed.[55]

4.1.3.2 Designed Threshold Rules

A varying threshold was designed and the steps to tune the threshold are detailed below:

- Step 1: Take |x| of AE signal
- Step 2: Identify $|x_{max}|$ from each particle distribution by inspecting the

maximum amplitude from all experiment repetitions of each particle distribution and set as default threshold amplitude (T)

- Step 3.1: Reduce the threshold amplitude level by 10%. Before the 10% value was chosen various other values were considered (2%,3%,5%) the 10% value chosen as suitable value based on the type of signals that are to be considered to ensure that the signal is divided into a reasonable amount of portions, as values below 10% made for too many signal divisions and more than this caused for the data portions to be too large.
- Step 3.2 Calculate the mean of the peaks above the threshold each time the threshold is reduced and correlate to particle sizes
- Step 4: Select threshold which provides best correlation fit for data as optimal threshold

A workflow diagram of the threshold approach can be seen in Figure 4.1

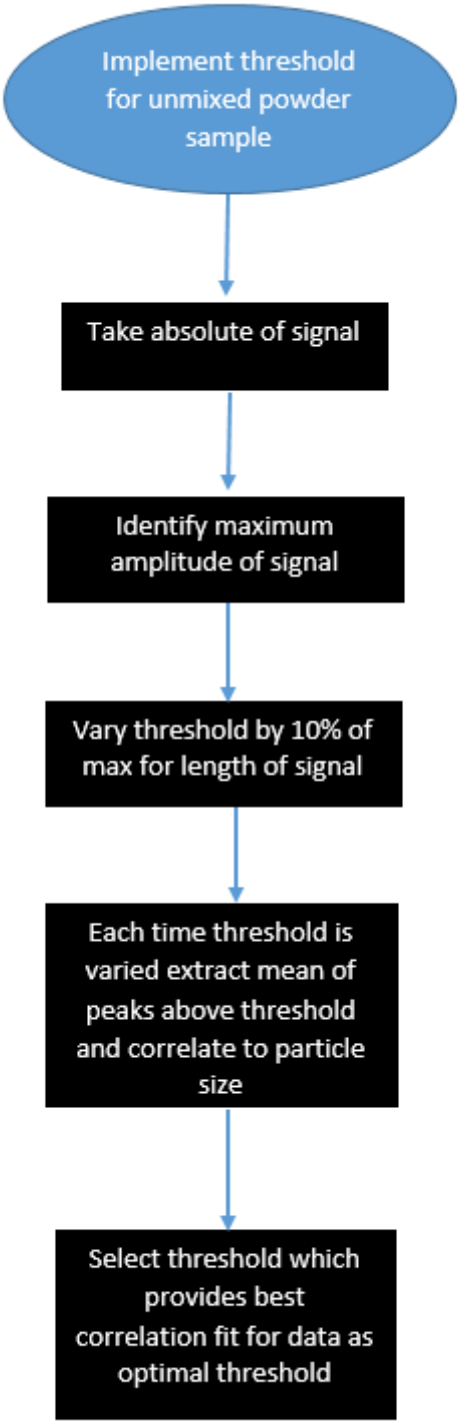

Figure 4.1: Workflow Diagram For Threshold Approach Of Unmixed Sample

Dispensing the particles through a funnel caused a variation in the amplitude of the acquired AE signal, as can be in Figure 4.2. Hence, for the data analysis procedure, 50,000 data points were extracted from a section of the data where the flow rate was maximum and fairly constant as illustrated with arrow in Figure 4.2.

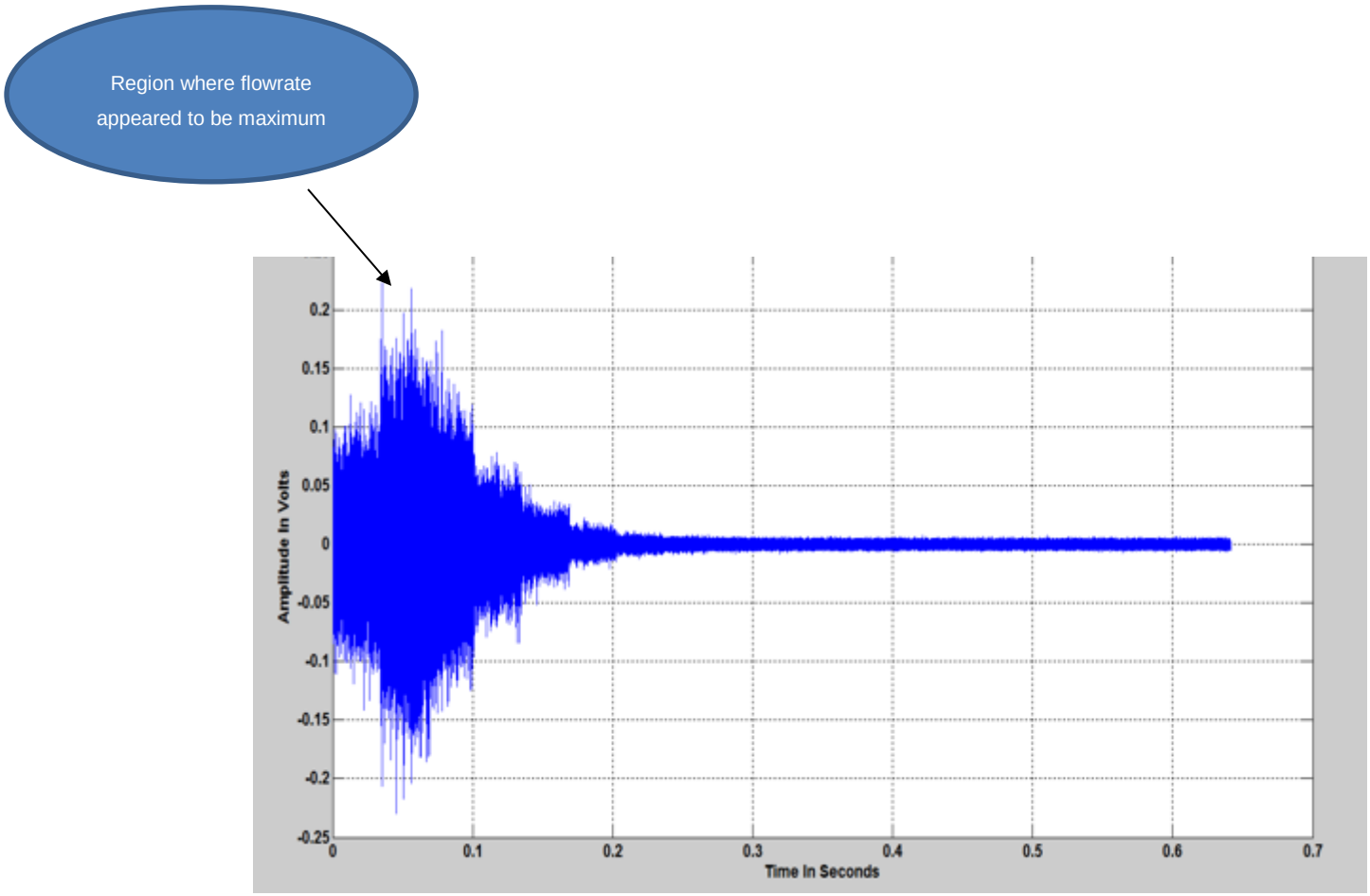

Figure 4.2: Acoustic Emission Plot Of 126-150 Microns Polyethylene Particles

The plot in Figure 4.3 shows a simple example of an isolated constant segment of 20,000 data points along with an example of how a 60% threshold would work.

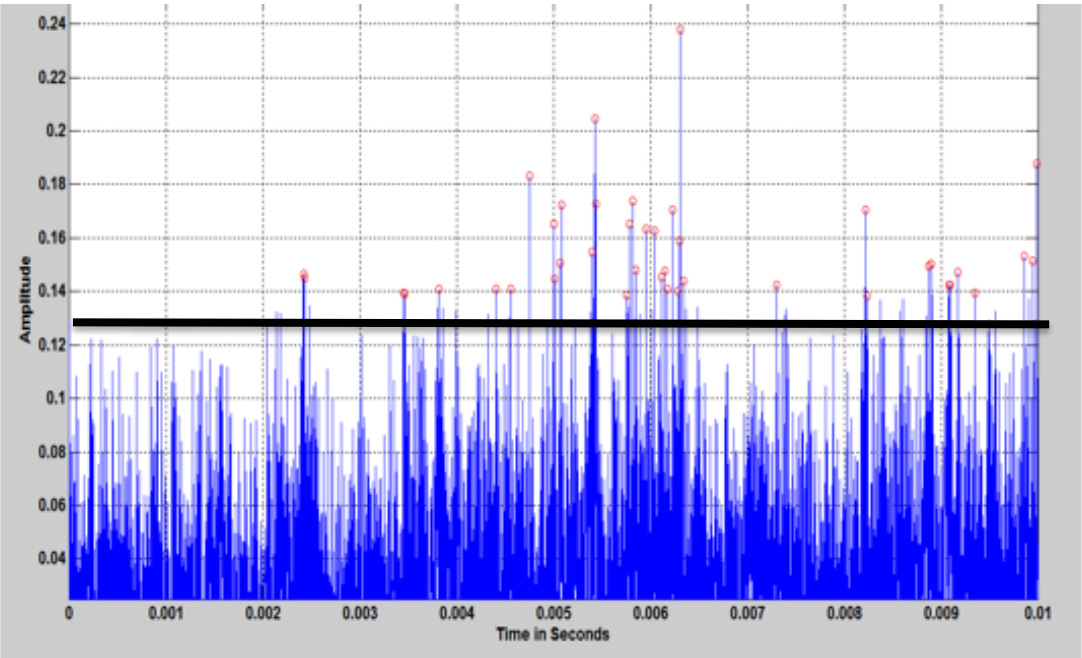

Figure 4.3: Amplitude (in volts) -time Graph with a threshold level of 60% (peaks above 0.138)

4.2 Results

4.2.1 Polyethylene Results

Once the data sections were isolated, the threshold method was applied and the linear correlation coefficient was calculated for each threshold level. The thresholding exercise began with a 90% threshold which reduced by steps of 10% and stopped at the 10% mark, as below this the correlation became worse due to the noise produced by the sensor. For all particle distributions, a measured mass of the particles was dispensed 4 times at each turn, after which the amplitude mean from the set threshold was extracted and correlated to the respective particle size.

Figures 4.4 and 4.5 show correlation figures of particle sizes against the mean of threshold peaks for 90% and 10% threshold levels, with 0.87 and 0.97 as their respective correlation coefficients. It can be noted from Figure 4.3, that certain experiment repetitions gave a threshold amplitude mean of 0v, this is due to the

method used to set the default threshold as described in step 2 in section 4.1.3.2 which meant that for the higher thresholds (i.e 90%), due to the overall variability of the particles, no peaks were present in some cases and therefore produced an amplitude mean of 0v.

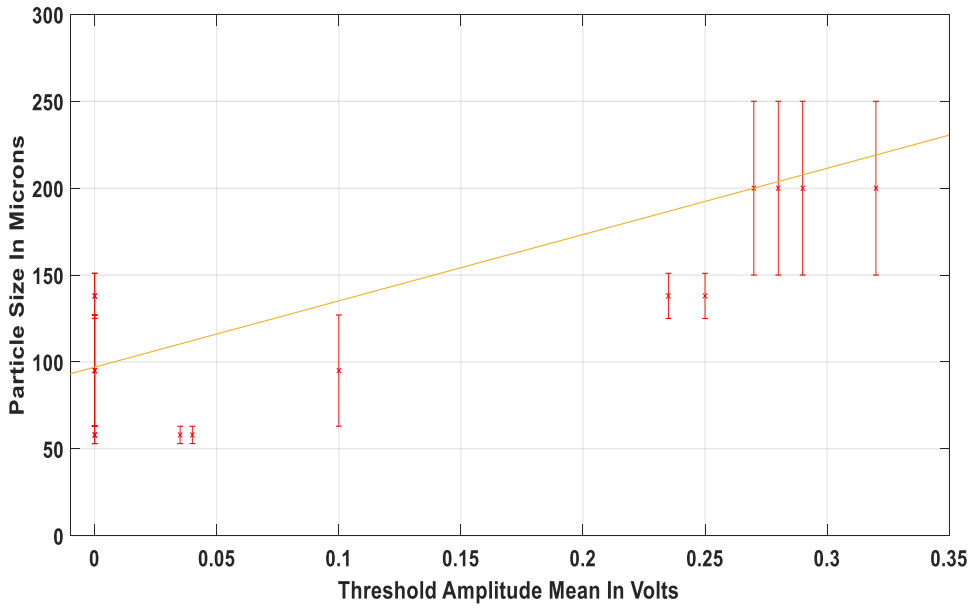

Figure 4.4: Correlation of Particle Size against Threshold Amplitude Mean For 90% Threshold (correlation factor 0.87)

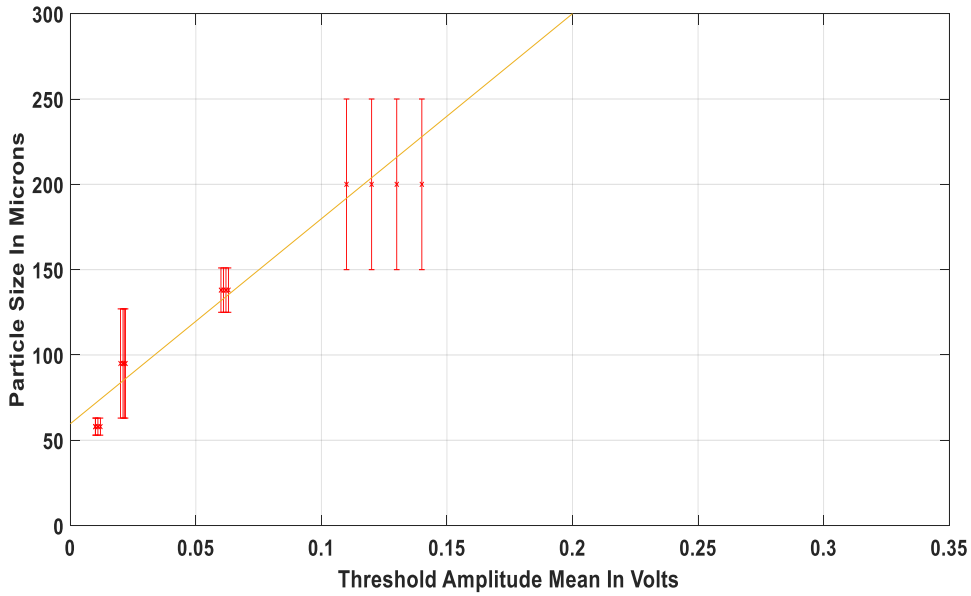

Figure 4.5: Correlation of Particle Size against Threshold Amplitude Mean For 10% Threshold (correlation factor 0.97)

It can be observed that the threshold amplitude mean showed greater variability as the particle sizes got bigger, as can be seen in Figure 4.5. This is thought to be due to the size of the particle distribution, as the smallest polyethylene particles ranged from 54-63 microns with a size variation of 9 microns, whereas the biggest particles ranged from 151-250 microns, which amounts to a variation of 99 microns and hence more variability in the acquired AE signal. The plot in Figure 5 was obtained using the 16 collected data points and it illustrates how the correlation coefficient between the particle size and the threshold amplitude mean increases with the lowering of the threshold level.

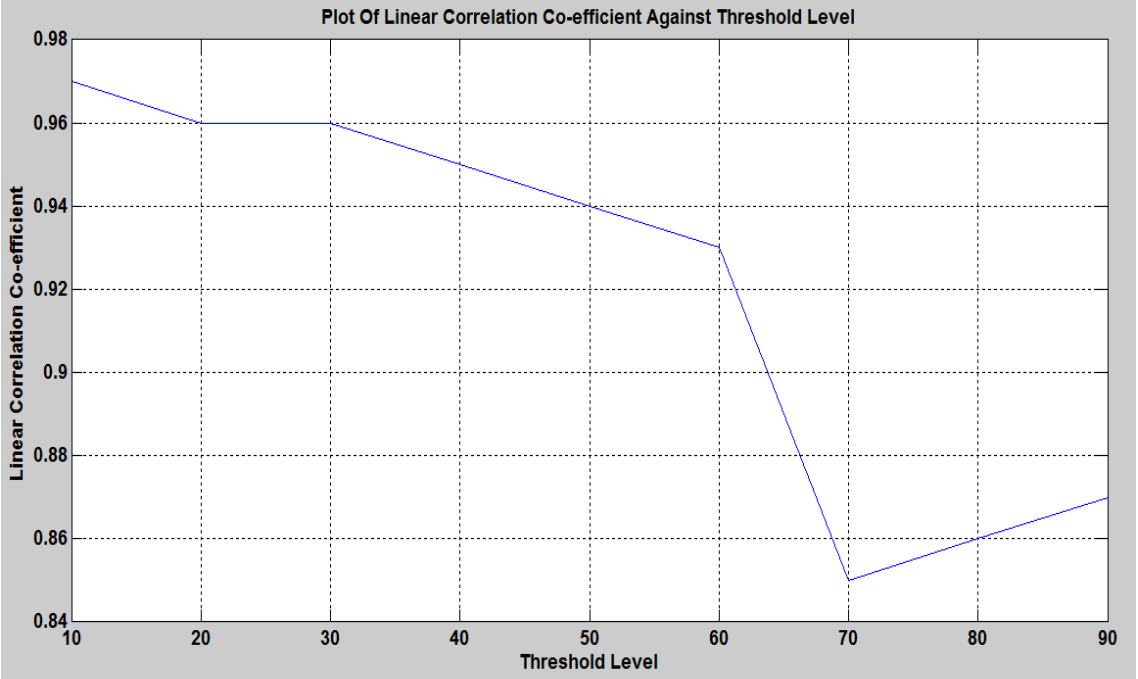

Figure 4.6: Plot Of Linear Correlation Co-efficient Against Threshold Level

4.2.2 Glass Beads Results

The threshold approach was implemented on a set of regular sized glass beads, with the aim of observing if the designed approach could also differentiate particles of a different geometry and physical nature. This capability is regarded as an important factor due to the nature of the washing powder compound - which

consists of a variety of different particles. Figure 4.7 shows a sample AE plot for the glass beads in the size range of 425-600 microns, and it can be observed that in contrast to the polyethylene particles, the glass beads produced a more consistent amplitude when the flow was constant.

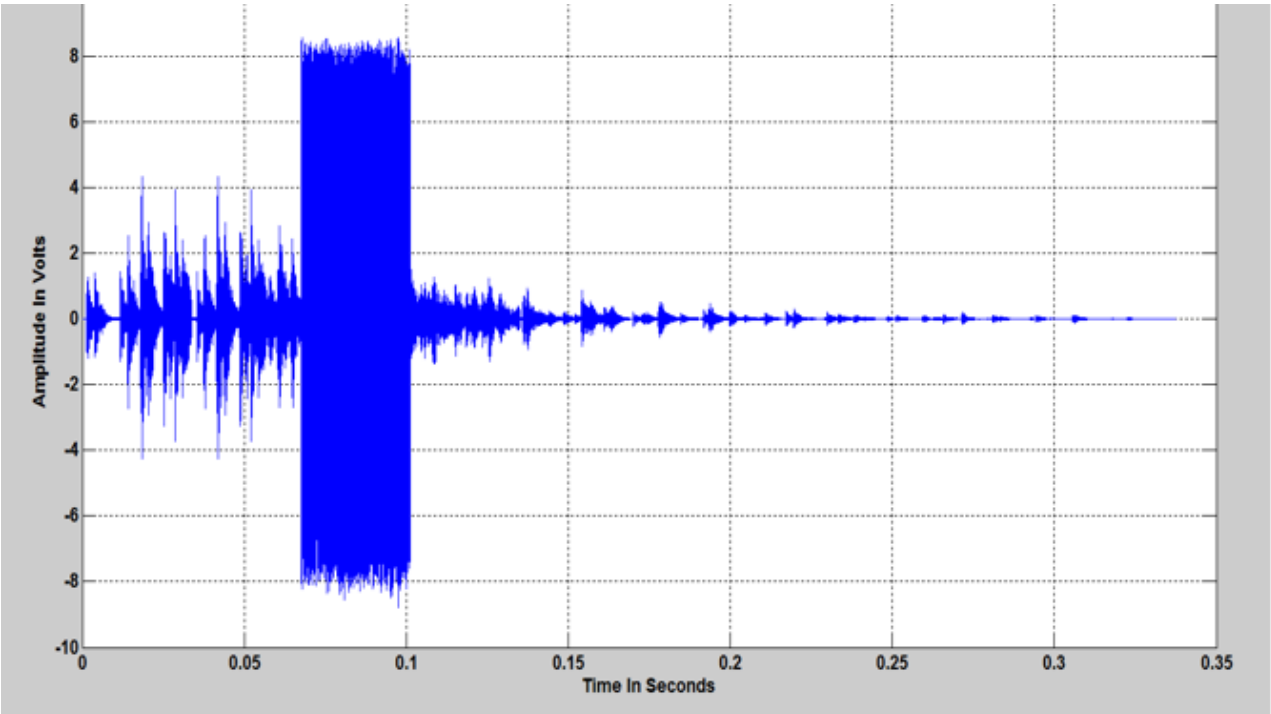

Figure 4.7: Acoustic Emission Plot of 425-600 microns Polyethylene Particles

The different glass beads in table 4.1 were classified using the same experimental approach and signal processing method used for the polyethylene particles along with a 10% amplitude threshold. A correlation plot of the different glass beads sizes and the threshold amplitude mean can be seen in Figure 4.8.

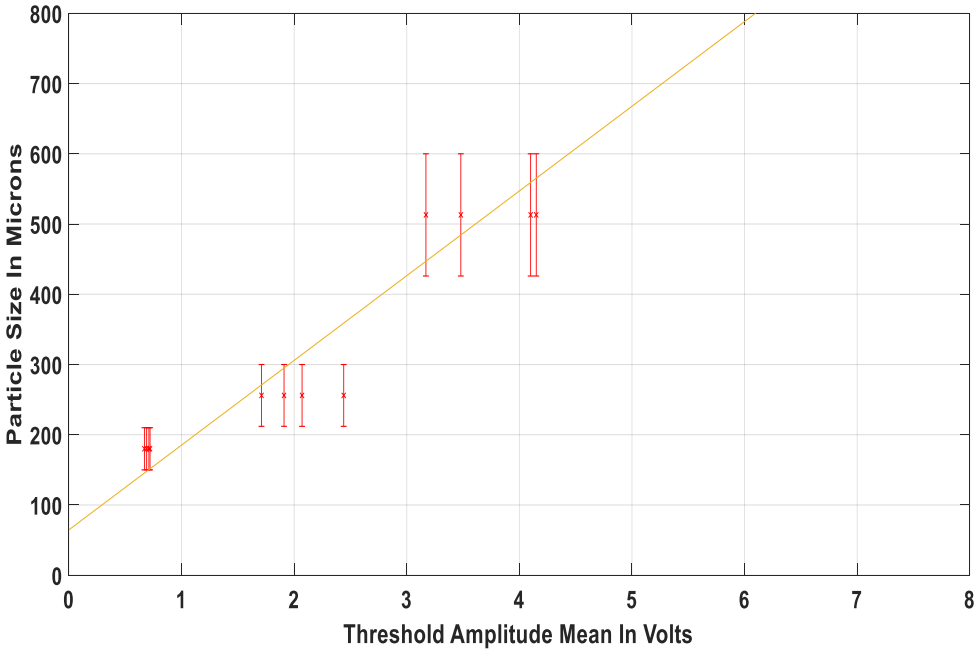

Figure 4.8: Correlation of Particle Size against Threshold Amplitude Mean For 10% Threshold (correlation factor of 0.99)

From the plot in Figure 4.8, it can be seen that a linear correlation exists between the glass beads of different sizes and their respective threshold amplitude means. This suggests that the signal processing technique can be used to effectively differentiate between particles of various sizes irrespective of the particle type and geometry, under the same conditions used in this experimental setup.

4.3 Conclusion

This chapter discussed an experiment aimed differentiating a sieved set of polyethylene and glass beads particles using their acoustic emission amplitude. By using a design threshold approach, it was observed from the results that a linear relationship exists between the sizes of the particles and the resulting AE amplitudes. These results helped to validate the hypothesis that a linear relationship exists between particles and their resulting amplitude; the results also provide evidence that the experimental setup can be considered as Linear Time Invariant (LTI).[40] The next chapter involves experiments with powder combinations of polyethylene and glass beads in order to observe the behaviour

of particles in a mixture, as well as to investigate the possibility of estimating particle sizes of mixtures of this kind.

5 Particle Size Distribution Estimation Of 2-Particle Mixtures

5.1 Introduction

This chapter details the steps taken to extend the designed particle sizing approach to deal with mixtures. As a first step in this direction, the experiments that were carried out involved the use of different combinations of a 2-particle mixture not just to observe the behaviours of particles in a mixture, but also to quantify the limitations, capabilities and performance of the designed method. The combinations experimented with in this chapter were influenced by the nature of particles present in the washing powder mixture; and these combinations do not appear to have been investigated in the literature reviewed for this thesis. The results showed the particle sizing approach is capable of estimating the PSD of different mixture types but has certain limitations in dealing with mixtures whose particles have certain physical properties.

5.2 Particle Mixture Threshold Method

The threshold approach that will be used for particle sizing of mixtures is still based on the theoretical model and signal shaping chain seen in Equation 3.1 and Figure 3.10. It involves separating the signal into a high amplitude region corresponding to the impact events of big particles in the mixture, and the low amplitude region which would correspond to the smaller particles in the mixture. In each amplitude region, the threshold is further varied until an optimal threshold region is found. The idea of this approach is to search the signal iteratively for the region that contains the rich content and can be correlated to particle size distribution.

Below is a list of steps required to tune the threshold for PSD estimation of a 2-particle mixture:

1. Expression of the signal in its absolute format |x| to rectify negative values.

2. Separation of the signal into high and low amplitude component parts corresponding to the impacts of big and small particle distributions in the mixture, respectively.
    - For this to be achieved, a default threshold first needs to be implemented whose signal amplitude level is equal to the maximum produced from the resulting impact of the distribution of the small particles in the mixture.
    - In order to gain an accurate calibration of the default threshold, it is advisable to carry out a good number of experimental runs of unmixed material containing only the small particles. Figure 5.1 shows an example of a signal and a number of thresholds with the described default threshold represented by the black line.
3. Within each signal, a varying threshold should be implemented to scan across the length of each signal component part for a region which contains signal information that can be linked to particle size.
    - The amplitude of the varying threshold should be varied in an ascending order in the high amplitude signal part and a descending order in the low amplitude signal part as can be seen in Figure 5.1. Due to the nature of the AE signals processed in this study, the threshold was adjusted by 0.5v each time it was varied.
4. For every time the amplitude of the varying threshold is changed, the mean amplitude of the signal within the corresponding thresholds should be extracted as shown in equation 3.5.
5. Different mixture ratios containing a measured mass of both particles of interests should be formed, after which steps 3 and 4 should be repeated for each powder mix ratio. In this chapter, the mix ratios shown in Table 5.2 was used. The acquired threshold amplitude mean should then be correlated to the respective powder mix ratio.
6. Each correlation plot produced from each threshold level should be validated using a new set of particle mixtures, with the correlation plot which produces the highest estimation accuracy selected as the PSD estimation model. The

amplitude parameters used to obtain the best correlation plot should be regarded as the optimal threshold level parameters.

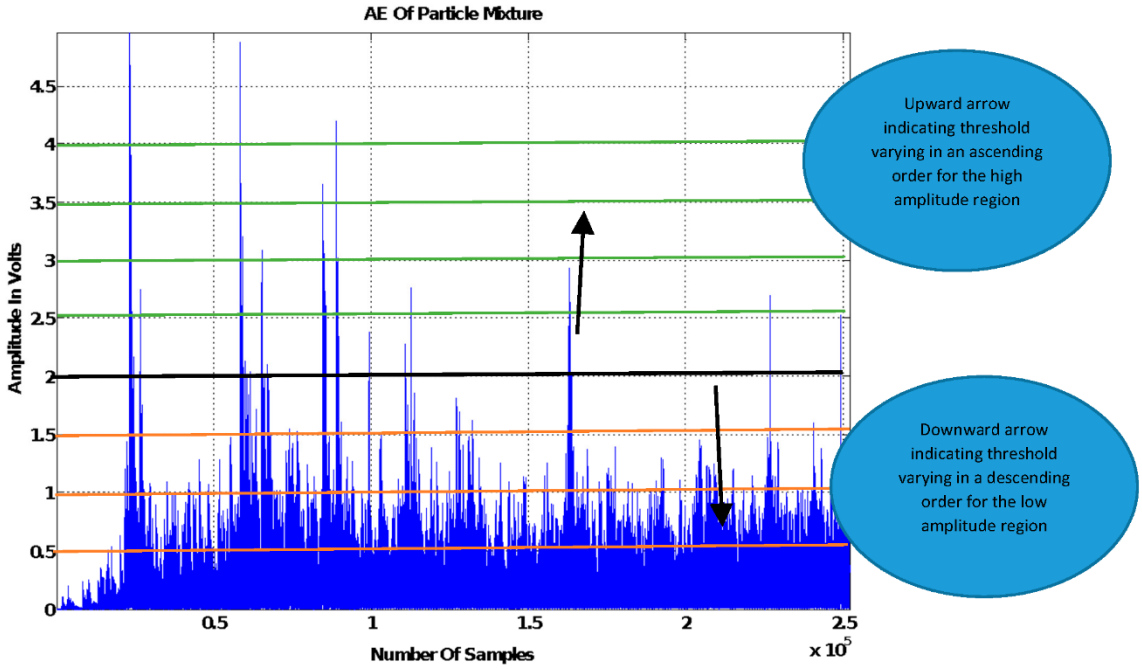

Figure 5.1: Visual Illustration of the Thresholding Method for a Two Particle Mixture

A workflow diagram of the threshold approach can be seen in Figure 5.2

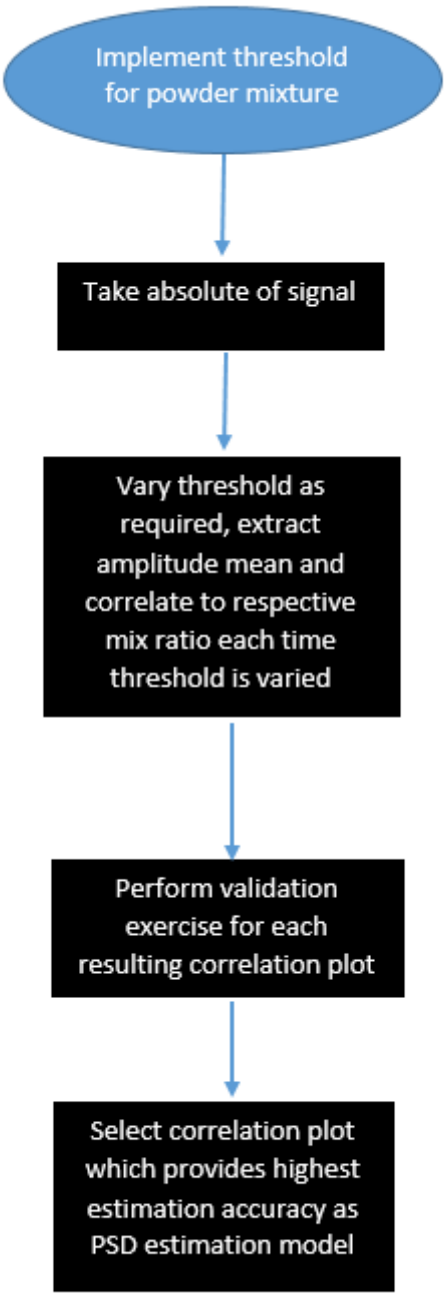

Figure 5.2: Workflow Diagram For Threshold Approach Of Mixed Sample

In this section, the designed threshold approach along with the signal processing method detailed in section 3 will be used to estimate the PSD of various mixtures

comprising of glass beads of regular geometry and polyethylene of irregular geometry.

5.3 Mixture of two sets of glass beads with regular geometry

The first set of experiments in this chapter involved the use of two glass beads of distinctively different sizes, which ultimately meant a different bulk density but their respective Young's Modulus and Poisson's Ratio are identical due to the properties of the two particles being the same, details of which can be seen in Table 5.1.

Table 5.1: Glass Beads Physical Properties

Particle Type	**Size Distribution**	**Bulk Density in g/cm^3**	**Percentage Bulk Density Difference**	**Young's Modulus In PSI**	**Poisson's Ratio PSI**
Glass Beads	150-212 microns	1.49	6.3%	10^6	0.21
	425-600 microns	1.59		10^6	0.21

This experiment was designed to represent what was viewed as a controlled experiment by means of a 2-particle mixture with a set of glass beads with high repeatability to investigate the performance and capability of the designed PSD estimation approach. Image of glass bead can be seen in Figure 5.3.

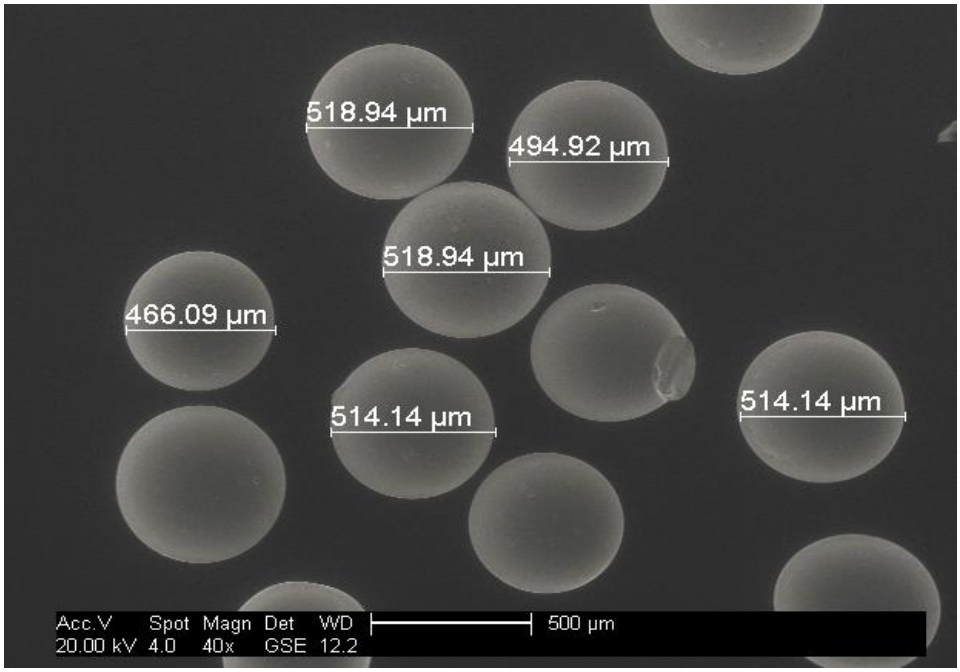

Figure 5.3: Image of Big Glass Beads

5.3.1. Experimental Method

Using the 2 sets of glass bead sizes detailed in Table 5.1, various particle mix ratios were formed as shown in Table 5.2 with a set mass of each powder mix ratio dispensed through the experimental rig 5 times to produces 5 experimental repetitions per mix ratio. This sequence was followed for all experiments described in this thesis.

The Acoustic Emissions (AE) acquired for each mix ratio was analysed using the designed signal processing method and a threshold amplitude mean was obtained for each experimental repetition. The acquired amplitude mean values were averaged to get a representative amplitude value for each mix ratio, and used to produce a correlation plot for each threshold.

Table 5.2: Particle Mix Ratio Table

	Mix Ratio
Big	**Small**
0	100
10	90
20	80
40	60
50	50
60	40
70	30
80	20
90	10
100	0

5.3.2 Results and Validation

The best correlation plot showed a sigmoidal relationship between the amplitude means and the particle percentages, and the threshold parameters used in obtaining the correlation plot helped determine the location of the optimal threshold region in the signal. For this particle mixture, the optimal threshold was located in the high amplitude section of the signal and the associated correlation plot can be seen in Figure 5.4.

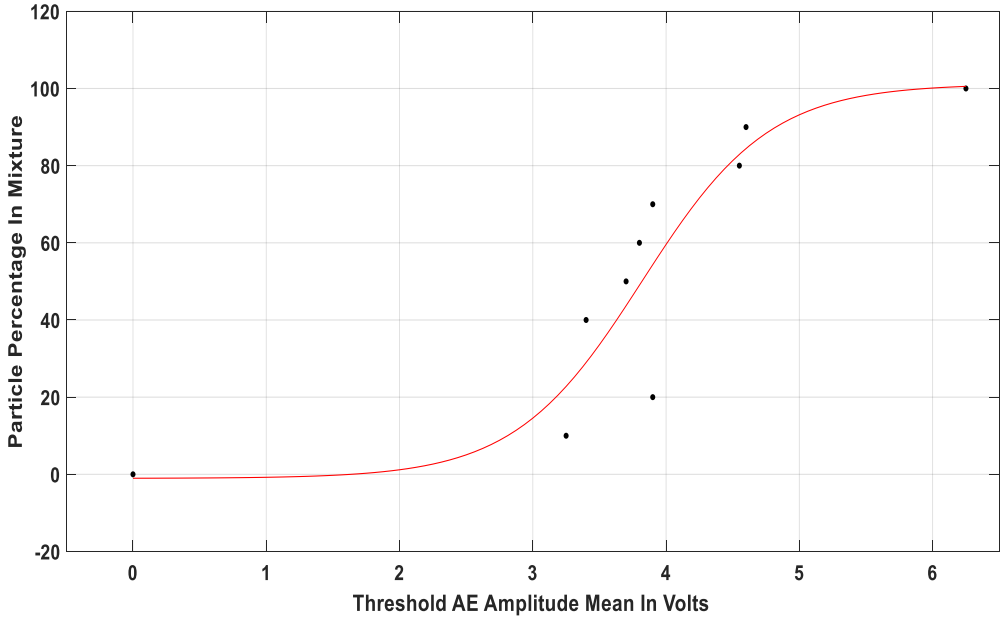

Figure 5.4: Correlation Plot of Percentage of Big Glass Beads in Mixture, Against Threshold AE Amplitude Mean from Upper Threshold

To quantify the accuracy of the designed PSD estimation model, a set of validation mixture exercises were carried out in the lab with different mix ratios as can be seen in Table 5.3.

Table 5.3: Mix Ratio Details of Experiments Used to Test Accuracy of the PSD Estimation Model

Experiment Number	**Mix Ratio (Small:Big)**	**Repetitions**
1	30:70	3
2	50:50	3
3	80:20	3
4	10:90	3

Results from the validation exercise showed that the model was capable of estimating PSD with an average absolute error of 10%. Figure 5.5 shows a chart

comparing the actual particle percentage with the respective amount estimated by the model for each experimental repetition.

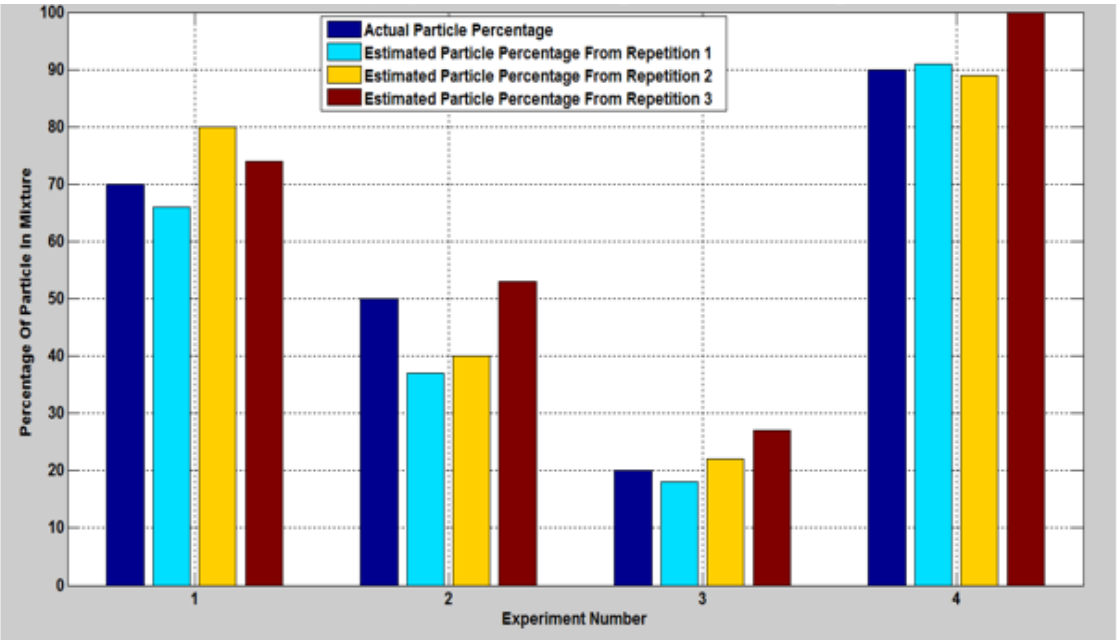

Figure 5.5: PSD Chart Comparing Actual Particle Percentage Of Big Particle In Mixture To Amount Estimated by Model

The results show that the designed signal processing method is capable of estimating the PSD of a mixture of two differently sized glass beads, with a marginal bulk density between them. This suggests that the theoretical model detailed in chapter 3 - which this signal processing approach is based on - can be extended to the sizing of a mixture of particles. A possible reason for the 10% error margin could be the small difference in bulk density between the pair of particles used to form the mixture, even though the particles are distinctively different in size. Density has been identified as a pivotal factor that influences the AE amplitude of a particle impact, hence for a set of particles with a density difference of only 6% the resulting AE amplitudes although differentiable, are similar to each other and this is - hypothetically speaking, - the cause of the associated estimation error. This hypothesis will be investigated in this chapter, and to further observe the capabilities and limitations of the designed signal

processing approach, the next set of experiments will involve a mixture of two particles with different geometries and distinctively different densities.

5.4 Mixture of a set of regular and irregular sized particles

This experiment involved a combination of regular sized glass beads and a set of irregular sized polyethylene particles, both of which are contained in the washing powder compound. The aim of this experiment is to examine whether the designed PSD estimation approach is capable of estimating particle sizes in mixtures of this nature.

Glass beads in the size range of 150-212 microns and polyethylene particles in the range of 150-250 microns were used for the experiments in this section and this made it possible to observe the PSD estimation approach when dealing with mixtures of similarly sized particles. Details of the physical properties can be seen in Table 5.4, and it can be seen that in addition to the large bulk density difference there are also difference in the Young's Modulus and Poisson's Ratio of the particles due to the different physical nature of the pair. An image of the polyethylene particles can be seen in Figure 5.6 and in contrast to the glass beads in Figure 5.3, a highly irregular geometry can be observed.

Table 5.4: Physical Properties of Experimental Particles

Particle Type	**Size Distribution**	**Bulk Density in g/cm^3**	**Percentage Bulk Density Difference**	**Geometry**	**Young's Modulus In PSI**	**Poisson's Ratio PSI**
Glass Beads	150-212 microns	1.49	76.9%	Regular	$1x10^6$	0.21
Polyethylene	150-250 microns	0.34		Irregular	$0.6x10^6$	0.40

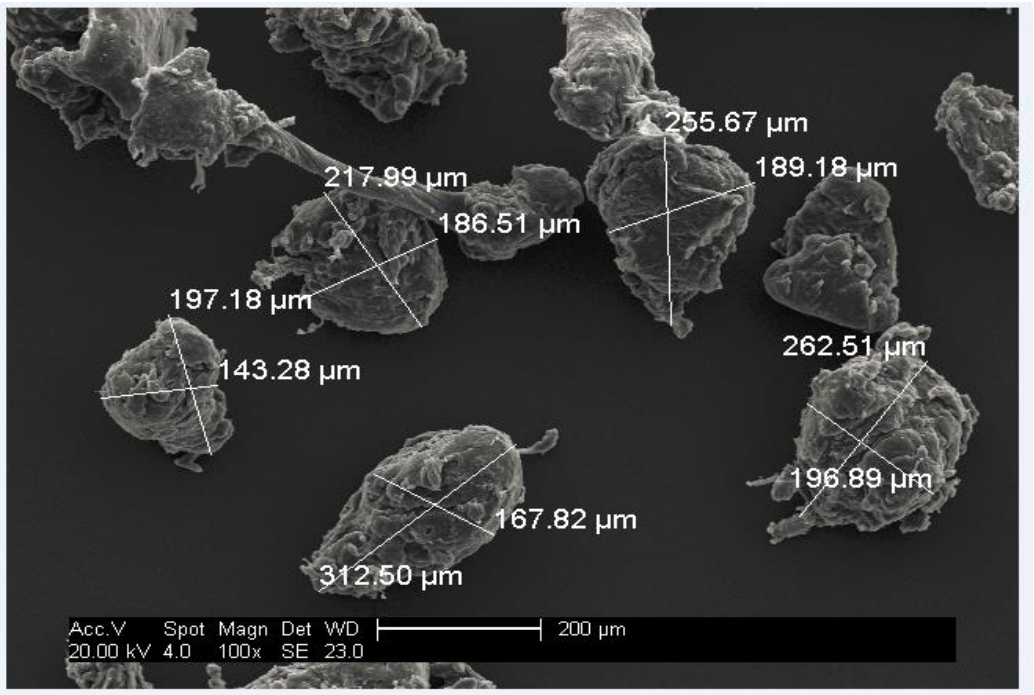

Figure 5.6: Image of Polyethylene Particles

The same experimental procedure was followed as detailed in section 5.3.1 and all acquired data was analysed using the designed signal processing approach. The optimal threshold region was found to be in the lower amplitude section for this particle mixture and a sigmoidal relationship was also observed between the different particle mixture ratios and AE threshold amplitude means. Validating the obtained PSD estimation model yielded an average absolute error of 3%, which is notably less than the mixture of two differently sized glass beads. A chart showing the results can be seen in Figure 5.7.

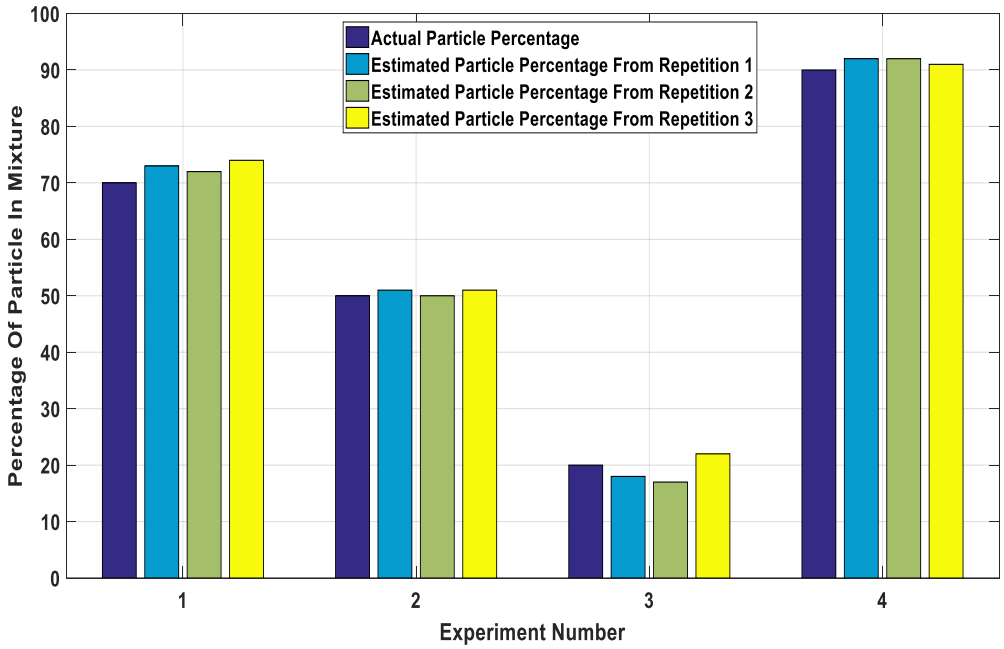

Figure 5.7: PSD Chart Comparing Actual Particle Percentage Of Big Particle to Amount Estimated by Model

The low average absolute error margin can be attributed to two possible reasons; the first is the large bulk density difference of 76.9% between the two particle types which would ensure that their AE signals are distinctively different from each other and therefore easily separable with the designed signal processing approach despite being in a mixture.[32,53] The second factor is the physical nature of each particle group in the mixture - the glass beads are harder and more crystalline, whereas the PE particles are less crystalline and not as hard as the glass beads; this factor is also believed to have contributed to the distinct AE amplitude of the particles which has made them easy to separate and made the resulting PSD easier to estimate than the previous mixture, even though both sets of particles are the same size. [32,53]

The obtained results go in hand with hypothesis stated in the theoretical model in chapter 3, which the designed signal processing method is based on. In the signal shaping chain shown in Figure 3.9 and equation 3.1, the resulting AE voltage is dependent on three preceding blocks which are merged together in a convolution

process to yield a resulting AE signal. The first is the source function block which consists of a set of equations that govern the impact dynamics of a particle on a surface.[32] Particle dependent features which include density, Young's modulus and Poisson's ratio are all variables within the source function equations, which would go in line with the obtained results and explain why two similar sized particles of different physical properties yield distinctly different AE amplitudes and when mixed together can be separated using the designed signal processing method, with a low average absolute error.[32,48,53]

To observe the limitations of this designed PSD estimation approach, the next set of experiments involved a mixture of two particle sets of the same type with the same physical properties. As it is assumed from the theoretical model which the particle sizing model is based on, a set of particles with near-identical physical properties when mixed together would be challenging to separate and hence should yield a considerable error margin in the estimation process. The next set of experiments investigated this assumption further and help define the limitations of this designed particle sizing approach.

5.5 Mixture of a set of similarly sized particles

In this section, a set of experiments involving similarly sized polyethylene particles and glass bead particles was conducted. This investigation is based on the theory stated in the source function of the signal shaping chain in Figure 3.10, which the designed signal processing method is based upon. Based on those assumptions (see chapter 3) it is expected that similarly-sized particles would possess the same physical properties which would mean their respective AEs are alike; with this hypothesis in mind it is also assumed that the designed signal processing method would be limited in estimating the PSD of mixtures of this kind. [53] The purpose of these experiments was to investigate this assumption further and observe the limitations of the designed particle sizing approach, using mixtures that comprise a pair of similarly sized irregular polyethylene particles and regularly sized glass bead particles.

5.5.1 Mixture of a set of similar sized particles with irregular geometry

Table 5.5 shows a summary table of the set of polyethylene particles used to form the various mixtures. Following the same experimental and data analysis procedure as detailed in the previous sections, the resulting correlation plot from the optimal threshold region can be seen in Figure 5.8.

Table 5.5: Physical Properties of Experimental Particles

Particle Type	**Size Distribution**	**Bulk Density in g/cm^3**	**Percentage Bulk Density Difference**	**Geometry**	**Young's Modulus In PSI**	**Poisson's Ratio PSI**
Polyethylene	150-250 microns	0.34	9.5%	Irregular	$0.6x10^6$	0.40
	250-500 microns	0.38		Irregular	$0.6x10^6$	0.40

It can be seen that the resulting correlation plot has a linear fit for this mixture when compared with previous results. The reason for this is assumed to be the similarity of particles in the mixture whose change in particle mix ratio and resulting AE amplitude is not sudden or sharp enough to result in a sigmoid, and instead yields a linear curve.

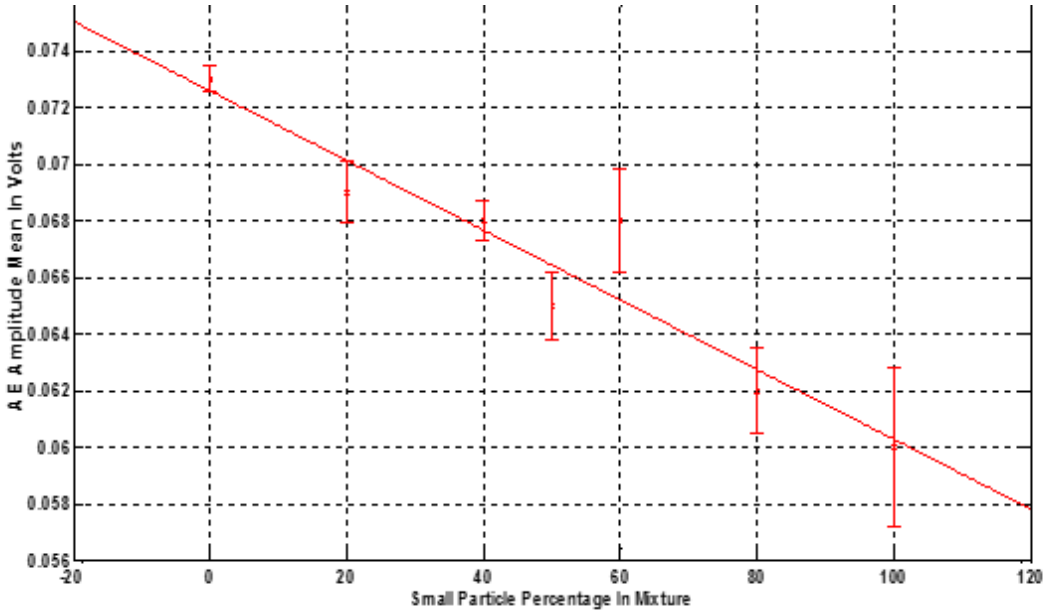

Figure 5.8: Correlation Plot of AE Amplitude Mean Against Small Particle Percentage in Mixture

Validation exercises conducted show that the linear model in Figure 5.7 is capable of estimating the PSD of this mixture despite the particle size similarity, with an average relative error of 13%. The error margin is due to similarity of particles in the mixture which ultimately appears to slightly limit the estimation accuracy of the particle sizing approach. The chart in Figure 5.9 shows the results of the validation exercise.

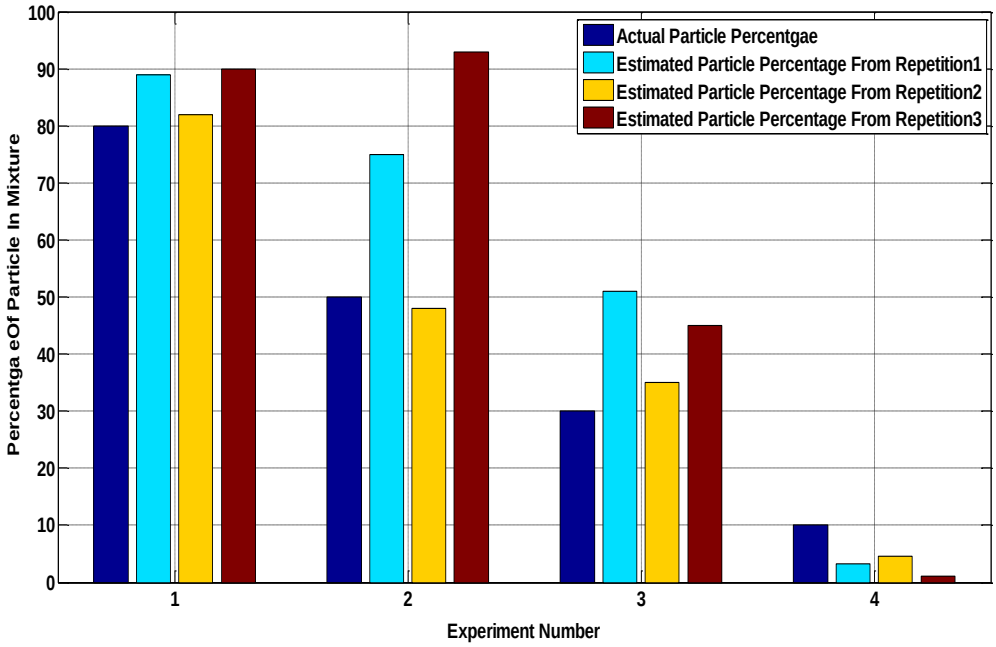

Figure 5.9: PSD Chart Comparing Actual Particle Percentage Of Small Particle To Amount Estimated by Model

5.5.2. Mixture of two sets of similar sized particles with regular geometry

Two sets of glass beads with similar sizes, physical properties and hence similar resulting AE amplitudes were used for the experiments in this section and details of their physical properties can be seen in Table 5.6.

Table 5.6: Physical Properties of Experimental Particles

Particle Type	Size Distribution	Bulk Density in g/cm^3	Percentage Bulk Density Difference	Geometry	Young's Modulus In PSI	Poisson's Ratio PSI
Glass Beads	151-212 microns	1.49	2.6%	Regular	1x10^6	0.21
	212-300 microns	1.53		Regular	1x10^6	0.21

Similar to the polyethylene results in section 5.5.1, the optimal threshold showed a linear trend between powder mix ratio variation and the resulting threshold AE amplitude mean, and this can be seen in Figure 5.10.

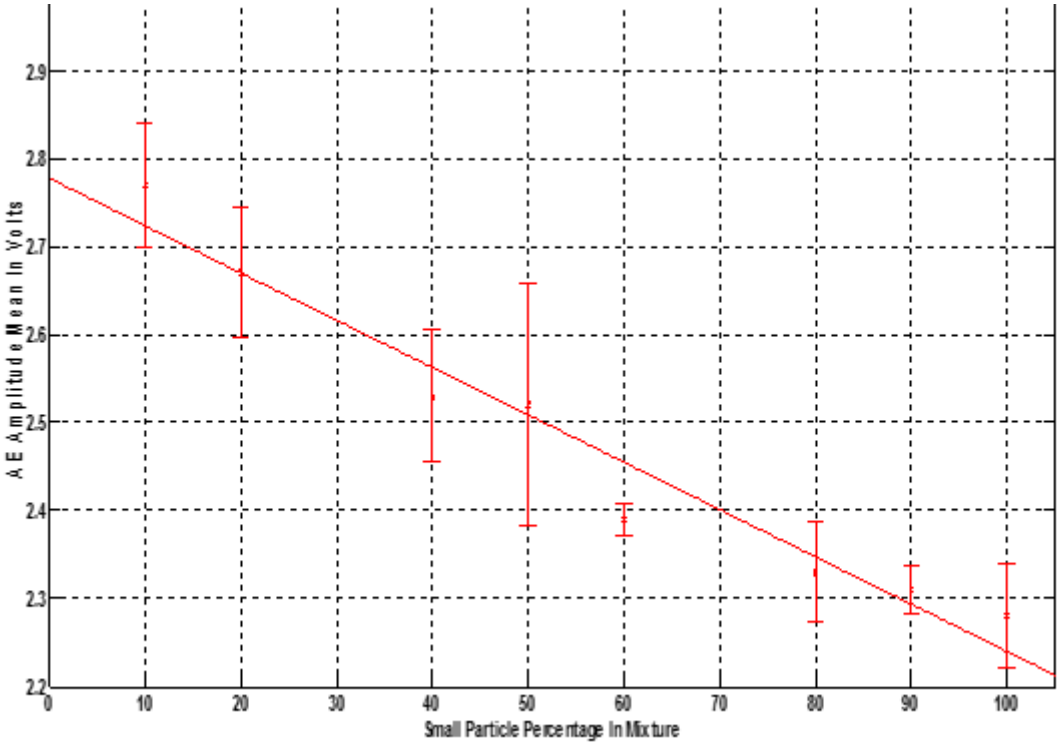

Figure 5.10: Correlation Plot of AE Amplitude Mean Against Small Particle Percentage in Mixture

The results in Figure 5.11 show that the validation exercise carried out suggests the linear model was able to estimate PSD with an average relative error of 12%, which is slightly less than the error margin obtained for the mixture of similarly sized polyethylene particles which possessed an even bigger density difference than the glass beads mixture in this section.

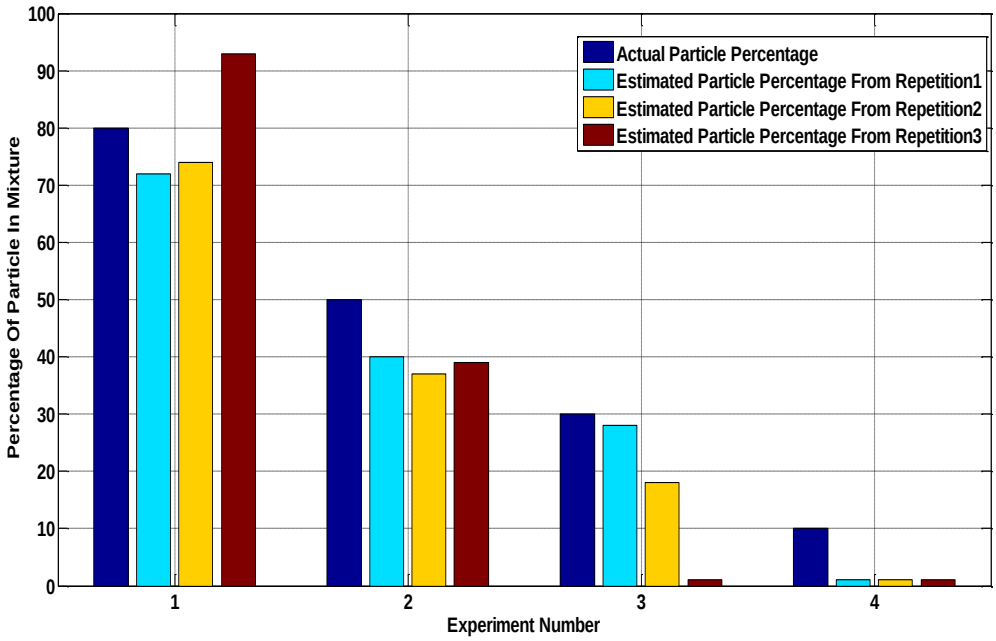

Figure 5.11: PSD Chart Comparing Actual Particle Percentage to Amount Estimated by Model

With respect to the sizing of irregularly shaped particles, Leach et al pioneered work in the sizing of particles using AE and saw that irrespective of their geometries, the sizes of particles can be determined with AE and this hypothesis was reproduced and validated with the experiments carried out in chapter 4. [39]

The theoretical studies carried out by Buttle et al in order to quantitatively size particles showed that a combination of oblique and normal impacts occur when particles fall on a target plate as can be seen in Figure 5.12, with each impact

type influencing the resulting AE magnitude. For spherical particles with a regular geometry, it is assumed that the effect of the impact type to the acquired AE is small and can be considered negligible, whereas in the case of irregularly sized particles the impact type can be said to cause notable variations in the resulting AE amplitude due to the geometry of the particle. [39,40,53] This theory can also be viewed in the sample AE acquired for the irregularly sized polyethylene particles and regularly sized glass beads in Figures 4.2 and 4.7 respectively in Chapter 4.

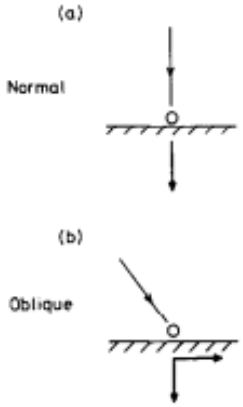

Figure 5.12: Image illustrating different particle impact types [40]

Comparing the two sets of results obtained from the mixture of similar sized particles, despite the polyethlene mixture possessing a much larger density difference, the obtained error margin appears to be larger than the glass beads mixture. This is thought to be due to variability induced by the irregular geometry and in addition, the brittle physical nature of the particles relative to the glass beads as well as cohesion between the particles due to electrostatic forces.[40,56] A summary table comparing the two particle mixtures can be seen in Table 5.7.

Table 5.7: Particle Comparison Table

Particle Type	**Density Difference**	**Particle Geometry**	**Cohesion Between Particles**	**Particle Nature**	**Average absolute Error**

Glass Beads	2.6%	Regular	Not present	Hard	12%
Polyethylene	9.5%	Irregular	Present	Brittle	13%

5.7. Conclusion

In this chapter, the designed signal processing method detailed in chapter 3 has been expanded upon with the inclusion of an additional threshold to estimate the PSD of mixtures comprising 2 particles mixed in different combinations. Four different combinations of mixtures were investigated in this section in order to observe the interaction of mixtures containing particles of a given set of physical properties. The first experiment involved a mixture of a pair of particles of regular geometry and different sizes. Using the designed signal processing method the PSD of different mixtures containing this set of particles was able to be estimated, with an average absolute error of 10%. Following the results obtained, the next set of experiments involved a mixture of particles with similar sizes and a combination of regular and irregular geometry; this time an average absolute error of 3% was obtained. The reason for this can be attributed to the distinct physical nature of the particles as can be seen in Table 5.8, which ultimately led to distinct resulting AE amplitudes as predicted in the source function equations in the signal shaping chain in chapter 3.[40,53]

Working with the assumptions set in the source function and the observed results from the experiments, it is thought that a set of particles in a mixture with the same physical properties and similar sizes would, when mixed together, produce amplitudes which would be difficult to separate. Hence, to investigate this phenomenon two more experiments were conducted; the first comprised a mixture of regularly sized particles with a density difference of 2.6%, while the second experiment involved a mixture of particles of irregular geometry and a density difference of 9.5%. A summary of experiments carried out can be seen in Table 5.8.

*In order to identify the mean size of each particle distribution, the particles were sieved and the results were plotted as a distribution with a weighted mean value extracted from the results of this.

Table 5.8: Experiment feature summary and results table

Difference in mean size of both particles	**Density difference**	**Geometry of particles in mixture**	**Average absolute error**
347 microns	6.3%	Both regular	10%
19 microns	76.9%	Regular and irregular	3%
75 microns	2.6%	Both regular	12%
175 microns	9.5%	Both irregular	13%

Results from the mixture containing a set of irregularly sized particles produced a higher average absolute error than the mixture containing regularly sized particles despite the pair of particles in the mixture possessing a notably higher density difference. This is thought to be due to electrostatic forces between the particles which cause cohesion between them, the brittle nature of the particles which influence amplitude dependent features such as Young's modulus, and the irregular geometry of the particles which is thought to produce variations in the resulting amplitudes of the particles.[40,53,56]

For PSD estimation of more complex mixtures with more particle groups, additional thresholds would be included in the signal processing stage as required. This is covered in greater depth in chapter 6 to estimate the full PSD of the washing powder compound. Having observed the behaviour of certain particle types in mixtures and performance of the designed signal processing method, subsequent steps would involve experiments with the actual washing powder compound. This represents an increase in complexity of the experimental work as the washing powder involves 12 different particle types - each with

different physical properties and a mix of geometries interacting with each other simultaneously, and with all the different impacts represented by an AE signal. A successful PSD estimation of the washing powder compound would provide evidence that the designed threshold based signal processing method is capable of dealing with complex particulate mixtures which result in highly variable AE signals.

6 Estimation Of The Ratio Of Fines To Oversize Particles In a Washing Powder Compound

6.1 Introduction

This chapter details the first set of experiments conducted to characterise the distribution of the washing powder compound. The experiments are structured similarly to how the offline check with the reference sieve is carried out at the P&G industrial site. The washing powder compound comprises a mixture of 12 different particles, each with unique physical properties combined to form a single compound. Authors who have designed online particle size monitoring platforms despite dealing with mixtures, have not investigated characterisation of the size distribution of a compound consisting of different particle types.[41] Ren et al considered a 7-particle mixture comprising differently sized polyethylene particles with different densities, but as the physical properties of the particles are the same, other AE amplitude dependent features such as Young's Modulus and Poisson's ratio would be the same.[4] Bastari et al - who dealt with the sizing of a mixture online - used coal particles of different sizes for their experiments, while Hu et al dealt with a mixture of glass bead particles.[3,41] Thus, it can be inferred that the experiments in this chapter represent the first investigation into estimating the size distribution of a compound comprising different particles with various physical properties, all of which interact with each other in a mixture and produce a signal from the simultaneous impact of particles hitting a target medium. A graph showing a sample AE plot of the washing powder compound can be seen in Figure 6.1, and the variability caused by the mixture of different particle types is reflected by the somewhat random nature of the signal. As described in Chapter 3, the variable impact peaks in the signal in Figure 6.1 are indicative of the fact that the mixture is of a heterogeneous type, in contrast the signal shown in Figures 4.1 and 4.6 which are from homogenous compounds appear to have a lot more uniform signal.

From the AE signal in Figure 6.1 it can be noted that the impact peaks are of highly varied heights, this is because the washing powder compound is a heterogeneous powder mixture and comprises of wide distribution.(53-1500microns)

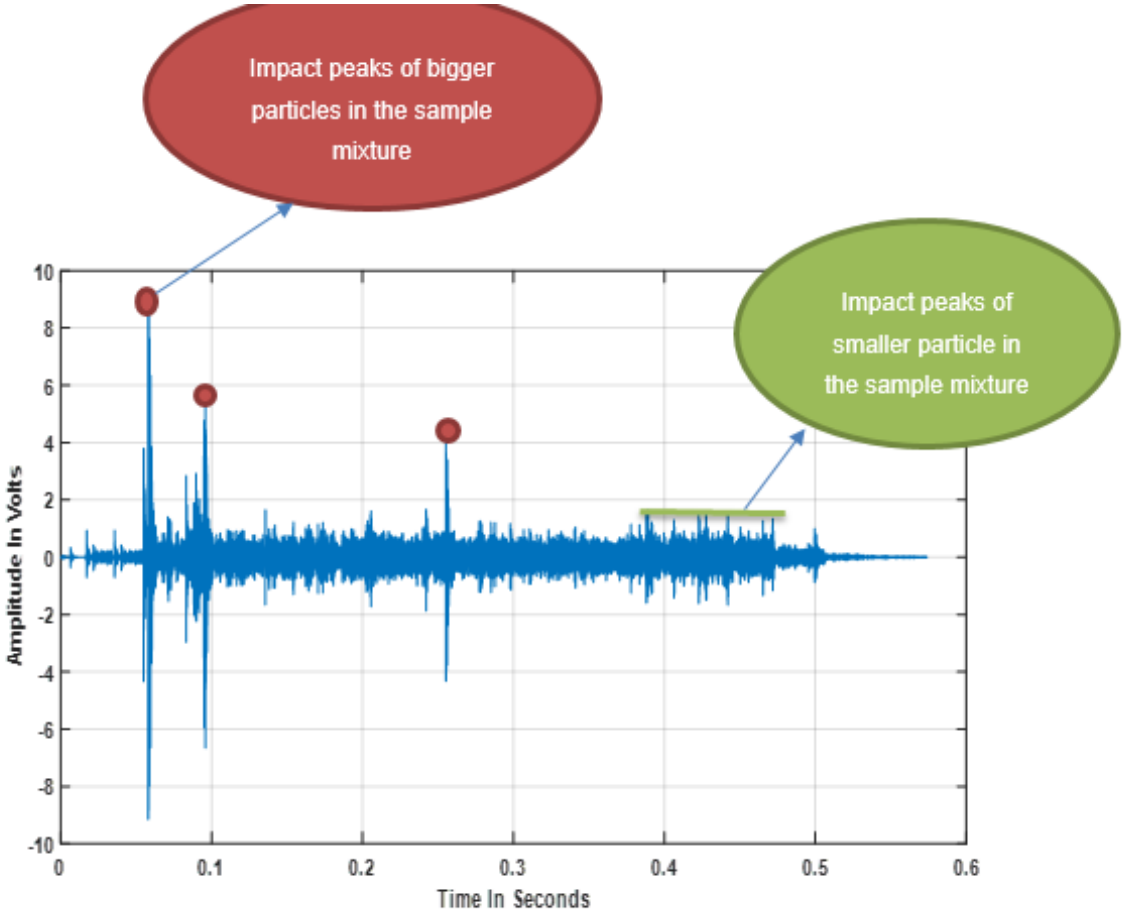

Figure 6.1: Sample Washing Powder AE Signal

6.2 Experiment Structure and Results

As reported by P&G, the traditional way of inspecting the washing powder compound involves the extraction of a set mass of powder from the mixing drum, and a sieving and weighing process where the ratio of oversized powders to fine powders is estimated. In this case, oversized particles refer to powders >500 microns while the fines refer to powders <500 microns. The aim of the first experiment performed on the washing powder in this section was to determine

the possibility of replicating the traditional inspection procedure, using AE. Ariel Actilift was used for all experiments in this chapter and was sieved using a layer sieve to create two different particle classes corresponding to <500 microns (fines) and >500 microns (oversize). An image of the two particle classes can be seen in Figures 6.2 and 6.3 respectively and it can be seen that the mixture of particles in each group consists of regular and irregular size particles.

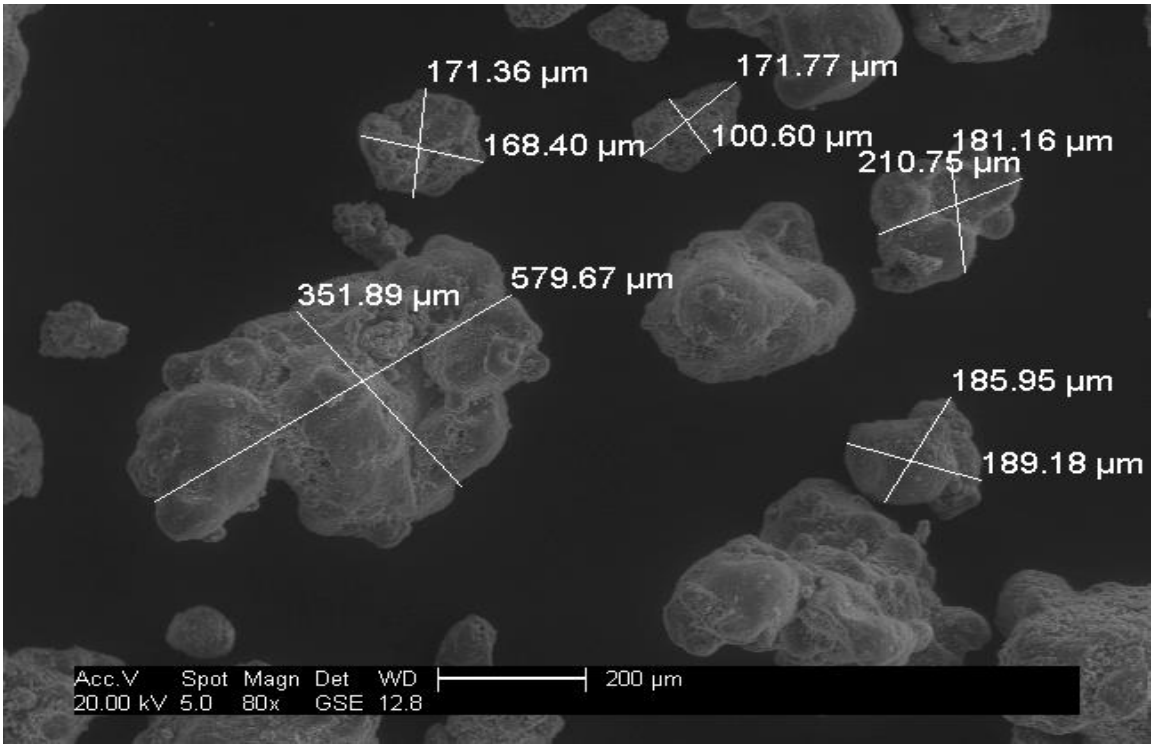

Figure 6.2: Image of Washing Powder <500 microns

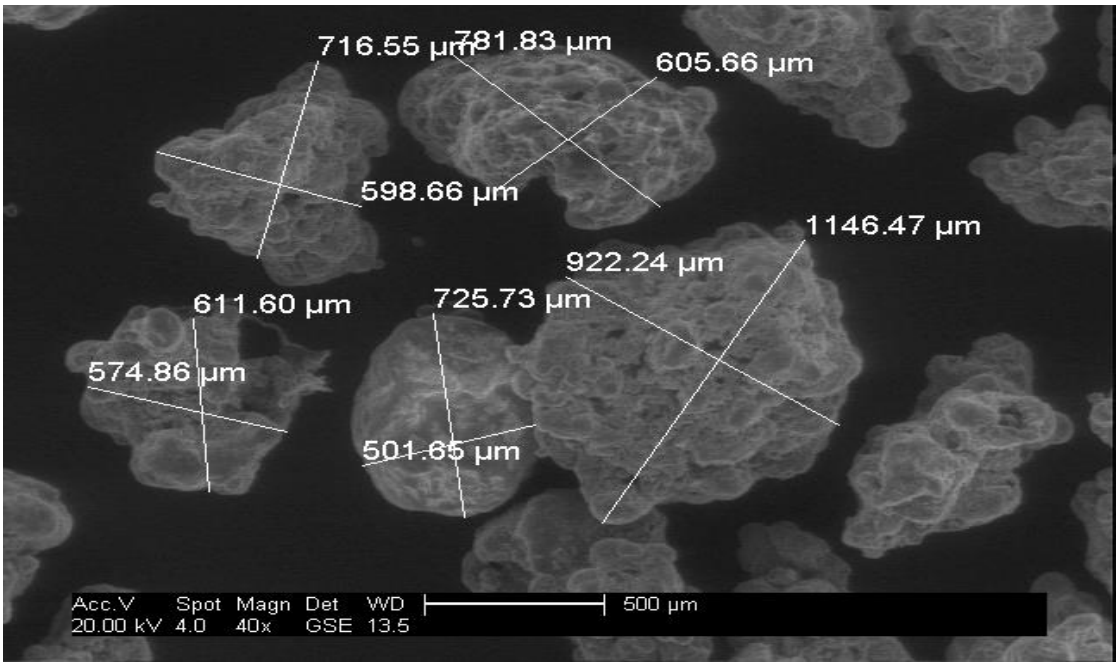

Figure 6.3: Image of Washing Powder >500 microns

A chart showing the full distribution of particles obtained by sieving can be seen in Figure 6.4, it can be noted that the distribution is skewed to the left with 67% of the powders in the oversize category and the median of the distribution being in the 500-700micron range.

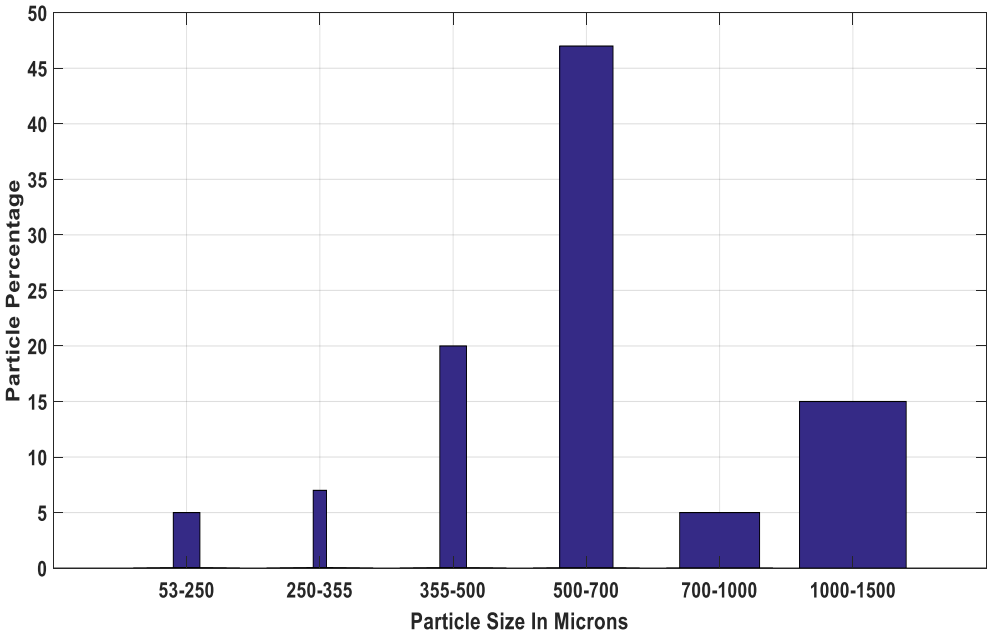

Figure 6.4: Actilift Washing Powder Full Distribution Obtained with Sieving

The physical properties of the particles can be seen in Table 6.1 and it can be noted that the two particle categories have a bulk difference of 8%, with the bulk density was noted in chapter 5 as a pivotal factor which influences the resulting AE produced by a particle, this provided evidence from a physical point of view that the particles could be distinguishable when in a mixture.

Table 6.1 : Physical properties of particles

	Size Range(microns)	**Bulk Density(g/cm^3)**	**Percentage Bulk density Difference**
Fines	53-500	0.58	8%
Oversize	501-1500	0.63	

The experimental procedure was the same as previous chapters where 5 experimental repetitions were carried out per mix ratio with their resulting threshold amplitude mean averaged out to give a representative point per mix ratio, which meant that the final correlation plot comprised of a total of 50 experimental repetitions. The optimal threshold was seen to be in the low

amplitude region and a graph of the optimal correlation plot can be seen in Figure 6.5.

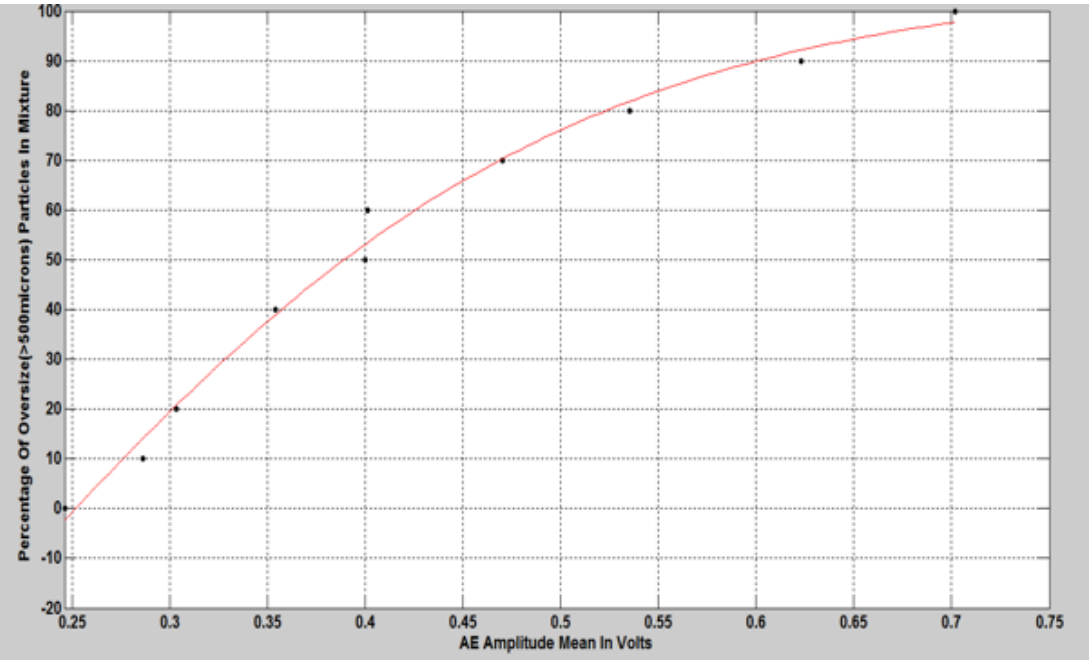

Figure 6.5: Correlation Plot of Oversize Particles against AE Amplitude Mean

Using a new set of experimental mixtures, the PSD estimation model in Figure 6.5 was validated and an average absolute error of 6% was obtained. A chart showing the results of the validation exercise can be seen in Figure 6.6, and it can be seen that the highest error margins were recorded for mixtures which were dominated by fine particles, but the error margin began to decrease as the percentage of oversize particles in the mixture began to increase.

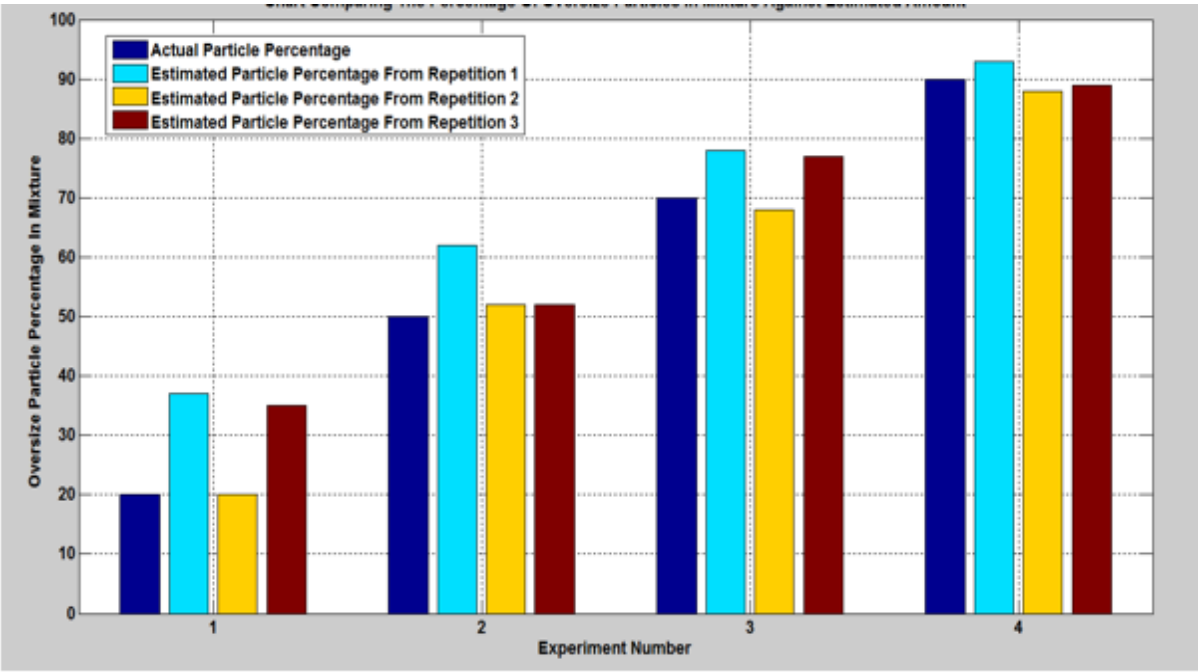

Figure 6.6: PSD Chart Comparing Actual Particle Percentage to Amount Estimated By Model

Results suggest that the designed threshold-based approach to PSD estimation is capable of dealing with mixtures as complex as the one in the experiment, and their resulting signals.

6.3 Conclusion

In this chapter the performance of the designed threshold based signal processing method was observed using an Ariel Actilift compound. The experiments were structured in a similar fashion to the P&G offline analysis which is done by sieving and weighing a localised sample extracted from a washing powder batch. Even though the powder was classified into fine and oversized categories, each category comprised particles with various physical properties and geometry which when mixed together produced a distribution range of 1450 microns. This produced a rather complex signal with very high variability, as can be seen in Figure 6.1.

The procedure was the same as detailed in previous chapters and the optimal threshold showed a modified sigmoidal trend in the particle ratio change, and the

validation exercises showed that the correlation plot was able to estimate the PSD of the mixture with an average absolute error of 6%.

Although the two particle groups have distinctly different sizes, from Table 6.1 it can be seen that there is only a percentage bulk density difference of 8% between the two particle groups, which can be explained by the bulk of the particles in the fines region being in the 355-500 micron range (63%), while in the oversize particle region 70% of particles are in the 500-700 micron range. Despite the apparent similarity in the bulk densities of the two particle groups, the different physical nature of the particles in each group help provide respective AE amplitudes for the pair which proved to be separable with the designed signal processing method.

The results obtained from this set of experiments suggest that despite the variability of the acquired AE signal induced by the wide distribution of particles in the mixture as well as their different physical properties, the designed threshold-based signal processing approach is capable of dealing with signals of this nature and ultimately estimating the related PSD. With the encouraging results obtained from the experiments in this chapter, subsequent work will involve the characterisation of the full washing powder PSD using AE.

7 Particle Size Distribution Estimation Of Washing Powder

7.1 Introduction

This chapter details the steps taken to expand the designed signal processing method in order to characterise the full washing powder distribution. This work builds on the results of the work done in a previous chapter which was based on the separation of the washing powder compound into a big and small category, the next step involves experimentation to observe if the designed signal processing method is capable of estimating multiple particle size bins within a distribution. The performance of the signal processing model was investigated for when the signal processing approach was modelled with a distribution which matched the real sample and a uniform distribution of particles.

7.2 Signal Processing Extension And Data Driven Modelling Technique

During the course of the research, the partners discontinued the sale of Ariel “Actilift”(domestically), which was used for the experiments in Chapter 6. As a result, Ariel original was used for all further experiments, a histogram obtained by sieving and showing the distribution of the powders can be seen in Figure 7.1. The histogram is seen to have a slight left skew with the bin divisions being a function of the standard sieve sizes once again. It is worth noting that the six specific categories which the powders were sieved into came about after interest was shown by the sponsors regarding the possibility of investigating the feasibility of using AE to measure these particle size categories within the washing powder.

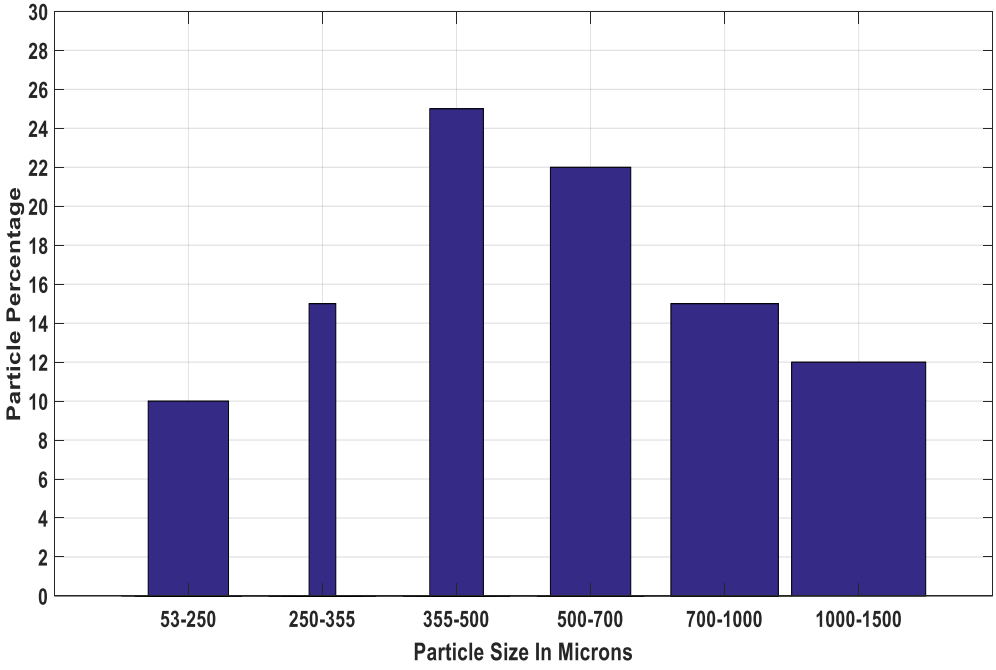

Figure 7.1: Histogram of Ariel Normal Washing Powder Distribution Obtained By Sieving By Weight

Table 7.1: Particle Separation Method

Bin Distribution(microns)	**Bin no./Particle Size Distribution estimation model no.**	**Sieve Separation(microns)**	
		Small	**Big**
53-250	1	53-250	250-1500
250-355	2	53-355	355-1500
355-500	3	53-500	500-1500
500-700	4	53-700	700-1500

700-1000	5	53-1000	1000-1500

In addition to this, the correlation plots were validated with more experimental mixture sets comprising 4 different particle mixtures and 12 repetitions in total in order to determine the best correlation plot and optimal threshold. In total, 57 experimental repetitions (45 training, 12 validation) were required to produce a PSD estimation model for one bin in the washing powder histogram in Figure 7.1 and 285 experimental repetitions were used to from the 5 models needed to estimate the full washing powder distribution with the designed Particle Size Distribution (PSD) estimation signal processing approach. After the AE amplitudes were correlated to their respective particle sizes, the following mathematical operations were used to calculate the particle percentage for each bin in the histogram:

$$B_1+B_2+B_3+B_4+B_5+B_6=100\% \quad (7.1)$$

B_1= can be estimated using PSD model 1 (7.2)

$$B_2= B_{3456}-B_1 \quad (7.3)$$

$$B_3= B_{456}-B_{12} \quad (7.4)$$

$$B_4= B_{56}-B_{123} \quad (7.5)$$

$$B_5= B_6-B_{1234} \quad (7.6)$$

$$B_6=100\%-B_{12345} \quad (7.7)$$

Where:

$B_{1\text{-}6}$=Particle bins 1-6

7.2 Results and Discussions

Two types of PSDs were used to train the PSD estimation model in order to investigate what the optimal distribution would be to use to train the model and would provide the best estimation accuracy.

7.3.1 Normal Distribution

In the first instance, the size estimation approach was modelled with a distribution which matched the real sample and was also a normal distribution. A histogram of this can be seen in Figure 7.1. The obtained PSD estimation models were tested with normal, left skew and right skew type distributions. Due to batch to batch variation was reported as a common issue in the washing powder production plant, it was important to observe the performance of the PSD estimation approach for different distributions.

The graphs in Figures 7.2-7.4 show a visual illustration of the threshold detection method for an AE signal of the normal distribution. The regions highlighted in the respective figures show the optimal threshold region which the threshold amplitude mean was extracted from and correlated to particle size for each bin in the distribution. In figures 7.2 and 7.4, it can be noted that the optimal threshold region was observed to be the same for certain bins, although despite the optimal threshold region being similar, their resulting correlation plots which served as the PSD estimation model was unique for each bin, therefore the threshold amplitude means correlated to different particle sizes.

Figures 7.5-7.7 show graphs comparing the actual particle percentage to the amount estimated by the model for the different distributions considered, and Table 7.2 shows the average absolute error obtained in each case. It is also worth noting that 3 validation experiment repetitions were carried out. The PSD value in each case was averaged, and the resulting value was plotted as the final model estimated amount.

From Table 7.2 it was noted that the estimation model recorded the lowest error margin when it encountered a distribution which matched the real sample as can be seen in Figure 7.5. As distributions different from the sample which the signal

processing approach was modelled with were considered, an increase in the error was observed. In the first case the estimation model was able to estimate the PSD of a distribution with a left skew with an average absolute error of 8%, which is slightly up from the from the error value recorded for a distribution which the model was designed with. The highest estimation error was observed for the distribution which was skewed to the right, which recorded an average absolute error of 16%, this is thought to be due to the mixture being dominated by particles over 500 microns which left only 35% of the particles in the mixture in the less than 500 microns, therefore it can be said that the high error margin is caused by the signal being dominated by the bigger particles(>500 microns) which in turn would make it difficult for the PSD estimation model to detect the peaks of the smaller particles(<500 microns). This is believed to be the reason why the highest error margin was recorded and also the anomalous results as can be seen in Figure 7.7 with the high peaks in Bins 3 and 6.

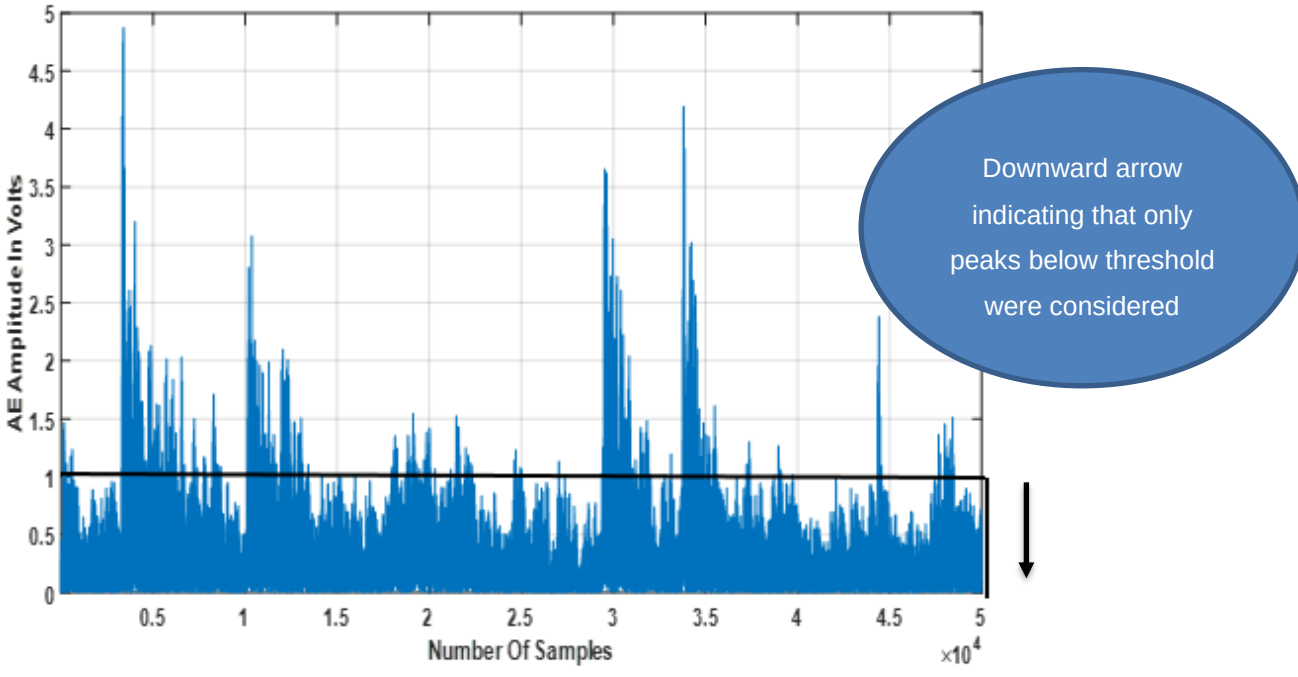

Figure 7.2: Graph Showing Optimal Threshold Region For Bins 1 and 3

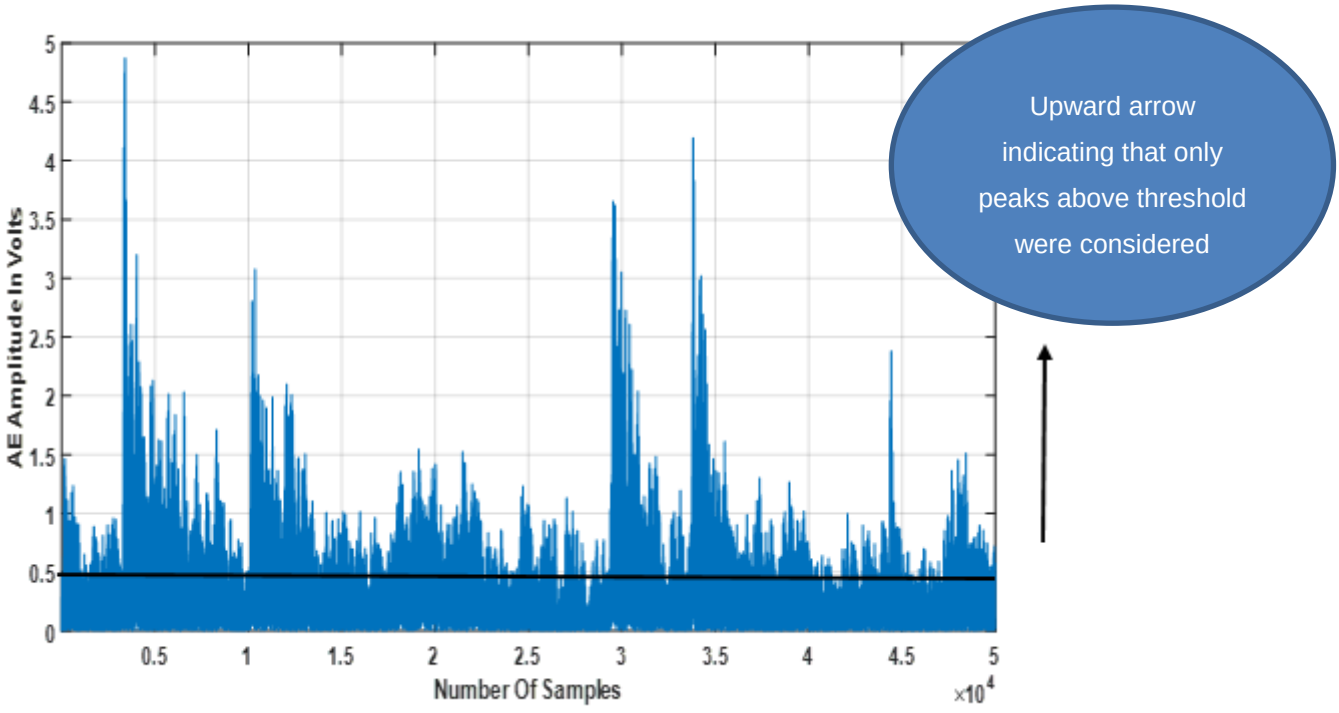

Figure 7.3: Graph Showing Optimal Threshold Region For Bins 2 and 4

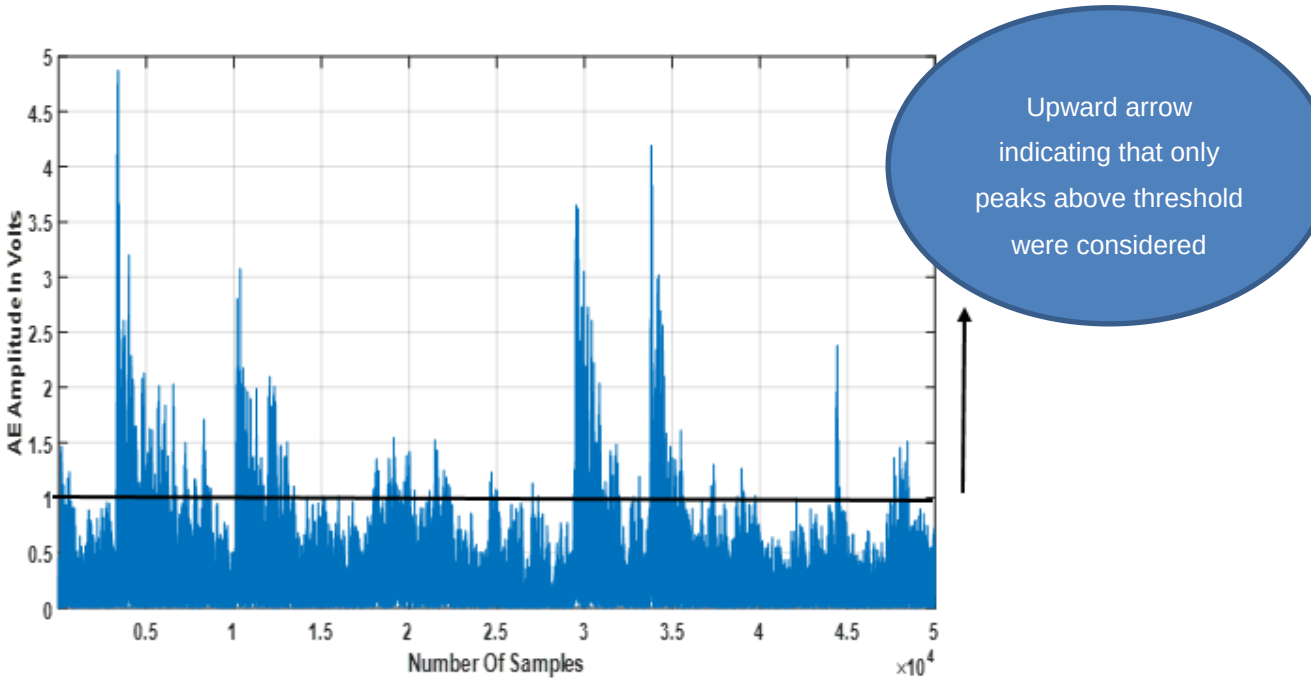

Figure 7.4: Graph Showing Optimal Threshold Region For Bins 5

Where;

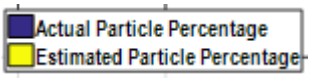

-Error bars represents the variations obtained using the designed PSD estimation model to estimate the respective particle percentage

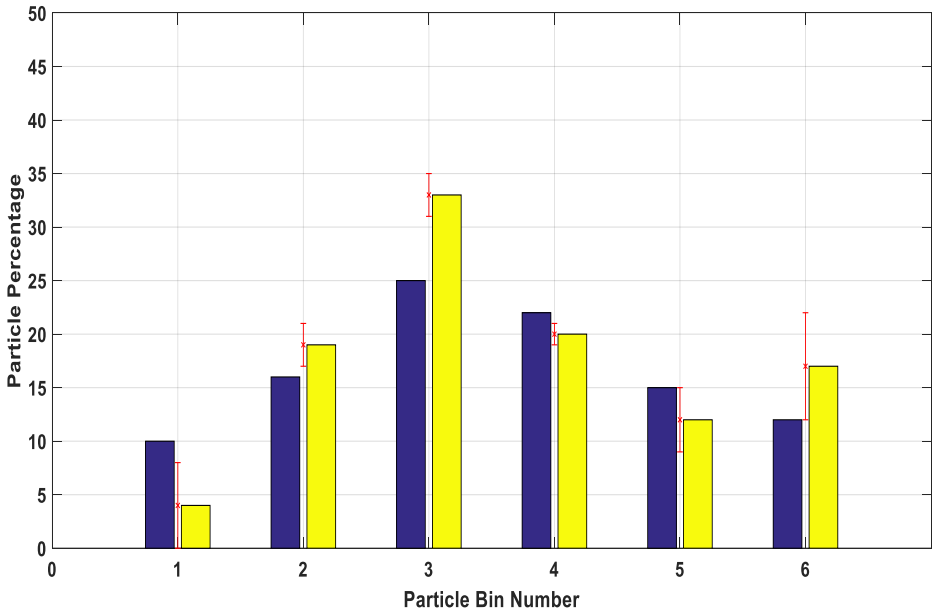

Figure 7.5: Chart Comparing Actual Particle Percentage to Estimated Amount for a Normal Distribution with a Mean of 580 Microns

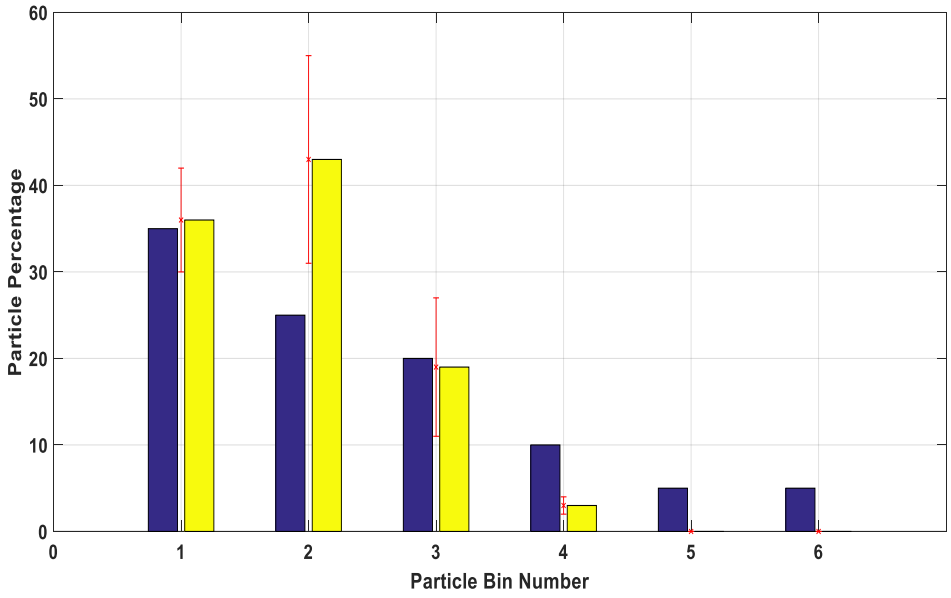

Figure 7.6: Chart Comparing Actual Particle Percentage to Estimated Amount for a Distribution Skewed to the Left with a Mean of 370 Microns

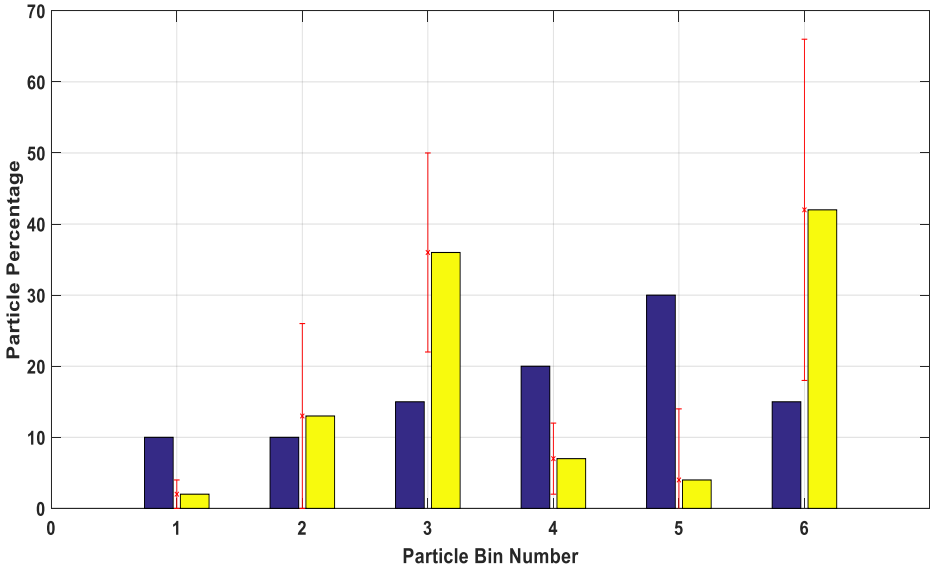

Figure 7.7: Chart Comparing Actual Particle Percentage to Estimated Amount for a Distribution Skewed to the Right with a Mean of 670 Microns

*In order to identify the mean size of each particle distribution, the particles were sieved and the results were plotted as a distribution with a weighted mean value extracted from the results of this.

Table 7.2: Table Showing Various Distributions Considered And The Associated Average Absolute Errors When PSD Estimation Approach Was Modelled With A Normal Distribution

Distribution Type	**Average Absolute Error**
Normal Distribution With A Mean Of 580 Microns	5%
Distribution Skewed To Left With A Mean Of 370 Microns	8%
Distribution Skewed To Right With A Mean Of 670 Microns	16%

7.3.2 Uniform Distribution

The second distribution with which the signal processing approach was modelled was a uniform distribution, as it was observed from previous results that the normal distribution produced a higher error margin when it encountered skewed PSDs. Hence, the motivation for investigating the performance of the PSD estimation approach when modelled with a uniform distribution was that, unlike with the normal distribution, a uniform distribution comprises an equal share for all PSD bins and is therefore expected to provide a smoothing effect which leads to a consistent estimation error for all considered distributions. To form the uniform distribution, the Ariel original washing powder was preliminarily sieved to separate all powder sizes into their various sieve categories, before they were mixed using the format detailed in Table 7.1 to form samples which were used for the experiments. A histogram of the uniform distribution can be seen in Figure 7.8.

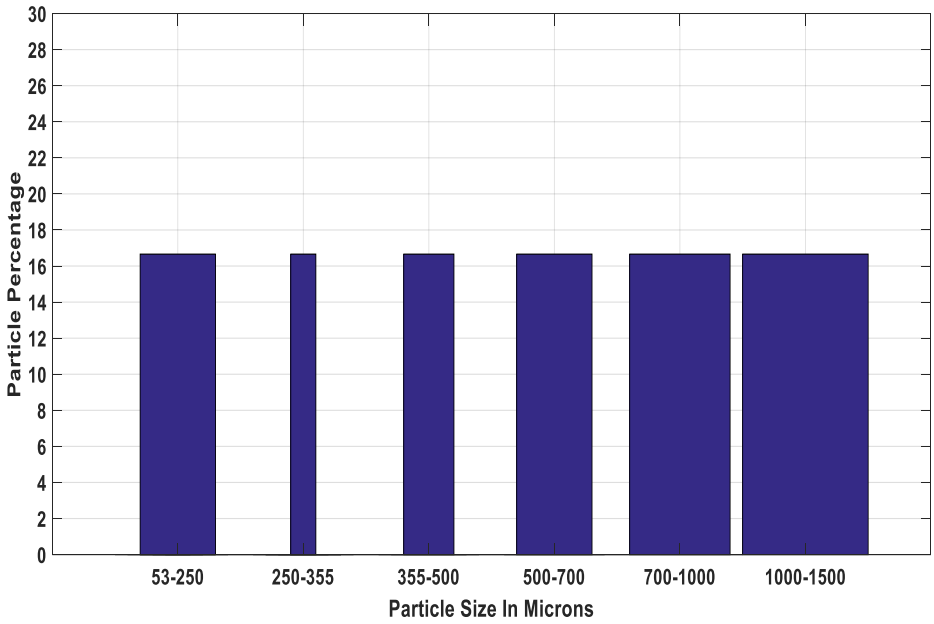

Figure 7.8: Histogram of Uniform Washing Powder Distribution Obtained By Sieving By Weight

The performance of the uniform distribution modelled PSD estimation system was investigated with a set of validation mixtures and Figures 7.9-7.11 show results of the validation experiments. A comparison of their associated estimation errors can be seen in in Table 7.3.

Where;

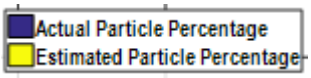

-Error bars represents the variations obtained using the designed PSD estimation model to estimate the respective particle percentage

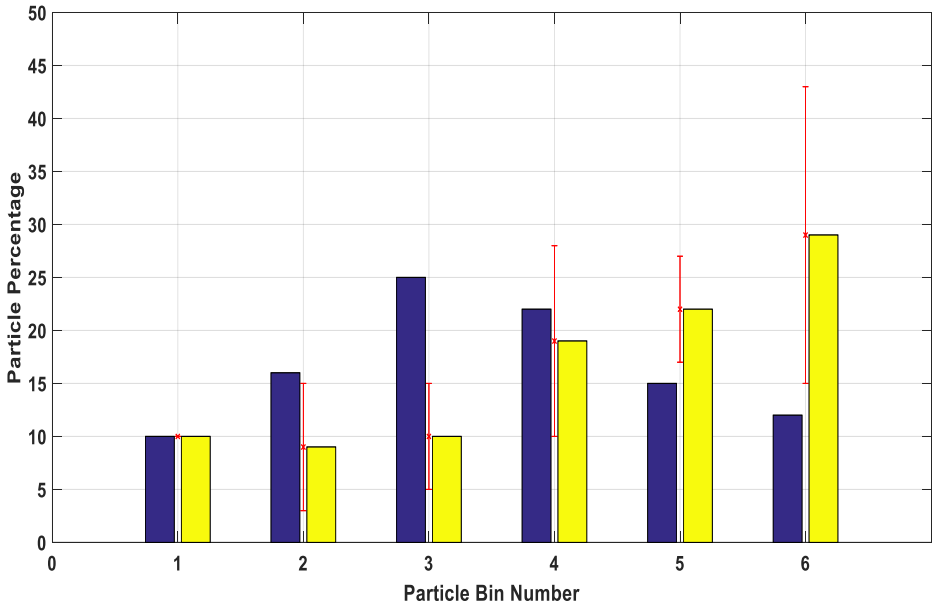

Figure 7.9: Chart Comparing Actual Particle Percentage to Estimated Amount for a Normal Distribution with a Mean of 580 Microns

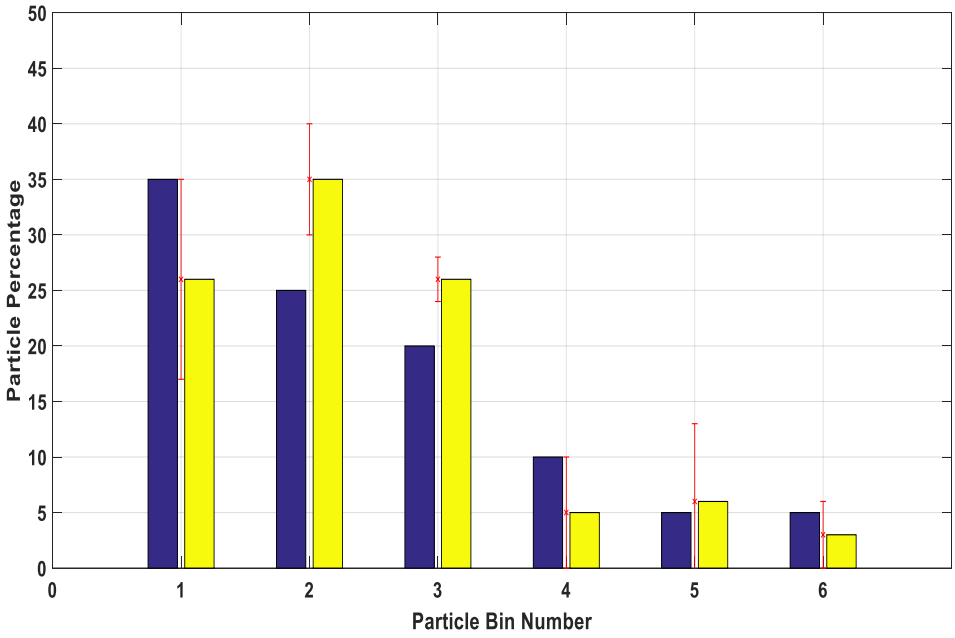

Figure 7.10: Chart Comparing Actual Particle Percentage to Estimated Amount for a Distribution Skewed to the Left with a Mean of 370 Microns

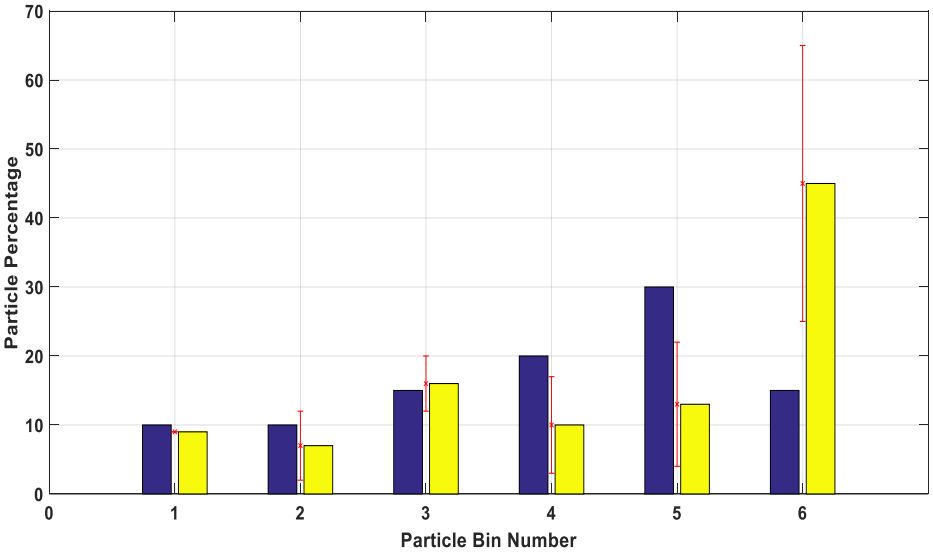

Figure 7.11: Chart Comparing Actual Particle Percentage to Estimated Amount for a Distribution Skewed to the Right with a Mean of 670 Microns

Table 7.3: Table Showing Various Distributions Considered and Associated Average Absolute Errors when PSD Estimation Approach Was Modelled with a Uniform Distribution

Distribution Type	**Average Absolute Error**
Normal Distribution With A Mean Of 580 Microns	8%
Distribution Skewed To Left With A Mean Of 370 Microns	6%
Distribution Skewed To Right With A Mean Of 670 Microns	10%

From the results in Table 7.3, it can be noted that the model whose data came from a uniform distribution appears to have undergone an increase in error when it encountered a normal distribution, with the graph in Figure 7.9 showing the model estimating the respective PSD with a mild right skew. The PSD estimation model showed an improvement when it estimated the PSD for a distribution skewed to the left; this is thought to be due to the smoothing effect induced by training the estimation model with a uniform distribution. While consistent with the results when the data used to design the model came from a normal distribution, the highest error margin is observed when the model encountered a distribution dominated by big particles and skewed to the right, although the result in this case is influenced by the smoothing effect of the uniform distribution, hence a lower error margin is obtained when compared with the result from section 7.3.1. A comparison of results of both model training cases can be seen in Table 7.4.

Table 7.4: Table Comparing Results From Both Training Distributions

Distribution Type	**Average Absolute Error – normal distribution**	**Average Absolute Error – uniform distribution**
Normal Distribution With A Mean Of 580 Microns	5%	8%
Distribution Skewed To Left With A Mean Of 370 Microns	8%	6%
Distribution Skewed To Right With A Mean Of 670 Microns	16%	10%

7.4 Discussion and Conclusion

In this chapter, the designed signal processing method was extended to estimate the PSD of a distribution comprising 6 bins. To find the optimal distribution to train the PSD estimation model with, two case studies were conducted where the signal processing approach was modelled with a normal distribution as found in a washing powder box and a uniform distribution, the performance of the PSD estimation model was observed for cases where skewed and normal distributions were encountered.

In the first case, the PSD estimation model was designed with a normal washing powder distribution which can be seen in Figure 7.1, and results showed that the model had the lowest estimation error(5%) when it encountered the same type of distribution as it was modelled with, but recorded a higher error margin(8%) when it estimated distributions skewed to the left - and was seen to record an even bigger margin(16%) for distributions skewed to the right as can be seen in Table 7.3. It is thought that for the distribution with a left skew, as the mixture is

dominated by fine particles (<500 microns), particles greater than that size would be distinguishable and thus enable the model estimate the PSD of the mixture. The increase in estimation error margin is thought to be due to a difference in skewed distribution from what the signal processing approach was modelled with. The case for the distribution skewed to the right had the highest estimation error, and in contrast to the mixture with a left skew which was dominated by finer particles, this mixture comprises mainly particles greater than 500 microns and only 35% of particles less than that. Thus, the high error margin is caused by the impact of the bigger particles which are expected to dominate the AE signal and hence appear to make detection of the finer particles more challenging.

In the second case, the PSD estimation model was sieved and mixed in a way that produced a uniform distribution as can be seen in Figure 7.8, and this was based on an assumption that the uniform distribution would produce a smoothing effect to help reduce the model's estimation error when dealing with skewed distributions.

When the model encountered a normal distribution it produced a higher estimation error in contrast to the previous case, because the normal distribution differed from what it was modelled with. But a better performance was achieved when the model encountered a distribution skewed to the left, thereby validating the hypothesis that training the estimation model with a uniform distribution does help in reducing estimation error for skewed distributions. For the distribution skewed to the right, as was the situation in the previous case, the error margin was highest in this case but in contrast the estimation error was lower. This suggests that in spite of the smoothing effect induced by the uniform distribution, the finer particles are still difficult to detect because the signal is dominated by the impact of bigger particles.

8 Algorithm Comparison Case Study

8.1 Introduction

To thoroughly benchmark the performance and capability of the designed Particle Size Distribution(PSD) estimation method, its performance was compared to a time-frequency method proposed by Ren et al.[4] Ren used the relationship between the energy of the signal and the particle size in the time-frequency domain, by way of the wavelet transform, to estimate the PSD, using the particle energies at various decomposition levels.[1] Ren et al's method was chosen for comparison as it is a hybrid signal processing method and his data analysis was done in the time-frequency domain as opposed to the time domain which the designed PSD estimation method is based on. This allowed not only for algorithm comparison, but also for observation of the behaviour of the AE signal in different analysis domains.

8.2 Wavelet Transform

Historically, the Fourier transform (and the fast Fourier transform algorithm) represents the most common method used to analyse the frequency content of a signal, but when signals undergo Fourier Transformation they lose details associated with their time signatures.[4,57] Although this is not a problem for time invariant stationary signals, the Fourier Transform has been noted as unsuitable for signals that depict a trend and thus vary with time or have abrupt changes, or non-stationary short events such as impacts and bursts.[57] In 1946, Dennis Gabor proposed a solution to this problem in form of the Short Time Fourier Transform (STFT) which was capable of providing a Frequency-Time representation of the signal - albeit with limited accuracy, and was dependent on the window selection size.[57,58] The downside of this approach was in the window selection, as once a window of a certain size was chosen, it was constant and could not be varied for all the different frequencies in the signal and most signals require a more adaptable approach. The solution to this came in form of the wavelet transform which allowed for a more flexible windowing approach -

long windowing for low frequency components of the signal when more information is required, and shorter time windows where high frequency details are required.[57,59] Figure 8.1 shows a comparison of the various signal analysis domains.

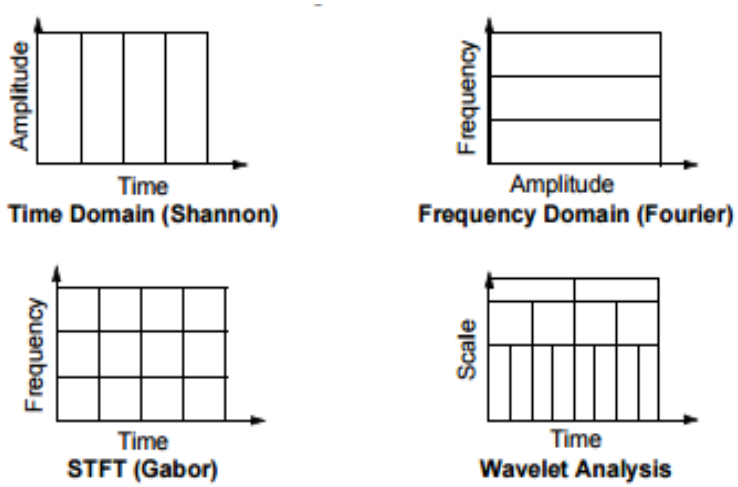

Figure 8.1: Comparison of the Various Signal Analysis Methods [57]

The wavelet transform is proficient in uncovering underlying features of a signal which would normally be difficult to uncover with other techniques; examples of these features include small breakdown points and signal trends.[57,59,60]

8.2.1 Wavelet Approximations And Details

Typically, signals consist of a low and a high frequency part; the low frequency part sometimes makes the signal unique while the high frequency part is usually made up of noise and other signal content. Hence the wavelet decomposition usually consists of the approximate and detail signal values. The wavelet approximations comprise the low frequency and high scale components, while the details represent the high frequency and low scale components of the signal [4,57]. Figure 8.2 shows an illustration of the filtering process and Figure 8.3 shows an example of how the wavelet decomposition approach would work for a multi-level decomposition scenario.

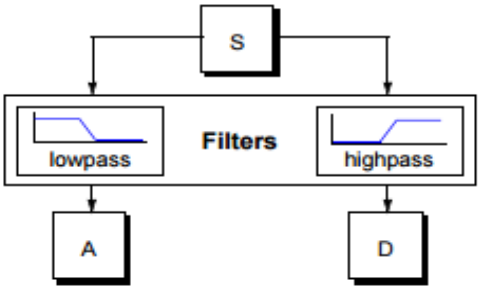

Figure 8.2: Picture showing how one signal is split into two frequency components [57]

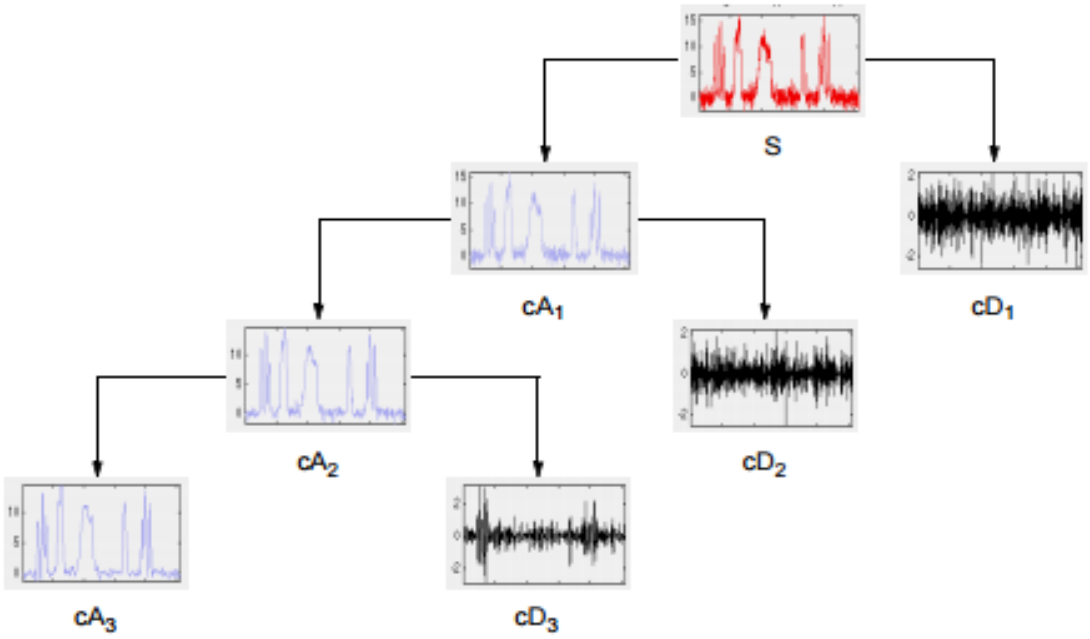

Figure 8.3: Picture showing how one signal is split into two frequency components for a multi decomposition scenario [57]

8.3 Theoretical Model

The theoretical model proposed by Ren et al - which established the relationship between AE and particle energy - can be described as follows [4]:

For a set of homogeneous particles with size D and mass m, impacting on a particular area of a surface ΔA, the resulting force can be written as:

$$F(t) = \sum_{t=1}^{n} 2mv_i\delta(t-t_1) \qquad (8.1)$$

Where δ(t) is related to time t, t_i is the particle arrival time and v_i is the velocity of the particle colliding with the surface. Therefore, it can be said that there are fp·T impacts within the time interval T, where fp represents the mean arrival rate of the particles on the area ΔA.[4] The mean force imposed by particles can then be written as:

$$F(t) = 2mv\text{fp} \qquad (8.2)$$

The acoustic pressure exerted on the surface as a result of the impact can be written as:

$$P_{AE} = \eta\frac{F(t)}{\Delta A} \qquad (8.3)$$

η represents the efficiency of the impact pressure which transforms to acoustic pressure. Assuming that the particle concentration impacting on the surface is C, which can be expressed as the inverse ratio to the projection area of the particles to the impacting surface:

$$C = \zeta/D^2 \qquad (8.4)$$

Where ζ is the coefficient.

The mean arrival rate of the particles on the surface can then be expressed as:

$$f_p = C\frac{\Delta Av}{\Delta A} = CV \qquad (8.5)$$

The average acoustic energy flux per unit time can thus be expressed as:

$$J = P_{AE}\Delta Av = 2\eta mv^2 f_p = 2\zeta\eta f_p = 2\zeta\eta mv^3/D^2 \qquad (8.6)$$

Thus, the acoustic energy E can be given as:

$$E = \int_0^T J dt = \int_0^T \frac{\pi}{3}\zeta\eta\rho_s V3D dt, \qquad (8.7)$$

Where E is the acoustic energy which is a function of the particle diameter D, density ρ_s, and time interval T. Thus if ρ_s and T are constant and do not vary, the acoustic energy E is related to the particle diameter D.

Hence, the relationship between the signal energy in the kth scale and the particle distribution can be expressed as:

$$P_D=\sum_{t=1}^{T} x^2_k = E^a_k(D_j) \qquad (8.8)$$

Where:

P_D=Particle Distribution

x_k=AE signal in kth level

k=decomposition level

$E^a_k(D_j)$ = Approximate energy of the particle j at the kth level

T= time signal takes to go from 1 to T

8.4 Particle Size Differentiation

To validate the relationship described in section 8.3, an investigation was run to determine if the signal energy could be used to differentiate the particle sizes of a sieved set of glass beads, whose physical properties can be seen in Table 8.1. As determined by Ren et al in his study, the Daubechies 2(dB2) wavelet was used to analyse the data and the optimal decomposition was observed to be at the 2nd level. The frequency range analysed in the second decomposition level can be seen in Table 8.2.

Table 8.1: Particle Class Information

Size Distribution	**Bulk Density In g/cm³**	**Particle Class**
150-212 microns	1.49	1
213-300 microns	1.53	2
425-600 microns	1.59	3

Table 8.2: Frequency ranges of the various scales

Energy Scale	Frequency(kHz)
d1	500-1000
d2	250-500
a2	0-250

5 experimental repetitions were taken for each particle class and used to form the correlation plot which can be seen in Figure 8.4.

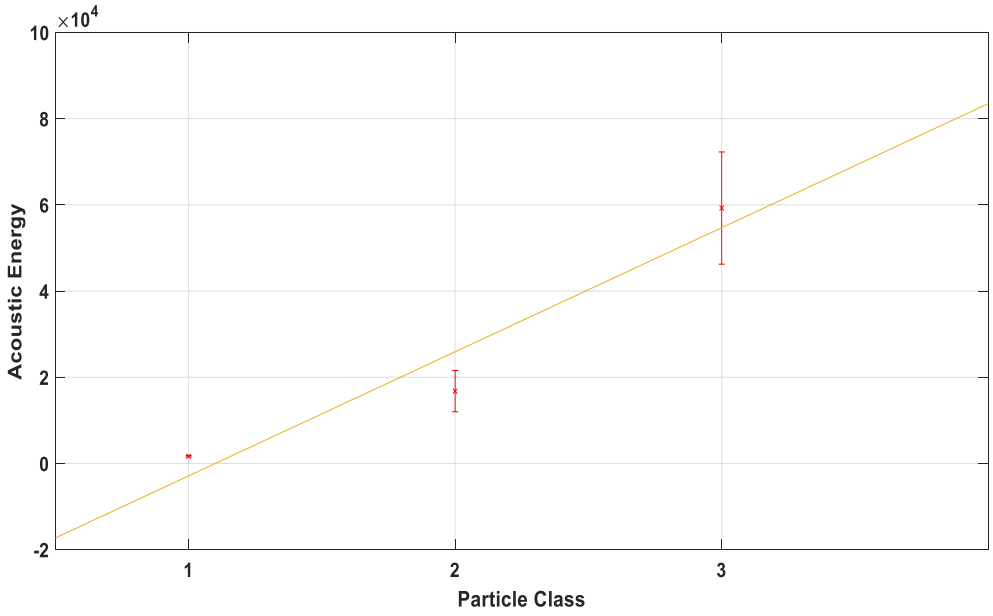

Figure 8.4: Correlation Plot of AE Signal Energy In Joules against Particle Class

From the plot in Figure 8.4, it can be seen that a linear correlation exists between the different glass bead sizes and the resulting signal energy from the optimal decomposition level, thus validating the hypothesis proposed in the theoretical model. The wavelet decomposition function works similarly to threshold tuning, where various regions in the signal are considered until the region which holds rich content from which a feature could be extracted and correlated to the particle size of interest. In wavelet analysis, this region is seen as the optimal

decomposition level, whereas in the threshold approach this is referred to as the optimal threshold level.

8.5 Glass Bead Mixture PSD Estimation

Following validation of the theoretical model, the approach to particle sizing was observed for a mixture of class1 and class3 glass beads. Using the same experimental method as detailed in Chapter 5 which meant that for each data point in the correlation plot comprised of 5 experimental runs with the average value of the results from all repetitions used as the representative point on the graph, which meant that 45 experimental repetitions were used to form the final correlation plot. The plot in Figure 8.5 was formed for the class3 particle percentage in mixture and the resulting Acoustic Energy in Joules. This plot can be seen in Figure 8.5.

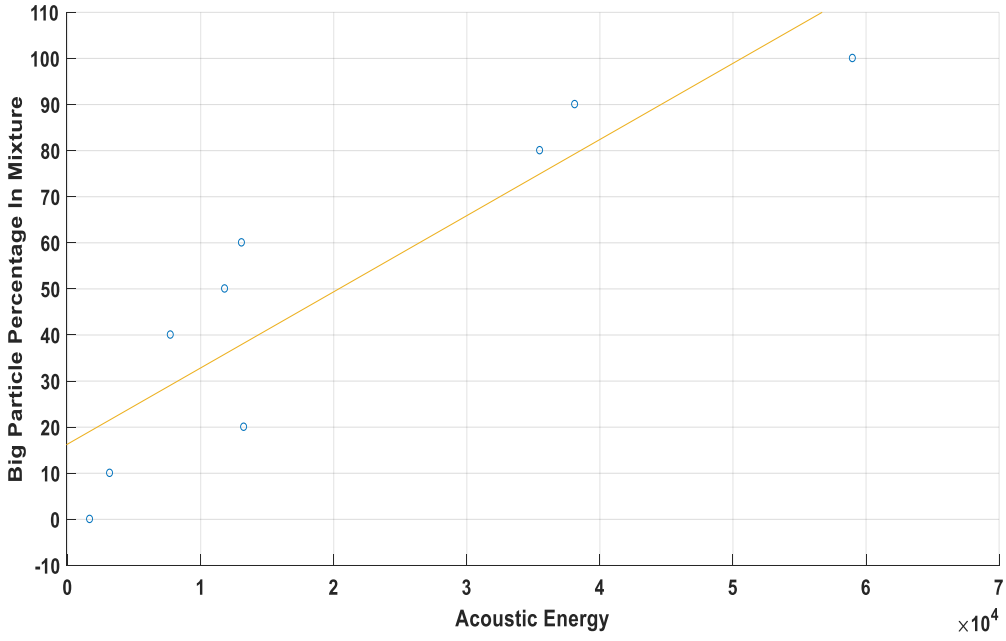

Figure 8.5: Big Particle Percentage in Mixture against Acoustic Energy In Joules For Glass Beads Mixture (R=0.9)

Validating the linear model in Figure 8.5 for a set of validation experiments provided an average absolute error of 7%, which is better than the 10% error

value recorded by the threshold method. A chart showing the results can be seen in Figure 8.6.

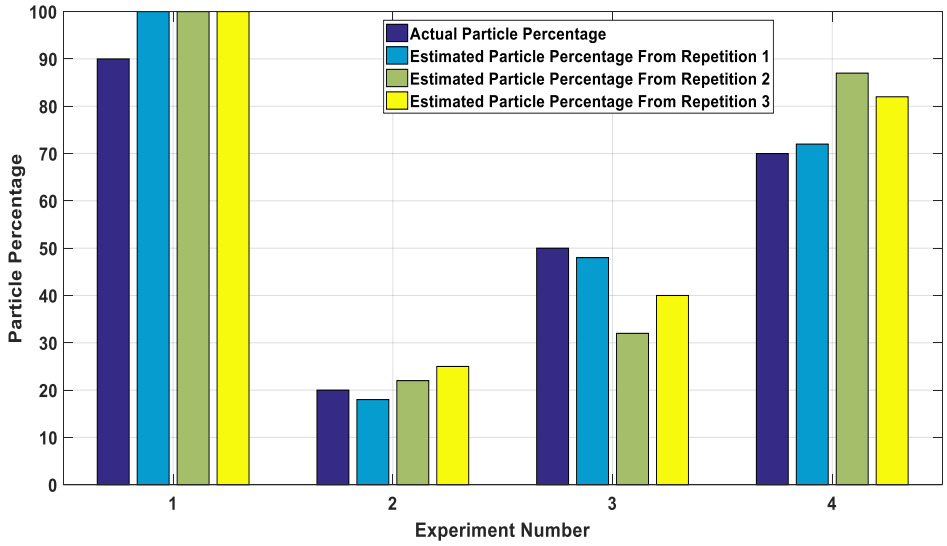

Figure 8.6: PSD Chart Comparing Actual Particle Percentage Of Class 3 Particles (Big) To Amount Estimated By Model

This result suggests that for mixtures of this kind, the energy feature in the time-frequency domain is more sensitive and provides a more accurate estimation accuracy in contrast to the time domain based threshold method.

The next step will involve observation of the wavelet performance for the washing powder compound, which would provide a much more complex signal.

8.6 Washing Powder PSD Estimation

Using the experimental methodology described in chapter 6, this section looked at the estimation of the ratio of fine(53-500micorns) and big(500-1500microns) particles using wavelet analysis to determine if this procedure was capable of dealing with a complex signal such as the washing powder, as well as estimate the PSD. Figure 8.7 shows the correlation plot of the big particles in the mixture against the respective acoustic energy.

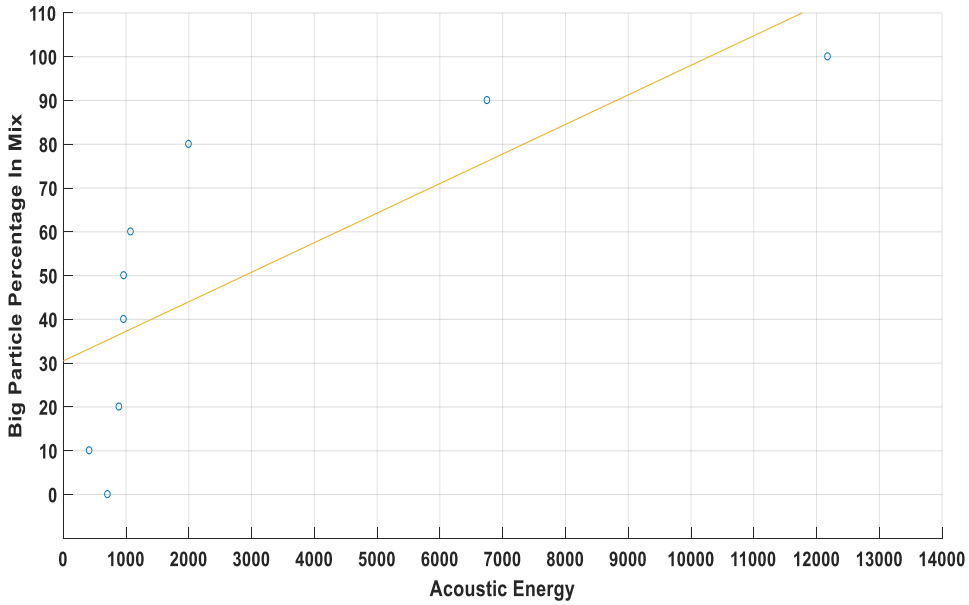

Figure 8.7: Big Particle Percentage in Mixture against Acoustic Energy In Joules Of Washing Powder Mixture (R=0.7)

It can be noted from Figure 8.7 that there does not appear to be a substantial difference in the resulting acoustic energy for mixtures in the range of 0-60% mark, after this a trend begins to form at the points at 80, 90 and 100. This ultimately led to the poor correlation as can be observed from Figure 8.7, the results suggests that in contrast to the designed threshold method, wavelet decomposition is not sufficient for analysing complex signals such as the washing powder, but produces better results than the threshold method for less complex signals as was seen in section 8.5.

8.7 Ren's PSD Estimation Algorithm For PSD Estimation In A Fluidised Bed

Working with a fluidised bed as can be seen in Figure 8.8, Ren et al further developed the principles set in equation 8.8 which relates particle size to resulting acoustic energy, and designed a model which suited his application and was based around the estimation of the particle mass fraction from the acoustic

energy and the mathematical representation for this can be seen in equation 8.9.[1]

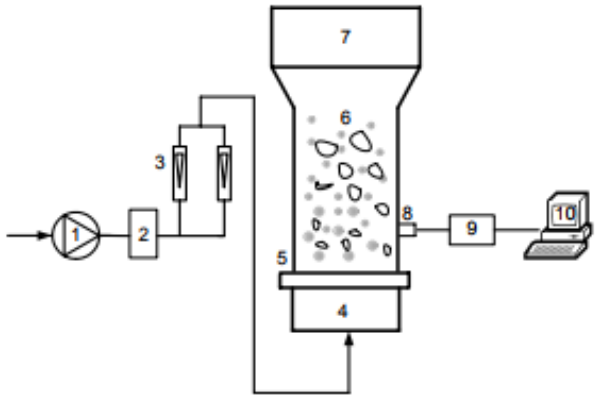

1: Fan; 2: Dryer and heater; 3: Flow meter; 4: Mixing room; 5: Distributor; 6: Fluidized bed; 7: Expanding section; 8: Acoustic sensor; 9: Data acquisition system; 10: Computer

Figure 8.8: Ren's Fluidised Bed Experimental Setup [1]

$$\sum_{j=1}^{N} \lambda_j P_k^a(D_j) x_j = P_{mix,k}^a, k = K \quad (8.9)$$

Where:

x_j= component particle mass fraction

$$P_k^a(D_j) = \frac{E_k^a}{E(D)}$$

k=decomposition level

E_k^a = Approximate particle energy at kth level

$E(D)$= total particle energy

j= component particle number

$$\lambda_j = E(D_j)/E_{mix}$$

Using the same wavelet parameters and dataset as used in section 8.6, the PSD estimation method shown in equation 8.9 was used and the results produced an

average absolute error of 0.38%. A results comparison chart can be seen in Figure 8.9.

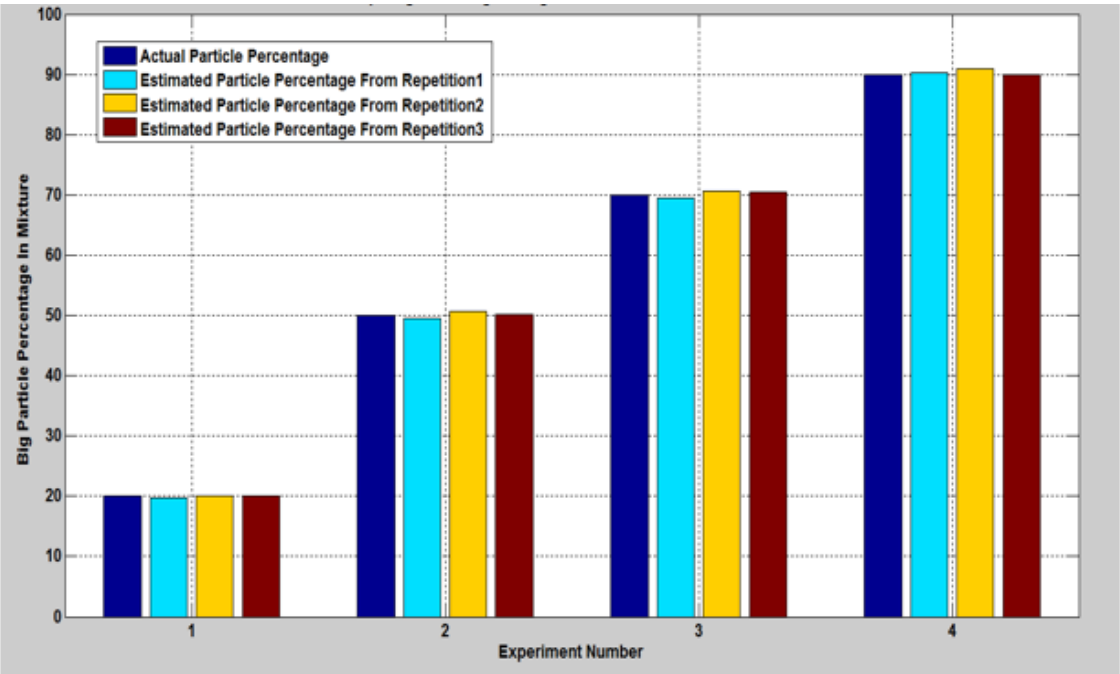

Figure 8.9: Chart Comparing The Percentage Of Big Particles In Mixture Against Estimated Amount

Commenting on the performance on the PSD estimation model designed by Ren for the fluidised bed, it can be noted that from a first observation that the capabilities appear to surpass that of the designed threshold based PSD estimation model. Despite of the impressive accuracy of Ren's PSD model, its limitation comes from the tuning process in the calibration stage where the expected PSD range needs to be input in order to assist the algorithm in making the estimation. [4]

Further validation experiments were carried out with mixtures of different PSD's but this time with the estimation model tuned to just one PSD range. The results of these experiments can be seen in Figure 8.10.

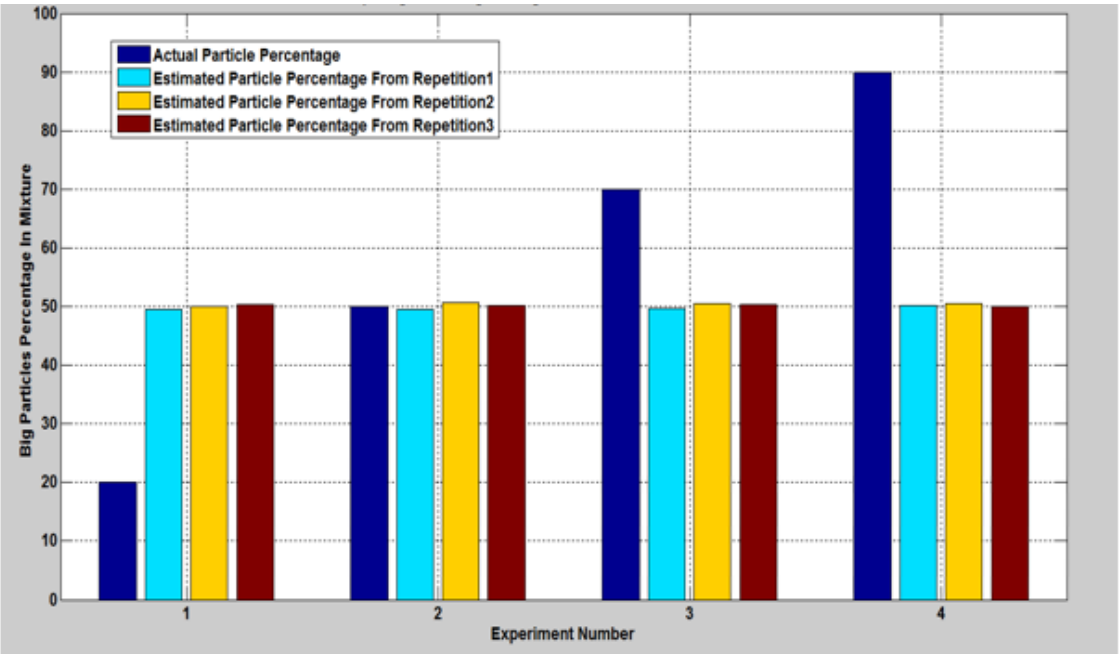

Figure 8.10: Chart Comparing The Percentage Of Big Particles In Mixture Against Estimated Amount

It can be seen from the results in Figure 8.10, that the tuning involved in the calibration stage appears to influence the estimation PSD estimation range possible by the model. This has led to the results shown in Figure 8.10 to be confined to the PSD range which the model was tuned to. For processes such as the fluidised bed considered by Ren et al where PSD variation is not significant, this approach would be suitable, but for other types of powder processes where powder segregation occurs and there is high PSD variance from batch to batch, this PSD model would be unsuitable in that case. In contrast, the threshold based approach would be versatile enough to detect this change as the algorithm is based around the estimation of the PSD of the powders based on the output amplitude which has been seen to vary with different powder mix ratios.[4]

8.8 Conclusion

In this chapter, an algorithm comparison case study was carried out, based on comparison of the designed time-domain based PSD estimation with a time-frequency based technique from the literature designed by Ren et al.[4] Ren et

al's theoretical model was based on the relationship between the particle impact with a surface and its resulting AE signal energy [4].

Ren's approach to PSD estimation was chosen for the algorithm comparison study because in addition to being a hybrid signal processing method, it also provided the opportunity for a performance comparison to be made between time-domain and time-frequency based approaches.

The first work done in this case study involved the differentiation of a set of sieved glass beads using their respective acoustic energies. The analysis was conducted with the Daubechies 2 wavelet family as was determined by Ren et al in his study, and the decomposition level which provided the best correlation was at the 2nd level and thus was referred to as the optimal decomposition level.[4] A linear correlation was observed between the particle sizes and the acoustic energy of each particle as can be seen from Figure 8.4, which helped to validate the relationship proposed by Ren et al's theoretical model. The next scenario involved a mixture of 2 sets of glass beads and an average absolute error of 7% was obtained for this mixture which is more accurate than the 10% error obtained with the designed threshold based approach. The results suggests that the wavelet appears to outperform the threshold method in this case, authors in the literature whom have implemented wavelet based algorithms online have stated the approach to be computationally intensive and thus it is expected to produce a slower online computation rime in contrast to time domain based algorithms.[60]

The wavelet based approach was used to estimate the ratio of fine to oversized particles in a washing powder compound, there appeared to be very little changes in the acoustic energy of mixtures dominated by fine particles which ultimately led to a poor correlation between the particle percentage and resulting acoustic signal energy as can be seen in Figure 8.7, suggesting that this wavelet based approach is incapable of dealing with complex signals such as the type produced by the washing powder compound.

Ren et al further developed an algorithm which was applied to a fluidised bed experimental setup and was based around the estimation of the respective mass

fraction of a mixture using the various particle energies as seen in equation 8.9.[4] It was observed that Ren's algorithm recorded an average absolute error of 0.38% which is lower than the amount recorded for the threshold method(6%) but it was noted that the successful application of Ren's method to PSD estimation was reliant on a tuning process in the calibration stage where the expected PSD range is input into the estimation model. Failure to do this, results in a high average relative error as can be seen in figure 8.9. In the fluidised bed which Ren was working with, it would appear as though the mix ratio does not vary significantly as it is assumed that particle segregation does not occur during mixing. This assumption was made due to the operating nature and tuning reliant nature of his PSD model and also because Ren only validated his PSD model both in the laboratory and in the operating plant for just one mix ratio.[4] If this assumption is true, this could provide an explanation for why Ren's PSD model can only be calibrated/tuned for a given mix ratio and detect what appears to be only slight deviations from the mix ratio which it was calibrated with. Therefore, in processes where mixing is not done efficiently enough and the PSD range post mixing varies significantly, this method of PSD estimation would be unsuitable in that instance.[4] In contrast, the threshold based signal processing method designed in this research would perform better in this case as it is based on the correlation of various AE amplitude mean from the relevant threshold with the associated particle mixture ratio which has been seen to vary with varying PSD's.

9 Conclusion And Further Work

9.1 General conclusions and novelty

The literature review suggested that a hybrid method did not exist for estimating particle sizes with Acoustic Emissions (AE) for powder processes where the final mix ratio varies does not exist. This was identified as a knowledge gap and formed this thesis. The contribution came in form of the design of a time domain based signal processing method which is based on the analysis of the impact peaks of the particles using an amplitude threshold approach. In addition to being able to detect powder mix ratio variation, other notable features of this approach include a simpler algorithm, which would allow for a simpler hardware setup and a quicker online computation time when compared with other particle sizing approach.

This research was Work Package 6s(WP6s) as can be seen in Figure 9.1, and this work package has provided evidence that with the use of an AE sensor and appropriate signal processing algorithms, particle information can be extracted from the powder mixer online.

The proof of concept rig which was designed to retain specific characteristics of the drum mixer was used for all experiments and helped to provide statistical evidence that online PSD monitoring is possible and the approach can also be extended to the detection of a suitable process end point.

This results presented in this thesis has helped to inspire Procter and Gamble(P&G) the quality check procedure can not only be improved but has also provided a possible sensing option which could be utilised in a Process Analytical Technology(PAT) system which will see the mixing process in closed loop.

At the time of writing this thesis, the proposed next steps for P&G based on the output of this work package is to have this sensing approach and designed signal processing approach validated on an industrial scale equipment.

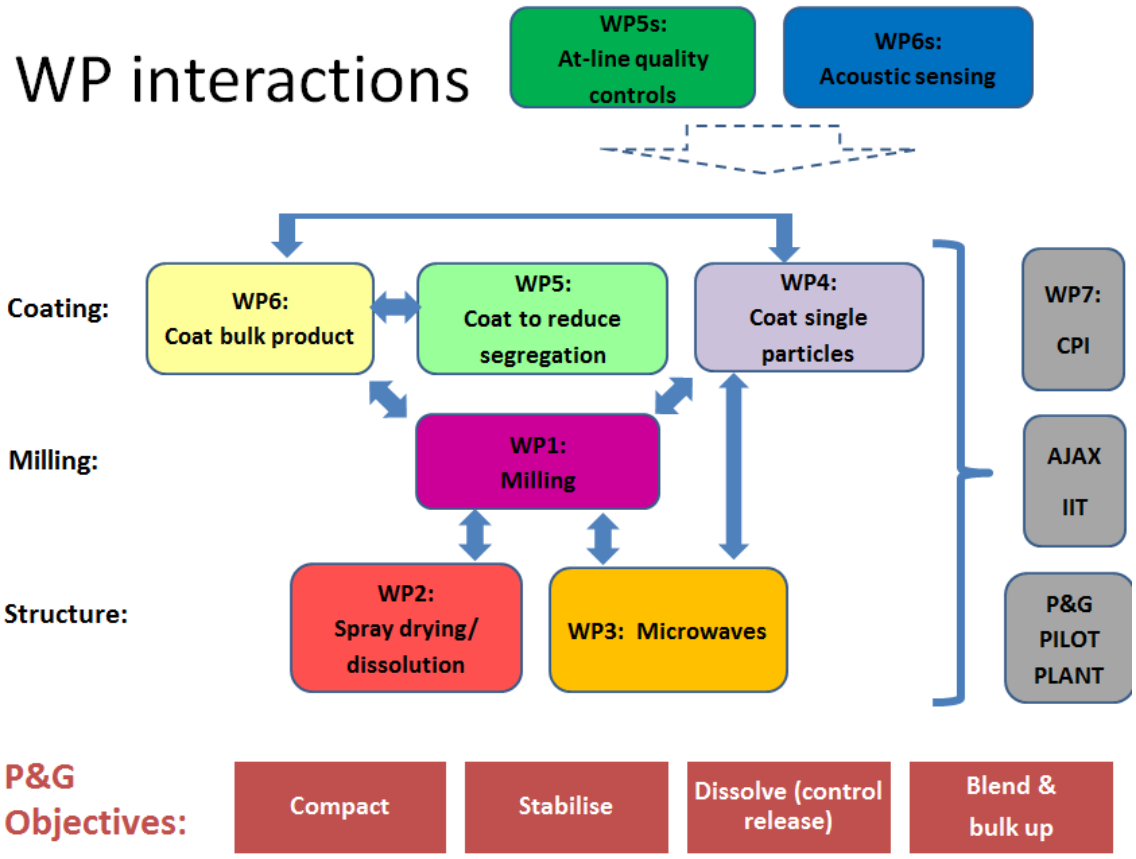

Figure 9.1: Schematic Views Of Work Packages Interactions

9.1.1 Specific Conclusions

The aim of the research was to develop signal processing method capable of estimating the Particle Size Distribution(PSD) of powder mixtures using AE, and objectives associated with this aim included the following;

- Establish the relationship between AE and particle size: the theoretical model established by Buttle et al helped show that AE signals carry the necessary information which can be used to estimate particle sizes. This theoretical model which showed the AE-particle size relationship formed the basis of the signal processing used in this thesis. The relationship was validated using a set of sieved high density glass beads with a regular geometry and low density polyethylene with an irregular geometry, and the experiments were carried out using a benchtop powder free flow experimental rig which by application of the Design OF Experiments(DOE)

methodology helped to design a controlled powder free flow setting. The results from the exercise helped show that a linear relationship exists between the various particle sizes considered and their resulting AE amplitudes. Thereby validating the theory proposed in the theoretical model, providing evidence that the experimental rig can be considered as Linear Time Invariant (LTI) and also showing that the signal processing method is applicable to more than just one particle type.

- Understand the variables that influence AE: Buttle et al established a relationship which accounts for the impact of a source particle(S(*t)*) of a given size on a on wave propagation medium(G*(t)*) and acquired by a sensor which possesses a unique response function (R*(t)*) and records the resulting AE magnitude. The mathematical equation for this can be seen in equation 1.

$$V(t)=S(t)*G(t)*R(t) \qquad 9.1$$

  For an LTI system, once the the wave propagation medium and sensor has been chosen and established, the mentioned functions can be deemed as constant for all acquisitions, thus in this case the acquired AE signal becomes directly dependent of the variables of the source of the impact. From the theoretical model of the source function, it was concluded that in addition to particle size and geometry, particle dependent physical parameters such as density, Poisson's ratio and the Young's Modulus would influence the resulting AE signal produced by a particle impacting a surface. In addition, controlled variations of some of the mentioned factors where possible helped to validate the conclusions made.

- Detect variations in the PSD of various mixtures using AE: the work done in chapter 5 was based around different combinations of a 2-particle mixture were considered to determine if the designed signal processing approach is capable of estimating the PSD of a mixture. The particles used for these experiments included polyethylene which was chosen to represent particles with irregular geometry and low density, and glass beads which was used to represent regular sized particles with a high

density in the washing powder compound. From the results, it was concluded that under the experimental conditions investigated, the designed particle sizing method was capable of estimating the PSD of mixtures but recorded a higher error margin (13%) when it encountered a particle mixture of similarly sized particles due to the similarity of their AE amplitudes.

Chapter 6 involved experiments with the washing powder compound and the experiments done in this chapter were based structured in similar fashion to the offline quality check procedure as reported by P&G, which involves the estimation of the ratio of fine (<500 microns) to oversized (>500 microns) particles in the mixture. From the results, it was concluded that despite the wide distribution of the powders and variability of the acquired AE signal, the designed PSD estimation method was able to estimate the desired ratio of the particles with an offline average absolute error of 6%, suggesting that irrespective of the variable nature of the powders and their respective AE signals, the designed single processing method is capable of dealing with mixtures of this nature and estimating the PSD.

The work done in chapter 7, saw the characterisation of the full washing powder PSD with up to 6 distribution bins in the histogram and detailed the steps taken to extend the signal processing method to adapt to performing the necessary PSD characterisation. Two case studies were conducted in this chapter as the designed signal processing approach was modelled with two distributions in each case in order to determine the optimal training PSD for the size estimation method. The final model in both cases was capable of detecting PSD variations of different mixtures, however it was observed that the model was more capable of detecting minor variations from the normal distribution when modelled with a normal distribution but was less sensitive in detecting the PSD of skewed distributions, whereas when the system was modelled with a uniform distribution, it was more sensitive in estimating the PSD of skewed

distributions. The results helped to conclude that that for processes where only minor deviations from normal distribution occur, the PSD estimation approach can be modelled with a normal distribution. On the other hand, in cases where significant deviations occur per process batch, the system should be modelled with a uniform distribution as this has been found to be more sensitive in estimating the PSD of skewed distributions.

9.1.2 Limitations observed

- One of the possible ways to reduce the error margin produced by the designed PSD estimation model is to use more data in the training phase. In the field. This would be preferably from different production batches and even as far from various seasons to ensure further robustness of the estimation method. This will mean that a large training dataset from a wide time frame will be required to effectively carryout the training phase of the PSD estimation model.
- For all experiments carried out, the PSD estimation model was seen to produce a high error margin for mixtures that comprised of similar sizes and the same physical properties. The similarities in the physical properties of the particles created similar AE signals which made it difficult for the PSD estimation model to effectively distinguish between the different particles and therefore yielded a high error margin. For the washing powder case study, this was not a problem as the mixture comprised of different particles each with their own unique properties. But for powder mixtures consisting of particles similar properties in a mixture, it is believed that high estimation error margin will be obtained in that case.

9.1.3 Proposals for further work

- The results obtained from this study suggests that the designed PSD estimation model which is based on a hybrid signal processing architecture can be implemented online and used in powder processes. The online setup could involve a computational device which will play the

role of a system which the estimation algorithm will be embedded in, and can also include other hardware components that carry out signal functions which are required in the signal processing phase. Typically when an AE burst event occurs, a maximum peak is produced which represents the maximum amplitude producible by the event and this is accompanied by a decay of the signal which is accompanied by a series of damped sequential amplitude peaks as shown in Figure 9.2, as the designed PSD estimation algorithm is based around the detection of the maximum peak, all other accompanying peaks associated with the same AE burst event can be regarded as false peaks and can be eliminated with a signal enveloper.

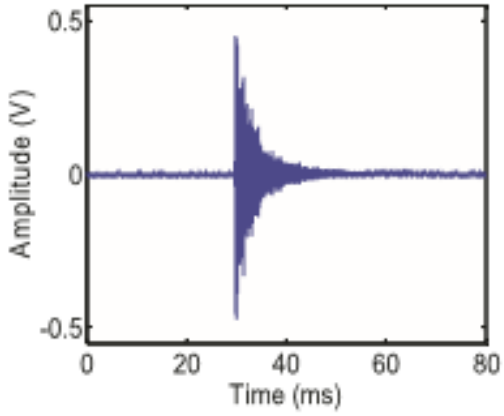

Figure 9.2: Picture Of A Single AE Burst Event [61]

An example illustrating the applicability of a digital signal enveloper for a sample AE signal can be seen in Figure 9.3, it is worth noting that the enveloped signal, has also been downsized from the original 1MHz which it was originally sampled at to 50KHz due to the enveloping phenomenon. The enveloping function carried out on the signal in Figure 9.3 presents two methods of enveloping a signal, which can be done either by the Hilbert's transform or moving average.

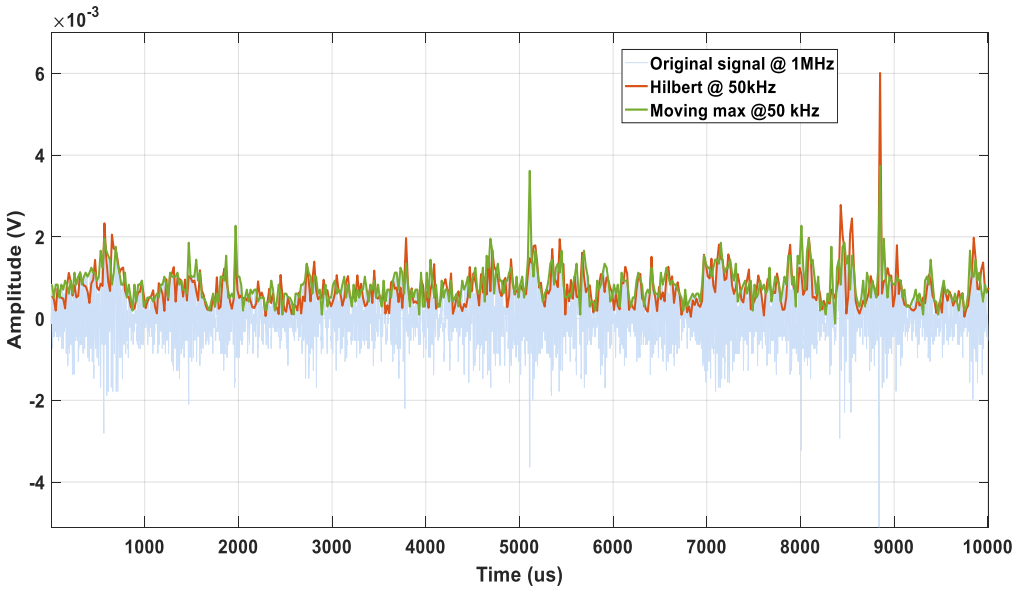

Figure 9.3: Graph Illustrating The Enveloping Phenomena

The signal enveloping step can also be implemented using an enveloper circuit which would aid in the reduction of overall hardware complexity and thus overall online computation time.

- Previous researches have managed to track process change and transition of particulate processes using AE, but despite this none of the authors were able to form a model around an appropriate endpoint for their respective processes. With an appropriate endpoint defined as the point where the measured AE signal indicates the achievement of the desired particle properties. Previous work suggests that it is indeed possible to track process transition, with the PSD estimation model developed in this thesis capable of identifying variations in different mixtures. The model could be extended to monitoring process change over time and detecting an optimal end point which would be defined by a set of PSD characteristics.

10 References

[1] Particle size tutorial. 2017. [ONLINE] Available at: http://www.dispersion.com/. [Last Accessed 9 July 2017]

[2] Nsugbe, E, Starr, A, Foote, P, Ruiz-Carcel, C and Jennions, I. Size Differentiation Of A Continuous Stream Of Particles Using Acoustic Emissions IOP Conf. Series: Materials Science and Engineering 161 (2016)

[3] Bastari, A., Cristalli, C., Morlacchi, R.,: Acoustic emissions for particle sizing of powders through signal processing techniques, Mech. Syst. Signal Process., 2011, 25, (3), pp. 901–916

[4] Ren, C.J., Wang, J.D., Song, D., et al.: Determination of particle size distribution by multi-scale analysis of acoustic emission signals in gas-solid fluidized bed, J. Zhejiang Univ., Sci A, 2011, 12, (4), pp. 260–267

[5] Bdaily Business News. 2013. Procter and Gamble Development Project. [ONLINE] Available at: https://bdaily.co.uk/articles/2013/10/14/iit-to-join-18m-procter-gamble-development-project. [Last Accessed 2 July 2017]

[6] UK-CPI. 2015. CPI in collaboration to develop novel powder processes. [ONLINE] Available at: https://www.uk-cpi.com/news/cpi-announce-world-leading-collaboration-to-develop-powder-based-consumer-products[Last Accessed 2 July 2017]

[7] Box G.E.P., Hunter W.G., Hunter, J.S. (1978). Statistics for experimenters: an Introduction to design, data analysis and model building. New York: John Wiley &Sons Inc.

[8] Papp MK, Pujara CP, Pinal R. Monitoring of high-shear granulation using acoustic emission: predicting granule properties. J Pharm Innov. 2008;3:113–122

[9] Guidance for industry: PAT – A framework for innovative pharmaceutical development, manufacturing and quality assurance; September 2004

[10] Hansuld E.M., Briens L. A review of monitoring methods for pharmaceutical wet granulation / International Journal of Pharmaceutics 472 (2014) 192–201 193

[11] Soravia S., Orth A. (2009). Design of experiments. Ulmann's encyclopedia of industrial chemistry. Retrieved from onlinelibrary.wiley.com. last accessed on 17 May 2017

[12] Mark Anderson and Patrick Whitcomb, DOE Simplified (Productivity, Inc. 2000). ISBN 1-56327-225-3

[13] Yang R.Y. , Yu A.B., McElroy L. , Bao J., Numerical simulation of particle dynamics in different flow regimes in a rotating drum 2008

[14] Staniforth J.N., Walker S., Flanders F., 1986. Granulation monitoring in a high speed mixer/processor using a probe vibration analysis technique. Int. J. Pharm. 31,277–280

[15] Rantanen J., Räsänen E., Tenhunen J., Känsäkoski M., Mannermaa J., Yliruusi J., 2000. In-line moisture measurement during granulation with a four wavelength near infrared sensor: an evaluation of particle size and binder effects. Eur. J. Pharm. Biopharm. 50, 271–276.

[16] Staniforth J.N., Quincey S.M., 1986. Granulation monitoring in a planetary mixer using a probe vibration analysis technique. Int. J. Pharm. 32, 177–185.

[17] Heywood H., Groves M.J. and Wyatt-Sargent J.L. (1970), Proc. Particle Size Analysis Conf., ed., See. Analyt. Chem., 1-18, 208, 210, 245

[18] Zhang J.Q., Yan Y., On-line continuous measurement of particle size using electrostatic sensors Powder Technology, 135–136 (1) (2003), pp. 164–168

[19]Watano S., Numa T., Miyanami K., Osako Y., 2001a. A fuzzy control system of high shear granulation using image processing. Powder Technol. 115, 124–130

[20] Heath A.R., Fawell P.D., Bahri P.A., Swift, J.D., 2002. Estimating average particle size by focused beam reflectance measurement (FBRM). Part. Part. Syst. Char. 19, 84–95.

[21] Rantanen J., Wikstrom H., Turner R. & Taylor L. (2005). Use of in-line near infrared spectroscopy in combination with chemometrics for improved understanding of pharmaceutical processes. Analytical chemistry, 77, 556-563.)

[22] Watson N.J., Povey M.J.W., Reynolds G.K., Xu B.H., Ding Y., Acoustic emission monitoring from a lab scale high shear granulator—A novel approach. International Journal of Pharmaceutics, 2014. 465(1–2): p. 262-274.

[23] Hidaka J., Shimosaka A., 1993. Parameters of radiated sound and state variables in flowing particles. Int. J. Mod. Phys. B 7, 1965–1974

[24] Xu R. Particle Size And Shape Analysis Using Laser Scattering And Image Analysis Using Laser Scattering And Image Analysis Revista Latinoamericana de Metalurgia y Materiales, Vol. 20, N°2, 2000, 80-84

[25] Watano et al., 2001b Feedback control in high shear granulation of pharmaceutical powders S. Watano, T. Numa, I. Koizumi, Y. Osako Eur. J. Pharm. Biopharm., 52 (2001), pp. 337–345

[26] O'Neil A. J., Jee R. D. and Moffat A. C., Measurement of the percentage volume particle size distribution of powdered microcrystalline cellulose using reflectance near-infrared spectroscopy. Analyst, 2003, 128, 1326–1330

[27] Makoto Otsuka, Comparative particle size determination of phenacetin bulk powder by using Kubelka–Munk theory and principal component regression analysis based on near-infrared spectroscopy. Powder Technology 141 (2004) 244 – 250

[28] Huang J., Kaul G., Utz J., Hernandez P., Wong V., Bradley D., Nagi A., O'Grady D., 2010. A PAT approach to improve process understanding of high shear wet granulation through in-line particle measurement using FBRM C35. J. Pharm. Sci. 99, 3205–3212.

[29] Kumar V., Taylor M, Mehrota A., Stagner W. Real-time particle size analysis using focused beam reflectance measurement as a process analytical technology tool for a continuous granulation-drying-milling process AAPS Pharm. Sci. Technol, 14 (2013), pp. 523–530

[30] Yu Z. Q., Chow P. S., Tan R. B. H. Interpretation of focused beam reflectance measurement (FBRM) data via simulated crystallization. Org. Process Res. DeV. 2008, 12, 646–654

[31] Greaves D., Boxall J., Mulligan J., Montesi A., Creek J., Sloan E. D., Koh C. A. Measuring the particle size of a known distribution using the focused beam reflectance measurement technique. Chem. Eng. Sci. 2008, 63 (22), 5410–5419.

[32] Hancke G.P., Malan R. A modal analysis technique for the on-line particle size measurement of pneumatically conveyed pulverized coal. IEEE Trans Instrum Meas 1998;47(1):118.

[33] Endecotts layer sieve website last accessed on 12/12/16

http://www.endecotts.com/products/sieve-shakers/

[34] Hertz H. R., 1882, Ueber die Beruehrung elastischer Koerper (On Contact Between Elastic Bodies), inGesammelte Werke (Collected Works), Vol. 1, Leipzig, Germany, 1895.

[35] Hunter S C. Energy absorbed by elastic waves during impact. Journal of the Mechanics and Physics of Solids, 1957. 5(3): p. 162-171.

[36]Learn Easy Website http://www.learneasy.info/MDME/projects/A1A2_project/robot_sensors/robot_sensors.htm last accessed on 11/2/16

[37] Leach M.F., Rubin G.A., Williams J.C., Particle size determination from acoustic emissions, Powder Technology 16 (1977) 153–158

[38] Leach, M.F. & Rubin, G.A, Williams J.C (1978). Analysis of Gaussian size distribution of rigid particles from their acoustic emissions, Powder technology, 19, 189-195.

[39] Leach, M.F. & Rubin, G.A. (1978). Size analysis of particles of irregular shape from their acoustic emissions, Powder technology, 21, 263-267.

[40] Buttle D. J.,. Martin S. R and Scruby C. B., “Particle sizing by quantitative acoustic emission,” Research in Non-destructive Evaluation, vol. 3, no. 1, pp. 1-26, 1991.

[41] Hu Y., Huang X., Qian X., Online particle size measurement through acoustic emission detection and signal analysis. Proc. IEEE Int. Instrumentation Measurement Technology Conf., May 2014, pp. 949–953

[42] Matero S., Poutiainen S., Leskinen J., Järvinen K., Ketolainen J., Reinikainen S., Hakulinen M., Lappalainen R., Poso A., 2009. The feasibility of using acoustic emissions for monitoring of fluidized bed granulation. Chemometr. Intell. Lab. 97, 75–81.

[43] Briongos J.V., Aragón J.M. & Palancar, M.C. (2006). Fluidised bed dynamics diagnosis from measurements of low-frequency out-bed passive acoustic emissions. Powder technology, 162, 145-156.

[44] Whitaker M., Baker G.R., Westrup J., Goulding P.A., Rudd D.R., Belchamber R.M. & Collins M.P. (2000). Application of acoustic emission to the monitoring and end point determination of a high shear granulation process. International journal of pharmaceutics, 205, 79-91.

[45] Gamble J.F., Dennis A.B. & Tobyn M. (2009). Monitoring and end-point prediction of a small scale wet granulation process using acoustic emission. Pharmaceutical development and technology, 14, 299-304.

[46] Chen. X.M., Chen D.Z, 2008. Measuring average particle size for fluidized bed reactors by employing acoustic emission signals and neural networks. Chem. Eng. Technol. 31, 95–102

[47] Miraslav Uher, Petr Benes (2012), Measurement of particle size distribution by acoustic emission method 2012, IEEE conference instrumental measurement Technology

[48] Pecorari C, Characterizing particle flow by acoustic emission, Journal of Nondestructive Evaluation, vol. 32, no. 1, pp. 104-111, 2013.

[49] Nsugbe E, Starr A, Ruiz-Carcel C, Monitoring The Particle Size Distribution Of A Powder Mixing Process With Acoustic Emissions: A Review. Engineering Technology Reference, pp. 1–12 ,doi: 10.1049/etr.2016.0139

[50] PCI-2 Based AE System User's Manual

[51] Honeywell Sensing and Control Website last accessed on 3/7/16 https://measurementsensors.honeywell.com/Pages/Product.aspx?pid=31

[52] Hirschman, I. I. and Widder, D. V. *The Convolution Transform.* Princeton, NJ: Princeton University Press, 1955

[53] McLaskey G, Glaser S. Hertzian impact: experimental study of the force pulse and resulting stress waves. J. Acoust. Soc. Am. 128, 1087–1096 (2010)

[54] Hsu N, Breckenridge F. Characterization of acoustic emission sensors. Mater. Eval. 39, 60–68 (1981)

[55] Ivantsiv V, Spelt J and Papini M 2009 Mass flow rate measurement in abrasive jets using acoustic emission, Meas. Sci. Technol. 20 095402.

[56] Electric Charge And Coulomb's Law Website. Accessed on 16/6/17

http://spiff.rit.edu/classes/phys213/lectures/coul/coul_long.html

[57] Michel Mistiti Wavelet Toolbox For Use With Matlab

[58] The Short Time Fourier Transform. Website accessed on 10/7/17

https://www.dsprelated.com/freebooks/sasp/Short_Time_Fourier_Transform.html

[59] The Wavelet Transform. Website accessed on 12/7/17

http://gwyddion.net/documentation/user-guide-en/wavelet-transform.html

[60] D. Sun On-line nonintrusive detection of wood pellets in pneumatic conveying pipelines using vibration and acoustic sensors,"IEEE Trans. Instrum. Meas., vol. 63, no. 5, pp. 993–1001, May 2014.

[61] Yong Yan, Xiwang Cui, Miao Guo and Xiaojuan Han. (2016). Localization of a continuous CO2 leak from an isotropic flat-surface structure using acoustic emission detection and near-field beamforming techniques. *Measurement Science and Technology* . 27 (11), 115105

APPENDICES

Training Log

Doctoral Training Courses Attended:

-Getting Started In Your Research

-Successful Planning For Your Personal Development

-Stages of Conducting Research

-An Intro To The Statistical Treatment of Experimental Data

-Research Integrity and Being An Ethical Researcher

-How To Succeed In The Global Research Community

-Keeping Up To Date In Your Field

-Visualising & Presenting Your Data

-Why Publication is Important for Your Research and Your Career

-Use The Business Model Canvas To Develop Your Business Idea

-Technical Writing Skills for Your Progress Reviews

-Introduction To Teaching in Higher Education

-Education Insights

-Using What You Read In What You Write

-Papercraft - Publishing In Peer Reviewed Scientific Journals

-Employability Skills

-IP and Commercialisation Strategies

-Keeping Up To Date In Your Field

-Statistics of Experimental Data

-Principles of Risk Management

-Introduction to Research Data Management

-Assisting In The Supervision of MSc Students

-Improving Your Employability : Leaders for Life

-Preparing For Your Viva

-Researchers Infokit - part 1

-Essential People Skills For Success

-Referencing and Avoiding Plagiarism

-Researchers Infokit - part 2

-Communicating Your Research Story

-Successful Planning For Your Personal Development

-Making An Impact With Your Publications

-Applying Systems Thinking To Your Research

-Writing A Literature Review

-Key Factors For Success In Starting Your Own Business

-Applying Your Technical Expertise as a Consultant

-Moving From Postgrad to Postdoc and into an Academic Career

-Doing A Systematic Literature Review

-Writing Up Your Thesis

-Papercraft - Publishing In Peer Reviewed Scientific Journals

-Making An Impact With Your Publications

Short Courses Taken:

- **BAE Online Course "**Principles Of Cost Engineering"-**Distinction Obtained**
- **BAE Online Course "**Principles Engineering Integration"-**Distinction Obtained**
- **University Of California Online Course "**Learning How To Learn: Powerful mental tools to help you master tough subjects**"-Distinction Obtained**

- **Week Long Short Course At The Cranfield School Of Management** “Principles Of Project Management And Introduction To Prince2”-Overall Grade of 69%
- Cranfield University Through Life Engineering Week Long Summer School
- Asset Management Coupling Business and Technology 3 Day Short Course

Related Work Experience:

-Assisted Supervisor With Lab Demonstration With Msc Group Based Around Modal Analysis Of Structures

-Completed 4 Hours Of Lecturing Shadowing With Professor Ian Jennions

Volunteering:

- Annual career advisor volunteer for sixth form students at the Green Power Final Racing event
- Nuffield Gold Star Award report reviewer
- School Liaison Officer with the Institute Of Engineering And Technology